STRATEGIES FOR DEVELOPING LENTIL PROTEIN STABILIZED CANOLA OIL IN WATER NANOEMULSIONS

A Thesis Submitted to the
College of Graduate Studies and Research
In Partial Fulfillment of the Requirements for the
Degree of Master of Science in the
Department of Food and Bioproduct Sciences
University of Saskatchewan
Saskatoon, SK

By
Maja Primozic

PERMISSION TO USE

In presenting this thesis in partial fulfillment of the requirements for a postgraduate degree from the University of Saskatchewan, I agree that the Libraries of this University may make it freely available for inspection. I further agree that permission for copying of this thesis any manner, in whole or in part, for scholarly purposes may be granted by the professor or professors who supervised my thesis work or, in their absence, by the Head of the Department or the Dean of the College in which my thesis work was done. It is understood that any copying, publication, or use of this thesis or parts thereof for financial gain shall not be allowed without my written permission. It is also understood that due recognition shall be given to me and to the University of Saskatchewan in any scholarly use which may be made of any material in my thesis.

Request for permission to copy or to make other use of material in this thesis, in whole or part, should be addressed to:

Head of the Department
Food and Bioproduct Sciences,
University of Saskatchewan
Saskatoon, SK, Saskatchewan
S7N 5A8
Canada

ABSTRACT

The overall goal of this research is to utilize the lentil protein isolate (LPI), prepared with isoelectric precipitation by POS Bio-Sciences (Saskatoon, SK, Canada), in the development of canola oil-in-water nanoemulsions. The effect of LPI concentration and the effect of high-pressure treatment of LPI on the formation, stability and rheological behaviour of canola oil-in-water nanoemulsions was investigated. According to a previous study of coarse emulsions, LPI showed the best emulsifying properties at pH 3; therefore, all nanoemulsions were prepared at this pH.

In the first study, nanoemulsions were prepared by adding 5 wt% canola oil to the LPI solutions at various concentrations (0.5 – 5 wt% LPI) in a citric acid buffer at pH 3 and homogenized at 20,000 psi pressure. The storage stability of the nanoemulsions was recorded for 28 days. All nanoemulsions showed bimodal droplet size distribution, where the smaller peak was attributed to the oil droplets while the larger peak was attributed to unadsorbed protein aggregates in the continuous phase which grew in the size with increasing LPI concentration. The protein aggregation was also confirmed with confocal microscopy. Concentration of 0.5 wt% LPI was not sufficient for long term stabilization of oil droplets therefore the nanoemulsion separated out over the 28 days. The best stability of the nanoemulsions was observed with 1, 1.5 and 2 wt% LPI, confirmed by a photocentrifuge, which evaluates oil droplet movement and hence emulsion stability under accelerated gravitational force. Nanoemulsions stabilized with 3 and 5 wt% LPI transformed to a thick gel, most likely due to a network formation between the oil droplets and free proteins in the continuous phase. The viscosity and the gel strength of nanoemulsions increased with increasing protein concentration because of increased aggregation of free proteins in the continuous phase of the nanoemulsions.

In the second study, the effect of high-pressure homogenization of LPI on the formation and stability of the nanoemulsions were investigated. The most stable and flowable nanoemulsions at 1, 1.5 and 2 wt% LPI concentrations were chosen based on the previous results. Prior to nanoemulsion formation, LPI solutions (1 -2 wt% LPI) were homogenized at 5,000 and 15,000 psi pressure for six cycles. Nanoemulsions were then prepared by adding 5 wt% canola oil to 95 wt% pre-treated LPI solutions at pH 3 and homogenized at 20,000 psi pressure. High-pressure homogenization of LPI significantly improved long term stability of the

nanoemulsions by decreasing the large protein particles into small ones, which was confirmed by particle size distribution, light microscopy and photocentrifuge dispersion analysis. Small particles improved migration of proteins to the oil-water interface and facilitated formation of oil droplets and resulted in a decrease in the average oil droplet size from ~ 250 nm to less than 200 nm. No significant difference was observed between 5,000 and 15,000 psi pressure indicating that 5,000 psi homogenization of LPI solution was sufficient to brake large protein particles into small ones. High-pressure homgenization of LPI solutions also decreased protein aggregation in the continuous phase of the nanoemulsions which was confirmed with the confocal microscopic imaging and this might be due to the lower surface hydrophobicity created by high-pressure homogenization of LPI. Results from the interfacial rheology indicated that weaker interfacial film was formed by the high-pressure homogenized LPI solutions compared to un-homogenized proteins. Storage stability of the nanoemulsions prepared with high-pressure homogenized LPI solutions was significantly improved compare to the nanoemulsions prepared without high-pressure treated LPI due to a smaller droplet size and less protein aggregation in the continuous phase. Lipid digestibility showed an increase for nanoemulsions prepared with high-pressure homogenized LPI solutions (1 wt%) due to a smaller droplet size and weaker interfacial film, however no significant difference was observed for 1.5 and 2 wt% LPI homogenized solutions. This might be due to a higher LPI concentration covering the oil droplet surface and preventing digestive enzymes to access the oil.

Overall, high-pressure homogenization improved emulsification properties of LPI and shelf life and lipid digestibility of the prepared nanoemulsions thereby increasing the nutritional value of the product. Lentil protein-stabilized nanoemulsions containing low oil volume fractions have many applications in the development of beverage type products due to their increased stability, flowability and longer shelf life.

ACKNOWLEDGEMENTS

First and foremost, I wish to express my sincere gratitude to my supervisors Dr. Supratim Ghosh and Dr. Michael Nickerson for their help and support, their attitude and passion for science and research truly inspired me and kept me going. Without their constant guidance this thesis would not have been possible. I would also like to thank my advisory committee Dr. Janitha Wanasundara and Dr. Qui Xiao for their invaluable feedback and advices throughout my project. Special thanks to my external examiner, Dr. Helen Booker for her time and careful review of a thesis on a very short notice.

I also appreciate and I wish to thank POS Bio-Sciences, Saskatoon, SK for kindly providing samples for this research.

I would like to thank my friends and colleagues (Vivek, Spuritha, Chang, Akaysha, Alexander, Aakash, Andrea, Dellaney, Natalie, Ivan, Athira, Saakshi, Kunal, and Sacha) for training and assistance during my time here. Special thanks to Akaysha Duchek who made a significant contribution to this research by helping me with experimental work as a summer student. For the administrative assistance I would like to thank Ann Harley and Donna Selby.

I would like to acknowledge the Agricultural Development Fund (ADF) from the Saskatchewan Ministry of Agriculture, CFI-John R. Evans Leaders Fund, Innovation and Science Fund (ISF) from the Saskatchewan Ministry of Advanced Education for providing financial support for my research. I am thankful for a Devolved Scholarship as an additional financial support from the Department of Food and Bioproduct Sciences.

I would like to thank my loving parents Vesna Primozic and Valentin Primozic, and my sister Nina Primozic who have supported and encouraged me throughout my life. Last but not least, special thanks to my fiancé Ales Ursic for his love and support in all the years we spent together and I should also thank to our son Luka who motivated us all to finish this thesis a little sooner.

TABLE OF CONTENT

LIST OF TABLES

LIST OF FIGURES

LIST OF SIMBOLS AND ABBREVIATION

°	angle
°C	Degree Celsius
<	Less
>	More
a.u.	Arbitrary unit
ANOVA	Analysis of variance
ANS	8-anilino-1-naphthalenesulfonic acid
AOAC	Association of Official Analytical Chemists
BBPI	Black bean protein isolate
BG	Bovine gelatine
ChPI	Chickpea protein isolate
CMC	Critical micelle concentration
d	Day
d_{32}	Droplet surface area mean (Sauter area mean)
d_{43}	Droplet volume mean
DH	Degree of hydrolysis
DLVO	Derjaguin, Landau, Verwey, Overbeek
DSD	Droplet size distribution
EWP	Egg white protein
$f(k_\alpha)$	Function associated with the ratio of the particle radius (α) Debye length (k)
F/m	Farad per meter
FFA	Free fatty acid
FG	Fish gelatine
g	Gravitational force (9.81 m/s^2)
G’	Storage moduli
G’’	Loss moduli
h	hour
kHz	Kilohertz

LPI	Lentil protein isolate
LVR	Linear viscoelastic region
M	Molarity
mm	Milimeter
mN/m	Mili-Newton per meter
MPa	Megapascal
MUFA	Monounsaturated fatty acid
mV	Milivolt
nm	Nanometer
O/W	Oil-in-water
Pa.s	Pascal second
pH-STAT	Titration method
pI	Isoelectric point
PIT	Phase inversion temperature
PPI	Pea protein isolate
PSD	Particle size distribution
psi	Pounds per square inch
PUFA	Polyunsaturated fatty acid
r	Particle radius
rad/s	Radian per second
RPI	Rice protein isolate
rpm	Revolutions per minute
S	Svedberg unit (sedimentation coefficient)
s	second
S_0-ANS	Surface hydrophobicity
SDS	Sodium dodecyl sulphate
SEM	Scanning electron microscopy
SGF	Simulated gastric fluid
SIF	Simulated intestinal fluid

SPI	Soy protein isolate
U/ml	Enzyme activity in one millilitre
U_E	Electrophoretic mobility
V	Volume
v/v	Volume to volume
V_{Stokes}	Creaming velocity
W/O	Water-in-oil
w/w	Weight to weight
W_{lipid}	Average molecular weight of canola oil
wt	Weight
γ	Interfacial tension (mN/m)
ΔA	Interfacial area between oil and water
ΔG	Free energy
ε	Permittivity
η	Viscosity (Pa.s)
μl	Microliter
μm	Micrometer
ξ	Zeta potential (mV)
ρ	Density (kg/m^3)
τ_d	Doublet fragmentation time
τ_{sm}	Collision time

1. OVERVIEW

Emulsions are used in a wide range of applications within food and pharmaceutical sectors, spanning from margarines to salad dressings to encapsulation matrices for controlled delivery of bioactive compounds. They are comprised of two immiscible phases formed in the presence of mechanical shear and a stabilizing compound (e.g., emulsifier), where one phase becomes dispersed as droplets within a continuous phase of the other as either water-in-oil (W/O) or oil-in-water (O/W) emulsions. Depending on the properties of emulsion (e.g., droplet size, viscosity, etc.), they can have an impact on the appearance, mouth feel, taste, morphology/structure and overall quality of the food products. Emulsions can also be tailored to give unique controlled release properties for entrapped bioactive molecules. Within coarse emulsions, droplet size may range from a few hundred nanometers to several microns, however depending on the formulations these emulsions tend to be inherently unstable and will phase separate over time, thereby adversely impacting the products shelf life. In the recent years, research has focused on the use of natural emulsifiers (e.g., proteins) for clean label purposes and in the formation of nanoemulsions. The latter is a class of emulsions formed under extremely high shear conditions to produce droplets with average radii < 100 nm, which can give very stable emulsions and long shelf lifes (McClements, 2005; Mason et al., 2006). In contrast to coarse emulsions, nanoemulsions allow for increased bioavailability of entrapped compounds because of extremely high surface area of the nano-sized droplets used for delivery in the small intestine (Mason et al., 2006).

The overarching goal of this research is to develop O/W nanoemulsions stabilized using plant proteins that have long-term stability and the ability to deliver a lipophilic bioactive ingredient (e.g., omega-3 fatty acid rich canola oil). Although nanoemulsions have been previously stabilized using animal proteins (e.g., derived from milk), research in the use of plant proteins has been limited for stabilization purposes. Pulse proteins are considered as emerging plant-protein within the protein ingredient sector The protein ingredient industry looks to replace animal derived proteins over concerns about allergens, high costs, perceived consumer fears (e.g., prion disease), therefore the emerging market segments of plant proteins are based on consumer dietary, religious or moral preferences. Pulse proteins, such as proteins extracted from

lentil, also tend to have fewer allergen concerns than soy, and represent an excellent source of essential amino acids (Duranti, 2006). As a crop, production of pulses is considered low input because of nitrogen fixing ability that contributes to environmental sustainability. In the present research, lentil protein-stabilized nanoemulsions were prepared with canola oil, which has a high level of the mono- and polyunsaturated fatty acids and low level of saturated fatty acids, making it a heart healthy oil that helps to lower the risks of cardiovascular diseases and stroke (Lin et al., 2013; Gillingham et al., 2011). As the nanoemulsions were developed with 5 wt% oil, they are most suitable for use in beverage applications.

1.1 OBJECTIVES

To reach the overall research goal of the thesis, three objectives was explored, including:

- Investigate the effect of lentil protein concentration on the stability and flow behaviour of canola oil-in-water nanoemulsions prepared with multiple passes through a high-pressure homogenizer.
- Investigate the use of high-pressure homogenization to create sufficient shear to modify the protein (derived from lentil) structure, and to form nano-sized oil droplets needed to prepare stable nanoemulsions.
- Examine the lipid digestibility by measuring the release of free fatty acids from the lentil protein-stabilized nanoemulsions using an *in vitro* digestion model system.

1.2 HYPOTHESES

The following hypotheses was tested to support the above objectives:

- Higher lentil protein concentration will reduce the droplet size, but increase the viscosity of the nanoemulsions due to increased protein aggregation.
- The size of lentil protein-stabilized droplets will be reduced by modifying the lentil protein using a high shear pre-treatment. Shear-modified proteins will act as better emulsifiers due to increased surface activity as a consequence of partial denaturation of protein molecules.
- Lipid digestion and release behaviour of free fatty acids will be affected by the interfacial layer of shear-modified lentil proteins surrounding the oil droplet.

2. LITERATURE REVIEW

2.1 Emulsions and nanoemulsions

Emulsions are mixtures of two or more immiscible phases where one droplet is dispersed within the continuous phase of another, in response to mechanical shear and then stabilized in the presence of an emulsifier (McClements and Rao, 2011). They may be either oil-in-water (e.g., milk, cream and mayonnaise) or water-in-oil (e.g., butter and margarine) in nature and give different texture, structure and mouthfeel of the food (McClements and Rao, 2011). Emulsions can also be designed to be carriers of both hydrophilic and hydrophobic bioactive ingredients in functional foods, supplements or other applications where entrapment and control release properties are desired.

Emulsions are thermodynamically unstable systems because of their positive free energy as a consequence of an increase in dispersed phase interfacial area after homogenization (Walstra, 2003). Inherently, the emulsions have a tendency to destabilize via gravitational separation, flocculation, coalescence, and Oswald ripening as the system tries to minimize free energy and move towards a more thermodynamically favorable state (i.e., separation into two distinct phases). The stability of formed emulsions is thus related to the magnitude of free energy or the activation energy (ΔG^*). In other words, emulsions that are in their local state of minimum free energy must overcome a energy barrier to reach the most thermodynamically favorable condition (Walstra, 2003). Hence, they may exist as a kinetically stable or metastable systems for a long time. Furthermore, because of the constant movement of droplets by Brownian motion, gravity, the presence of external forces (e.g., environmetal factors, such as temoerature, pH and ionic strength) and various colloidal interactions, droplets may remain separated or aggregate together in solution to facilitate stability or instability, respectively (McClements, 2005).

Nanoemulsions are defined as emulsions that consist of droplets in the nanoscale size range where the average diameter is <200 nm (Mason, 2006; Rao and McClements 2011). Average droplet diameter for conventional emulsions, on the other hand, are generally considered to be in the range of >200 nm to several micrometer. In contrast to conventional

emulsions, nanoemulsions are more stable to gravitational separation because Brownian motion dominates the flow behaviour within the system, keeping the droplets dispersed and limiting cases of flocculation and coalescence (Mason et al., 2006; McClements and Rao, 2011). They also tend to be much less turbid or translucent than the opaque appearance of a conventional emulsion, as the nano-scale droplet are smaller than the wavelength of light and therefore scatter much less light (McClements and Rao, 2011). Although, in some instances nanoemulsions may appear opaque when the number of oil droplets increases due to high oil volume fraction or when the concentration and size of biopolymer and other ingredients (e.g., proteins) in the continuous phase increases (Graves, 2008; Chantrapornchai & McClements, 2002).

Formulations of O/W emulsions

In contrast to conventional emulsions, O/W nanoemulsions typically require high concentrations of both emulsifiers and co-emulsifiers, along with many other compounds to foster stabilization. For instance, within the dispersed phase, the oil may contain many non-polar ingredients such as: triacylglycerol, di- and monoacylglycerol, free-fatty acids, essential oils, mineral oils, fat substitutes, waxes, weighting agents, oil-soluble vitamins or various lipophilic bioactives (e.g., carotenoids, curcumin, phytosterols, phytostanols) (McClements and Rao, 2011). The composition of the oil phase will then have an influence on its polarity, solubility and viscosity, which will subsequently impact nanoemulsion stability (Wooster et al., 2008; McClements and Rao, 2011). In contrast, the continuous aqueous phase of a nanoemulsion also contains a number of polar and amphiphilic molecules such as, emulsifiers, proteins, carbohydrates, salts, acids and bases. These compounds can influence polarity, interfacial tension, viscosity, density, pH and ionic strength of the nanoemulsions, and subsequently can enhance or adversely affect stability (McClements and Rao, 2011).

In any case, emulsifiers are necessary components of nanoemulsions to prevent the oil and the aqueous phases from instantaneous separation by gravitational force, flocculation, and coalescence. The most common emulsifiers used during emulsion preparation are small molecule surfactants which are very effective even using low-energy approaches (e.g., spontaneous emulsification) (Lawrence et al., 2012; McClements & Rao, 2011). In contrast, protein-based emulsifiers require high-energy approaches (e.g., high-pressure homogenization or microfluidization) to obtain nano-sized droplets (McClements and Rao, 2011). Co-emulsifiers or

co-surfactants are surface active molecules (e.g., short or medium chain alcohols and propylene glycol), that are not able to stabilize emulsions themselves but act synergistically to reduce the interfacial tension alongside the emulsifier, improve solubility of the oil and helps facilitate droplet disruption and emulsion formation (Yaghmur et al., 2002).

Formation of nanoemulsions

There are many different methods for preparing nanoemulsions, and are usually divided into high- or low-energy approaches. High energy approaches need mechanical devices, such as high-pressure homogenizers or microfluidizers to apply intensive forces that are sufficient enough for the formation of nanoscale droplets. In contrast, low-energy methods are based on spontaneous emulsification that happens in the mixture of water-oil-surfactant when the composition of solutions or environmental condition is changed in a controlled manner (Qian and McClements, 2011, Tadros, 2004). For example, when oil volume fraction increases above 0.65 under high shear forces and in the excess of surfactant, a phase inversion happens (Meleson et al., 2004). In phase inversion temperature (PIT) method an O/W emulsion stabilized with non-ionic emulsifier is heated and at a certain temperature converts to W/O emulsion (Tadros, 2004).

In high-energy approach, the effectiveness of the homogenizer depends on the operating condition, such as energy intensity or pressure, and the type of homogenizer (Qian and McClements, 2011). High-pressure homogenizers generate high-shear stress to reduce the droplet size, whereas in microfluidizers the mixture flows through microchannels under very high-pressure and collide with each other creating small droplets under intense force. Microfluidizers are more effective at creating smaller droplets at certain emulsifier concentrations relative to high-pressure homogenizers (Pinnamanemi et al., 2003). By placing a coarse emulsion through multiple passes in a homogenizer, their polydispersity and average droplet size can be further reduced. Multiple passes allow larger droplets to be disrupted in the subsequent passes. The average droplet radius of an emulsion can also be reduced by: a) applying higher pressure to generate higher shear stress; b) raising the emulsifier concentration so that interfacial tension can be further decreased; or c) reducing the dispersed phase viscosity (Meleson et al., 2004). Droplet size of an emulsion also highly depends on the nature of the emulsifier. For instance, Qian and McClements (2011) found that average droplet size of emulsion stabilized with sodium dodecyl sulfate (SDS) was much smaller than that with β-

lactoglobulin. It was hypothesized that the β-lactoglobulin film is more resistant to disruption under shear and absorbs to the oil-water interface at a much slower rate than SDS, which allows re-coalescence of droplets leading to a larger droplet size (Qian and McClements, 2011).

The difference in the free energy (ΔG) between an inhomogeneous mixture of oil and water and a homogeneous emulsion is equal to the increase in the interfacial area between the oil and water phases (ΔA) multiplied by the interfacial tension (γ), given by the equation (McClements, 2005):

$$\Delta G_{formation} = \gamma \, \Delta A \qquad \text{[Eq. 2.1]}$$

When the surface area increases due to the formation of smaller droplets, the interfacial tension has to decrease to lower the amount of energy required for a new interface to form. By lowering the interfacial tension, unfavorable contacts between the two immiscible phases are minimized thus the free energy of the system is lowered, thereby increasing the stability of the emulsion. Interfacial tension can be reduced by increasing emulsifier concentration until the interface is saturated. Different types of emulsifiers have different surface activity, for example, the rate of decrease in interfacial tension happens at a lower concentration for proteins compared to small molecule emulsifiers because they can cover more surface area due their bigger size. However, small molecule emulsifiers lower the absolute value of interfacial tension more effectively compared to proteins (McClements, 2005).

2.2 Emulsion stability and destabilization mechanisms

The stability of nanoemulsions relates to how well the system can resist structural changes over time or in response to changes in the environmental or processing factors. According to the DLVO (Derjaguin, Landau, Verwey, Overbeek) theory for colloidal interactions, oil droplets remain stable when the repulsive electrostatic forces dominated over that of the van der Waals attractive forces. In contrast, droplet aggregation is favored when the van der Waals attractive forces dominate within the nanoemulsion. For protein stabilized oil-water interfaces, the magnitude of the electrostatic forces depends greatly on the intrinsic properties of the protein (e.g., amino acid profile, surface charge and hydrophobicity) and the extrinsic properties of the continuous phase (e.g., pH, salt concentration and temperature).

Stability of nanoemulsions can also be significantly impacted through steric forces arising from the presence of large protein at the oil droplet surface and depletion flocculation from excess unadsorbed proteins (McClements, 2005).

An emulsion can be destabilize by both physical and chemical processes. Physical instability is induced by the structural reorganization of emulsifiers at the oil-water interface caused by either flocculation, coalescence or Oswald ripening to form larger oil droplets, which then cream to the surface due to gravity induced separation eventually forming a distinct oil layer. In another instance, when the emulsifier is at insufficient quantities to support high phase volumes, a phase inversion can occur (McClements, 2005). In the case of chemical instability, the oil phase can be oxidized or protein hydrolysis may occur, leading to the breakdown of the oil-water interface (McClements, 2005). In the context of this research thesis, only the physical instability mechanisms are considered.

Gravitational separation

Nanoemulsions typically consist of at least two phases that have different densities and hence will separate because of gravitational forces acting upon them over time. Since oils are less dense than water, oil droplets within an O/W nanoemulsion will migrate upwards to form a cream layer, whereas, in the case of W/O nanoemulsions, water droplets will sediment to form an aqueous serum layer at the bottom. Gravitational separation is undesirable within nanoemulsions because it can induce undesirable changes to a product's appearance and texture. It also brings droplets closer together, which can lead to flocculation, coalescence and eventually complete separation of oil and aqueous phases (McClements, 2005). The creaming velocity of oil droplets in an O/W nanoemulsion can be calculated using the Stokes equation:

$$v_{Stokes} = 2gr^2 (\rho_2 - \rho_1) / 9\eta_1 \qquad \text{[Eq. 2.2]}$$

where, v_{Stokes} is the creaming velocity [Note: the sign of v (positive or negative) dictates whether the migration of droplets is upward (+) or downward (-)], g is the gravitational acceleration, r is particle radius, ρ_1 and ρ_2 are densities of the continuous and dispersed phases, respectively, and η is the viscosity of the continuous phase (McClements, 2005). The use of the Stoke's equation is advantageous from a practical standpoint since it allows factors or variables to be altered, in

order to develop strategies for reducing the rate of separation. For instance: 1) densities of the continuous and dispersed phases can be reformulated to reduce their differences; 2) decrease the droplet diameter by increasing energy input during homogenization or by reformulation of the emulsion itself; or 3) increasing the viscosity of the continuous phase by addition of non-adsorbed polysaccharides (Protonotariou et al., 2013). However, Stokes theory considers only very dilute nanoemulsions and describes the rate of sedimentation of a single droplet (Walstra, 2003). The theory fails to account for: 1) the influence of frictional forces between multiple droplets; 2) higher viscosities associated with absorbing polymers to the droplets; or 3) an increase in the effective volume and size associated with aggregated droplets. In contrast to the creaming behaviour within dilute nanoemulsions, creaming in more concentrated nanoemulsions can be completely retarded because of the close packing of droplets (McClements, 2005). Stokes theory also does not consider the Brownian motion of droplets, which favours a random motion in all directions and opposes gravity. Below a critical droplet diameter (70 nm), Brownian motion dominates gravity to prevent creaming.

Flocculation

Flocculation is a reversible form of aggregation where two or more droplets associate with each other but keep their individuality, and can separate with gentle shaking (Walstra, 2003). Flocculation can be defined as time between two collisions (τ_{sm} - collision time) and the time for doublet being broken into individual droplets (τ_d - doublet fragmentation time): if time between two collisions (τ_{sm}) is greater than doublet fragmentation time (τ_d) ($\tau_{sm} >> \tau_d$) then the flocculation is reversible. In the opposite case, when the time of doublet fragmentation is greater than the time of collision ($\tau_{sm} << \tau_d$), the flocculation is irreversible. If the attractive interactions between the droplets are strong and could not be re-dispersed into individual droplets, this type of flocculation it is called coagulation (Mishchuk et al., 2002; McClements, 2005). The result of flocculation usually shows as creaming and increase in the viscosity of the system due to irregular shape of flocculated droplets and increase in the effective droplet volume fraction. Flocculated nanoemulsions usually show a thixotropic flow behaviour at high droplet concentrations where apparent viscosity decreases with increase in shear rate (McClements, 2005). In highly concentrated nanoemulsions strongly flocculated oil droplets can lead to the

formation of a droplet network, which severely restrict flow behaviour and gravitational separation (McClements, 2005).

There are two types of flocculation: depletion and bridging flocculation. In the case of the former, non-adsorbed biopolymer (e.g., proteins or polysaccharides) within the continuous phase of O/W nanoemulsions create an attractive force between the droplets. As two droplets approach one another, these non-absorbed molecules are pushed out of the way to create an osmotic gradient between the biopolymer-depleted region between the droplets and the region rich with the biopolymers. Consequentially, the osmotic pressure causes the continuous phase between the droplets to flow towards the bulk solution, causing the droplets to come in closer proximity to each other (McClements, 2005). In the case of bridging flocculation, there may be insufficient molecules to completely cover the oil-water interface of an individual droplet, since it's absorbed to the interface of more than one oil droplets (McClements, 2005).

Coalescence

Coalescence is a process whereby two or more droplets come in close proximity to each other and fuse together to form one large droplet leading to increase in creaming and sedimentation rates (Walstra, 2003). Coalescences occurs in three stages: 1) droplet formation, 2) film thining, and 3) film rupturing. When droplets are in close contact with each other, they might remain as spheres or have their surface become flattened (Walstra, 2003). Droplets will start to deform when the external forces, such as mechanical stress, are greater than the internal forces that are keeping the droplet in its spherical shape. During deformation, the film thickness at the O/W interface is stressed, causing emulsifiers to be dragged along the surface leaving gaps within the viscoelastic film. These gaps will then rupture due to hydrophobic forces arising between the disperse oil phases allowing for the exchange of material and the formation of a large droplet (Walstra, 2003; McClements, 2005).

Ostwald ripening

Ostwald ripening is a diffusion of dispersed phase molecules from smaller to a larger droplet through the continuous phase because of the higher Laplace (internal) pressure in the smaller droplets. It is the only destabilization mechanism that is more pronounced for smaller droplets than the larger ones, hence nanoemulsions are more susceptible to destabilization by

Ostwald ripening compared to conventional emulsions. However, in O/W nanoemulsions containing triacylglycerols as dispersed phase, Ostwald ripening is negligible because they are virtually insoluble in the water (Walstra, 2003).

2.3 Proteins as emulsifiers

Proteins are comprised of long polymers of amino acids joined together by peptide bonds, and folded into higher ordered (i.e., secondary, tertiary and quaternary) structures. They are held together by van der Waals attractive forces, hydrophobic and electrostatic interactions, and hydrogen and disulfide (in some cases) bonds. Proteins may be globular [e.g., proteins derived from pulses (lentil, pea, chickpea and faba bean), milk (whey and casein) or egg (ovalbumin)] or fibrous (e.g., gelatin) in nature. Both hydrophilic and hydrophobic amino acid moieties are exposed at the surface of protein molecules allowing them to act as an effective emulsifier because of their surface chemistry. During emulsification, proteins migrate to the oil-water interface from the bulk solution, absorb to the interface and then orient or unfold to position its hydrophobic amino acids towards the dispersed oil phase and the hydrophilic amino acids towards the aqueous continuous phase (Damodaran, 2005). The absorption process acts to lower the interfacial tension and decrease the energy required to form the droplets (Walstra, 2003). Once the proteins are on the interface, they further aggregate to form a viscoelastic film. In the case of globular-type proteins, diffusion to interface is slow, however once the film is formed they remain quite stable due to the presence of thick interfacial layer. In the case of a fibrous protein, such as gelatin, or an open protein with little higher-ordered structure (e.g., casein), migration to the oil-water interface tends to be faster, however the film is less thick.

The oil droplets-stabilized by proteins take on properties of the protein itself in terms of their charge, response to pH and salts. At solution pHs that are away from the proteins isoelectric point (pI), the oil droplets take on a net positive or negative charge (depending whether the pH is < or > pI, respectively), which provides stability through electrostatic repulsive forces (Lam & Nickerson, 2015). In contrast, at solution pH near the pI, oil droplets assume no net charge and flocculation, aggregation and coalescence ensues (McClements, 2004; Lam & Nickerson, 2015). The addition of salts to an emulsion can function in the same way as moving the solution pH close to the proteins pI, by screening the thickness of the electric double layer to promote droplet-droplet aggregation according to the DLVO theory (Keowmaneechai &

McClements, 2002). In contrast, low molecular weight emulsifiers (e.g., lecithin, phospholipids, polyoxyethylene (20) sorbitan monolaurate or Tween 20) diffuse rapidly to the oil-water interface and forms a thin interfacial film around the oil droplet leading to smaller droplet formation but poorer long-term stability than proteins (McClements, 2005).

Chang et al. (2015) investigated the effect of acidic and natural pH (3, 5, and 7) on the physicochemical, interfacial and emulsifying properties of pea, lentil, canola and soy protein isolates in coarse emulsions. The authors reported that the emulsifying properties of all proteins studied were improved at pHs away from the pI of the protein isolate where electrostatic repulsion dominated. Emulsifying properties were found to be the greatest for all proteins at pH 3, followed by pH 7 and then minimum at pH 5 (which was close to the pI value). The authors also reported that at pH 3, protein surface hydrophobicity were the greatest relative to the other pHs, while droplet size was the smallest. For solubility, it was found that for lentil, pea and soy proteins the values were similar at pH 3 and 7. Although at pH 7, proteins were able to lower interfacial tension better than at the other pHs, the viscoelastic film formed was weak. Interfacial rheology at the different pHs for all of the protein isolates indicated that pH 3 produced the strongest films to give the highest emulsion stability. At pH 3, the canola and lentil protein isolates have showed better emulsifying properties than pea protein isolates, and also had greater solubility and hydrophobicity. Solubility of lentil protein was Lentil protein had higher surface hydrophobicity than pea, soy or canola protein, at the pH 3, thereby it was able to form the most viscoelastic film that contributed to the long-term stability of the emulsion.

Proteins are typically used to stabilize coarse emulsions rather than nanoemulsions. The large size of protein molecules and subsequent slower diffusion to the interface during homogenization can lead to poor coverage of oil-water interface and a greater tendency to coalesce. As such, proteins are often modified in some capacity prior to use as stabilizers for nanoemulsions. For instance, ultrasonication has been previously used to improve solubility of soy protein isolate (SPI) by partial unfolding and reduction in intermolecular interactions thereby increasing free sulfhydryl group and surface hydrophobicity (Hu et al., 2012). Lee et al. (2016) studied the functional properties of nano-scale soy protein aggregates generated by an acidic (pH 2-4) or alkaline (pH 9-12) treatment accompanied with ultrasonication to break down the protein into smaller sized units. O'Sullivan et al. (2015) studied the effect of ultrasonication on the structural, physical, and emulsifying properties of animal (bovine gelatine (BG), fish gelatine

(FG), egg white protein (EWP)) and plant (pea protein isolate (PPI), soy protein isolate (SPI), rice protein isolate (RPI)) proteins. Ultrasound treatment reduced the protein size for most of the proteins studied and reduced the droplet size in the emulsion for BG, EWP, and PPI compare to untreated protein solutions. Jiang et al. (2014) investigated the effect of ultrasound treatment on the structure and physical properties of black bean protein isolate (BBPI). The analysis of fluorescence spectra showed changes in tertiary structure of ultrasound treated proteins. Moreover, the charge, hydrophobicity and solubility increased due to breaking of intramolecular hydrophobic bonds. Arzeni et al. (2012) studied the functionality and emulsifying properties of egg white protein (EWP) treated with high intensity ultrasound. After high intensive ultrasound treatment the surface hydrophobicity increased and the initial droplet size of emulsion was smaller compared to untreated one.

Can Karaca et al. (2011) studied the emulsifying and physicochemical properties of chickpea (ChPI), faba bean, lentil (LPI) and pea (PPI) protein isolates produced by salt extraction or isoelectric precipitation when used in a coarse emulsion. The authors reported that the isolate production method had a significant effect on the emulsifying and physicochemical properties. Isolates produced by isoelectric precipitation had higher surface charge and solubility than isolates generated by salt extraction because the isolate preparation conditions affect the protein structure differently which influence the exposure of hydrophilic and hydrophobic groups. The highest surface charge and solubility was observed for ChPI and LPI prepared by isoelectric precipitation, which formed the smallest droplet size that was more stable to creaming. LPI formed the smallest droplet size among the isolates prepared by salt precipitation. In another study Can Karaca et al. (2011) reported optimization of formulation and processing condition of chickpea and lentil protein-stabilized emulsions. The emulsions were prepared at different conditions; pH (3.0 – 8.0), protein concentrations (1.1 – 4.1 wt%) and oil volume fractions (20 – 40%) and their droplet charge, size and the creaming stability were analysed. Both proteins showed the highest surface charge, smallest droplet size and the best creaming stability at pH 3 or 8, protein concentration of 4.1 wt% and oil volume fraction of 40%.

In the present study, lentil protein isolate was chosen to stabilize nanoemulsions at pH 3 building on the work by Chang et al. (2015) on coarse emulsions. Lentil protein is dominated by salt soluble globulin proteins: legumin and vicilin. The former is classified as an 11S (S is a Svedberg Unit) hexamer protein with a molecular mass of 350-400 kDa (Jarpa-Parra et al.,

2015). Each subunit is comprised of an acidic α-chain (molecular mass ~40 kDa) and a basic β-chain (molecular mass ~20 kDa), which are held together by a disulfide bond (Barbana & Boye, 2011; Oomah et al., 2011). The six subunits within the hexamer structure are held together by non-covalent interactions. Vicilin is a 7S trimeric protein with a molecular mass of ~150 kDa. Each trimer is ~50 kDa and has no disulfide bond to stabilize the structure, allowing it to unfold easier upon processing or at the oil-water interface than legumin (Dagorn-Scaviner et al., 1987; Oomah et al., 2011). The use of lentil protein as a stabilizer in nanoemulsions has not yet been explored despite its excellent emulsifying properties exhibited in coarse emulsions.

2.4 Protein pre-treatment for improved emulsification

The formation and stability of emulsions highly depends on the emulsifier characteristics. To prevent flocculation and coalescence it is crucial that emulsifier is immediately adsorbed at the freshly created oil droplet interface, as well as its ability to provide a strong steric and/or electrostatic repulsive force. Proteins possess good emulsifying property due to their amphiphilic nature but they tend to migrate slowly to the oil/water interface because of large molecular weight compared to low molecular weight emulsifiers. Surface hydrophobicity of proteins also affects their emulsifying property. A high value of surface hydrophobicity may lead to increase in protein aggregation and decrease in solubility, while a low value would lead to weak adsorption at the oil droplet interface and poor emulsion stability. Therefore, right balance of the hydrophobic/ hydrophilic amino acids is important for the formation and stability of emulsions (McClements, 2017).

In general, seed storage proteins are larger in size compare to many of the animal proteins and have globular conformation with hydrophobic groups buried inside, therefore a certain degree of unrevealing is needed to improve their emulsification property (Day, 2013). It has been demonstrated that some plant proteins provide very stable emulsions against coalescence compared to animal proteins due to the formation of a thicker film. For example, Wong et al. (2011) showed that deamidated wheat gliadins formed 18 nm thick interfacial layer, while for heat-treated soy protein, it was 30 – 40 nm (Keerati-U-Rai & Corredig, 2010). On the other hand, β-lactoglobulin (a dairy protein) was found to form only 3.6 nm thick interfacial layer (Zhai et al., 2011). Plant proteins such as, chick pea, faba bean, lentil and pea can be a good alternative to

animal proteins but their functional properties are still not fully understood (Can Karaca et al., 2011).

Protein unrevealing or even dissociation into smaller subunits can be stimulated by chemical, enzymatic (Tavano, 2013) or physical (Messens, 1997) modifications which can increase in the charge, enhance the solubility by lowering the molecular weight and improve the surface activity by the exposure of hydrophobic domains. Chemical and enzymatic modification involves protein hydrolysis by cleavage of peptide bonds. Chemical hydrolysis is nonspecific and it is more difficult to control the extent of hydrolysis, besides the use of chemicals and extreme reaction conditions may not be acceptable for human consumption. On the other hand, enzymatic hydrolysis is more specific and the degree of hydrolysis (DH) is easier to control, but the complex food matrix may contain enzyme inhibitors that can affect the DH (Tavano, 2013). Zhao et al. (2011) reported that enzymatic hydrolysis (DH > 10%) improved the solubility of peanut protein isolate because of the formation of soluble peptides with charged amino acid residues. An increase in surface hydrophobicity was also observed due to the exposure of hydrophobic domains but the emulsification properties were decreased. Severin et al. (2006) reported a decrease in emulsification properties of whey protein concentrate (WPC) with an increase in DH from 5 to 20%. Although solubility of WPC was increased due to lower molecular size as a result of hydrolysis, the proteins were not able to form a strong viscoelastic film at the oil/water interface. It was proposed that hydrolysis significantly increased net charge on the protein, which prevented protein-protein interactions at the interface due to repulsive forces. Avramenko et al. (2013) investigated limited enzymatic hydrolysis (DH 4, 9 and 20%) on the physicochemical and emulsifying properties of lentil protein isolate (LPI). The surface charge on the protein did not change with the increase in DH, but their surface hydrophobicity significantly decreased. According to their explanations, exposure of hydrophobic groups after hydrolysis of LPI caused aggregation of the peptides due to hydrophobic interaction and buried them again into large hydrolyzed particles. Interfacial tension was lower for the hydrolysed LPI solutions due to improved solubility and migration to the oil-water interface; however the emulsification properties decreased for all hydrolysed LPI solutions due to low surface hydrophobicity which caused weaker attachment to the oil-water interface.

High-pressure treatment of proteins usually does not cause break down of their covalent bonds but affects the hydrophobic and electrostatic interaction and hydrogen bonds which are

involved in stabilizing quaternary, tertiary and secondary structures of a protein (Messens, 1997). High-pressure treated proteins change their conformation from native to a different degree of denaturation which depends on pressure level, cycles, treatment time, temperature, pH and ionic strength (He et al., 2016). Quaternary and tertiary structure can be affected at pressure less than 300 MPa (Silva & Weber, 1993), while modifications in secondary structure occurs at higher pressures, from 300 to 700 MPa (He et al., 2016; De Maria et al., 2016). He et al. (2016) studied the effect of high-pressure treatment on the structural and functional properties of bovine lactoferin (LFb). The protein was processed at 300 – 700 MPa, at pH 4 or 6, for 30 or 60 min. Modifications happened at 400 MPa for 30 min, or 300 MPa at 60 min at pH 4, resulting in partial denaturation of LFb with significantly modified tertiary structure and looser secondary structure. The surface charge of LFb increased from around +15 to +30 mV which improved protein solubility, foaming and emulsifying properties due to higher electrostatic repulsion of LFb stabilized droplets. In contrast, at higher pressure and treatment time the foaming and emulsification abilities of LFb were decreased. For 700 MPa, 30 min treated LFb the droplet surface charge decreased to around +10 mV and average droplet size increased from 275 to 350 nm. While for 700 MPa, 60 min treatment average droplet size increased to 470 nm, which was ascribed to the lack of electrostatic repulsion, causing the droplets to coalesce.

De Maria et al. (2016) studied the effect of high-pressure treatment on the structural and functional properties of bovine serum albumin (BSA) at 50 and 100 mg/ml concentrations at 100 – 500 MPa for 15 or 25 min. At 100 - 400 MPa pressure an increase in the number of sulfhydryl groups involved in the stabilization of tertiary and secondary structure was observed. This unfolding of BSA improved the foaming and emulsifying ability. In contrast, pressures above 400 MPa for 15 min or 300 MPa for 25 min decreased the number of sulfhydryl groups due to disulfide bonds formation which caused aggregation of BSA and reduction in the foaming and emulsifying ability. Formation of protein aggregates was observed at a higher concentration due to increased interaction between the protein molecules.

Molina et al. (2001) studied the effect of high-pressure treatment on the emulsification properties of soy protein isolate (SPI). At 400 MPa the hydrophobicity of 7S fraction was at the highest level with maximum emulsifying activity due to disruption into subunits and exposure of the hydrophobic groups. On the other hand, surface hydrophobicity of 11S fraction decreased at 400 MPa due to re-aggregation because of the disulfide bond formation. These results showed

that high-pressure treatment of SPI improved the emulsifying activity but decreased emulsion stability. Similar results were reported by Wang et al., (2008) who also studied the effect of high-pressure treatment on the physicochemical properties of soy protein. They found that at 200 MPa treatment number of sulfhydryl (SH) group increased, indicating unraveling due to disruption of disulfide bonds. At higher pressures above 200 MPa, the number of SH groups decreased due to re-aggregation and formation of disulfide bonds and hydrophobic interactions. Treatment at 200 MPa improved emulsifying activity because of exposure of hydrophobic groups and better surface activity of protein but it decreased emulsion stability because of loss of flexibility. Donsi et al. (2010) developed pea protein stabilized nanoemulsions with the droplet size less than 200 nm. They reported that high-pressure treatment (100 – 300 MPa) caused changes in a protein structure by disruption of disulfide bonds, which affected the exposure of hydrophobic groups. Keerati-U-Rai & Corredig (2009) investigate the effect of high-pressure homogenization (HPH) on the aggregation state of soy protein. The soy protein dispersion was homogenized at 26 and 65 MPa (equivalent to 3,770 and 9,427 psi). It was demonstrated that HPH caused disruption of soy protein aggregates and that glycinin (11 S) was more affected by HPH than β-conglycinin (7S). No further changes occurred after the pressure increased from 26 to 65 MPa, which indicates that 26 MPa pressure was sufficient to disrupt soy protein aggregates.

In the present research LPI solutions were high-pressure homogenized at two different pressures (5,000 and 15,000 psi for 6 cycles) prior to using them in the emulsification with canola oil. The long-term stability, droplet size distribution, flow behaviour and microstructure of the nanoemulsions made with modified LPI solutions were compared with the nanoemulsions made with unmodified LPI.

2.5 Nanoemulsions as a delivery medium for lipid bioactive ingredients

Nanoemulsions are now being considered in controlled release applications for the delivery of lipophilic bioactive compounds (e.g., beta-carotene, curcumin and oil soluble vitamins) or oils rich in omega-3 fatty acids (Sagalowicz and Leser, 2010; McClements, 2010). Depending on the use of protein and other ingredients in the formation of oil droplets, different external cues can be used to trigger their destabilization and release of internal bioactives. For instance, the droplet interface can be designed to protect the entrapped core material during transit through the highly acidic condition of stomach, and then release upon change in pH in the

small intestines, or in response to certain enzymes found in the gastrointestinal tract (Acosta, 2009; Norton, 2015). The release of the bioactive ingredient can also be controlled by altering the thickness and hence, the permeability of the interfacial layer. The presence of nano-sized droplets also acts to enhance the bioavailability of the entrapped active ingredient. The smaller droplet size provide larger surface area for the digestive enzymes to act, and can also be adsorbed directly into the bloodstream by passing through the gaps in-between the epithelium cells of the intestine wall (Acosta, 2009; McClements and Rao, 2011). Wang et al. (2008) compared the activity of curcumin delivered through an O/W coarse emulsion with a droplet size of 618 nm to a nanoemulsion with a droplet size of 80 nm, both stabilized with Tween 20. The anti-inflammation activity of curcumin was enhanced when the nanoemulsion was administered to the mice with ear edema relative to the coarse emulsion. The digestibility of protein-stabilized nanoemulsions is typically assessed using *in vitro* methods, as *in vivo* animal studies are costly and require numerous regulatory and ethics approval to undertake. *In vitro* method simulates the biochemical conditions and reactions of the human gastrointestinal (GI) tract, for instance pH, ionic strength, enzyme activity, temperature of the mouth, stomach or small intestine (McClements & Li, 2010).

In this study, nanoemulsions were prepared with canola oil. Canola oil is an excellent source of monounsaturated fatty acids (MUFA) and ω-3 polyunsaturated fatty acids (PUFA) linolenic acid, and it is low in saturated fatty acids (Gillingham et al., 2011). Many studies showed that canola oil-based diet reduced low-density lipoproteins in serum, increased tocopherol levels and improved insulin sensitivity compared to other sources of fats which have a positive effect on the prevention of cardiovascular diseases (Lin et al., 2013; Gillingham et al., 2011).

2.6 *In vitro* lipid digestion

Digestion is a complex process of physicochemical and enzymatic reactions. *In vitro* digestive models are meant to imitate physiological conditions of the GI tract. Compared to *in vivo* studies on live animals or humans, *in vitro* models are cheaper and easier to perform because there are no ethical issues and exclude the biological differences between individuals (Sing & Sarkar, 2011). In recent years, many studies have investigated how emulsion structure influences lipid digestibility. When emulsions are exposed to different conditions during transit

through the GI tract their stability, droplet size and the composition of oil droplet interfacial layer (thickness and surface charge) are significantly affected (Golding & Wooster, 2010). For instance, in the mouth, emulsions are exposed to shear forces (~100 s^{-1}), enzymes (e.g., amylases, lipases), proteins (e.g., mucins), changes in temperature (37^{o}C), pH (7.1-7.5) and ionic strength, all of which can act to destabilize protein-stabilized interfacial layers (Siletti, 2007; Sing & Sarkar, 2011). In the stomach, emulsions are exposed to acidic pH conditions (pH 1.5-3.5) and digestive juices containing enzymes (e.g., pepsin) and electrolyte salts which can also act to breakdown protein-stabilized interfacial layers to promote flocculation and coalescence of oil droplets (Sing & Sarkar, 2011). In the intestine, most of the lipid digestion happens due to the secretion of pancreatic lipase from the pancreas and bile salts from the gall bladder. The bile salts act to displace the protein from the oil droplets surface to allow lipase and co-lipase adsorption and start lipolysis. The triacylglycerols are then hydrolysed to monoacylglycerols and free fatty acids (Maldonado-Valderrama et al., 2011).

Furthermore, the physicochemical properties of emulsions have also been found to influence lipid digestibility in the GI tract. Many studies have shown that emulsions with smaller droplet sizes have higher lipid digestibility due to their larger surface area. Armand et al. (1999) reported that individuals who ingest emulsions with droplet size of 10 μm had lower blood lipids, measured over a 7 h period relative to individuals who ingested emulsions with 0.7 μm droplet sizes. The authors explained this is due to better accessibility of the lipase at the oil droplet interface because of the higher surface area. Salvia-Trujillo et al. (2017) demonstrated in an *in vitro* study that the rate of lipid digestion was faster in emulsions with small droplet sizes. The thickness of the interfacial layer has also been shown to impact lipid digestion. Lee et al. (2011) investigated lipid digestibility from β-lactoglobulin-stabilized conventional emulsions (average droplet size 325 nm) prepared with homogenization and nanoemulsions (average droplet size 66 nm) prepared with homogenization followed by solvent evaporation. Lipid digestibility in the nanoemulsion was slower than in the conventional emulsion because of the thicker interfacial layer surrounding the droplets in the nanoemulsion. It was proposed that the β-lactoglobulin protein layer became thicker when the oil droplets shrank during solvent evaporation, making it less susceptible to bile salt displacement and lipase actvity.

The nature of the surfactant and the type of oil present within the emulsion also play a significant role in lipid digestion. Mun et al. (2007) investigated the influence of emulsifier type

on the *in vitro* lipid digestibility of sodium caseinate, whey protein isolate (WPI), lecithin and Tween 20 stabilized emulsions. The release of free fatty acids (FFA) was measured in the absence and presence of bile salts. In the presence of bile salts, the release of FFA increased for all emulsions, but larger difference was observed for Tween 20 stabilized emulsion and the smallest for sodium caseinate stabilized emulsions. The results suggested that the emulsifier displacement from the oil droplet surface was significantly affected by the nature of emulsifier, which can influence the rate and extent of lipid digestibility. Maldonado-Valderrama et al. (2012) studied *in vitro* gastric digestion of β-lactoglobulin-stabilized emulsions containing two types of oil (tetradacane and olive oil). The viscoelasticity of the olive oil-water interface decreased to a greater extent upon addition of pepsin compare to the tetradecane-water interface. Also the digestibility of β-lactoglobulin in olive oil emulsions was higher than that for tetradecane emulsions. Only 24% of β-lactoglobulin remained intact at the olive oil-water interface while 47% of protein remained at the tetradecane-water interface. The authors proposed that β-lactoglobulin at the tetradecane-water interface had more hydrophobic groups turned into the oil phase due to lower polarity of tetradecane compare to olive oil. In contrast, β-lactoglobulin at the olive oil-water interface had bigger portion of the molecule oriented towards the water phase than the oil phase, thereby making β-lactoglobulin more exposed to hydrolysis by pepsin.

In this study lipid digestibility of the LPI-stabilized nanoemulsions were determined using *in vitro* stomach and intestine digestion as a function of LPI concentration and whether the proteins were modified prior to emulsification. The mechanism of lipid digestibility as influenced by protein modification was also investigated using interfacial shear rheology measurements of the LPI at the oil-water interface.

3. EFFECT OF LENTIL PROTEIN ISOLATE CONCENTRATION ON THE FORMATION, STABILITY AND RHEOLOGICAL BEHAVIOUR OF OIL-IN-WATER NANOEMULSIONS[1]

3.1 Abstract

The formation and stability of nanoemulsions as a function of lentil protein isolate (LPI) concentration (0.5 to 5.0 wt%) at pH 3.0 was investigated over a four-week period. The nanoemulsions were characterized by droplet size distribution, zeta potential, rheology and microstructure. The long-term stabilization potential of the nanoemulsions was determined in a photocentrifuge using accelerated gravitation. All nanoemulsions, except 1 wt% LPI, showed bimodal droplet size distribution (DSD) where the larger diameter peak was ascribed to protein aggregates and entrapped oil droplets. After 28 days DSD shifted towards the larger diameter peak, indicating formation of a stronger protein network with time. The average droplet size for all nanoemulsions measured from the lower diameter peak of DSD ranged from 300 nm to < 200 nm, which did not change over time. Nanoemulsions with 0.5 wt% LPI phase separated over 28 days. Stable flowable nanoemulsions were formed at 1-2 wt% LPI concentrations. All nanoemulsions showed shear thinning behaviour and the storage moduli (G′) higher than the loss moduli (G″) in the low strain regime of oscillatory strain sweep measurements, indicating structure formation in the quiescent state. Nanoemulsions with 3 and 5 wt% LPI formed strong non-flowable gel which showed a two-step yielding behaviour, first by rupturing the interconnected clusters of protein aggregates and oil droplets at the G′ and G″ crossover, and then by the break down of the individual aggregates of proteins and oil droplets into fine dispersions at a higher strain. This study demonstrated that lentil protein has a potential to be utilized as an emulsifier in the development of stable nanoemulsions, as well as in the formation of emulsion gels at higher LPI concentrations.

[1] Published in Food Chemistry 237 (2017) 65 - 47

3.2 Introduction

An emulsion is a mixture of two or more immiscible liquids where one phase is dispersed within the continuous phase of another in the presence of an emulsifier and with the help of mechanical energy. Emulsifiers are important in the reduction of interfacial tension between two immiscible phases, which reduces energy required to form an emulsion. They also adsorb on the freshly-formed droplet surface and provide stability against coalescence. Proteins make excellent emulsifiers as their amphiphilic nature (i.e., presence of hydrophobic and hydrophilic amino acid) enable them to become surface active, to align and aggregate at the oil-water interface to form stabilizing films. In general, during emulsion formation, proteins migrate from the bulk solution to the interface, where it absorbs and re-aligns to position its hydrophobic amino acids towards the apolar phase and the hydrophilic amino acids towards the polar phase (Damodaran, 2005; Dickinson, 1994). Proteins then aggregate to form an interfacial viscoelastic film. Improved stabilization of protein-stabilized emulsions against flocculation and coalescence occurs through electrostatic repulsive forces arising from the interfacial film at pH's away from the protein's isoelectric point, through steric stabilization and an increases in the continuous phase viscosity from un-absorbed proteins (McClements, 2004). In the case of globular-type proteins (e.g., seed storage protein such as from lentil), diffusion to the interface is relatively slow, however once the film is developed, the emulsion remains quite stable due to the presence of the thick interfacial layer (Wilde et al., 2004). In the case of a fibrous protein (e.g., gelatin), migration to the oil-water interface tends to be faster, however the interfacial film is less thick and more susceptible to rupturing (Lobo, 2002). In contrast, low molecular weight synthetic emulsifiers (e.g., phospholipids, polyoxyethylene sorbitan monolaurate (Tween 20)), diffuse rapidly to the oil-water interface and forms a thin interfacial film around the oil droplet producing smaller droplet sizes, but poorer stability under long-term storage conditions (McClements, 2005). Proteins, being natural products, are of high demand for their use in emulsion stabilization for food application. Among the various types of proteins, plant proteins have recently become particularly popular for their ability to replace animal proteins and synthetic emulsifiers (Lam & Nickerson, 2013).

Chang et al. (2015) investigated the effect of pH (3, 5, and 7) on the physicochemical, interfacial and emulsifying properties of protein isolates obtained from pea, lentil, canola and soy in coarse emulsions. The authors reported that the emulsifying properties were the greatest for all

proteins at pH 3 and followed by pH 7 and then pH 5 (closer to their isoelectric point). At pH 3, protein solubility and surface hydrophobicity was higher relative to the other pHs. Further, the lentil protein isolate (LPI) at this pH was found to have higher surface hydrophobicity compared to the other proteins studied, and formed the strongest interfacial viscoelastic film among the pulse proteins. Can Karaca et al. (2011) studied the emulsifying and physicochemical properties of chickpea (ChPI), faba bean, lentil and pea protein isolates (PPI), produced by isoelectric precipitation and salt extraction in coarse emulsions. The authors reported that isolates produced by isoelectric precipitation had higher surface charge and solubility than the isolates generated by salt extraction, and that ChPI and LPI extracted by isoelectric precipitation produced the most stable coarse emulsions against creaming.

Nanoemulsions are similar to coarse emulsions but are formed using high-pressure homogenizers, microfluidizers or using solvent evaporation techniques to produce droplets with radii <100 nm (McClements & Rao, 2011). The majority of research in the literature involving protein-stabilized nanoemulsions has involved dairy proteins such as casein (Dickinson et al., 2003; Surh & McClements, 2008; Ye, 2008) and whey proteins (Euston et al., 2000; Reiffers-Magnani et al., 2000; Ye, 2008) with very limited work involving plant proteins. Donsi et al. (2010) developed pea protein stabilized nanoemulsions (average droplet diameter <200 nm) using high-pressure homogenization. The authors reported that the homogenization process altered the protein's quaternary and tertiary structure by disrupting disulfide bonds to allow for a partial unraveling of its composition to expose a greater amount of hydrophobic sites. Yerramilli et al. (2017) investigated the use of PPI to partially replace sodium caseinate in the formation and stabilization of nanoemulsions and showed an improved stability against depletion-induced destabilization. Other researchers have also developed plant protein-stabilized emulsions with droplets size in the range 200 – 500 nm (Fernandez-Avila et al., 2016; Liang & Tang, 2013; Peng et al., 2016). However, plant protein-stabilized nanoemulsions with droplet size in the range of < 200 nm are rarely reported in the literature.

In the present study, oil-in-water nanoemulsions was stabilized by LPI at pH 3, building on the initial work by Chang et al. (2015). Lentil protein is dominated by two types of globulin proteins: legumin and vicilin. The former is classified as an 11S (S is a Svedberg Unit) hexamer protein with a molecular mass of 350-400 kDa, with each subunit being comprised of an acidic α-chain (molecular mass ~40 kDa) and a basic β-chain (molecular mass ~20 kDa) held together

by a disulfide bond (Barbana & Boye, 2011; Jarpa-Parra et al., 2015; Oomah et al., 2011). In contrast, vicilin is a 7S trimeric protein with a molecular mass of ~150 kDa. Each trimer of vicilin is ~50 kDa in mass, and contains no disulfide bridging, allowing it to unfold easier during processing or at the oil-water interface than legumin (Dagorn-Scaviner et al., 1987; Oomah et al., 2011).

The overall goal of this study is to investigate the effect of LPI concentration on the formation and stabilization of O/W nanoemulsions using high-pressure homogenization and to identify the best formulation to produce the smallest sized droplets with the greatest stability. To our knowledge, no study so far has reported development of O/W nanoemulsions with LPI as the sole emulsifier.

3.3 Materials and methods

3.3.1 Materials

Lentil protein isolate (protein content 79.5% w/w, w.b.) was kindly provided by POS Bio-sciences (Saskatoon, SK, Canada), that was produced by alkaline extraction followed by isoelectric precipitation and spray dried at pilot scale. Canola oil (containing 0.7 g omega-3 fatty acid per 10 ml of oil) used in this study was purchased from the local supermarket (Saskatoon, SK, Canada). The citric acid was purchased from VWR International (Edmonton, AB, Canada), whereas all other chemicals were purchased Sigma-Aldrich (St. Louis, MO, USA) and were of reagent grade.

3.3.2 Preparation of lentil protein solutions

Lentil protein solutions were prepared by dispersing the protein powder at different concentrations (0.5, 1, 1.5, 2, 3, and 5 wt%) based on the protein content, in a 0.1 M citrate buffer (pH 3) using a magnetic stirrer at 500 rpm for 24 h at room temperature (22-23 ^{o}C). To prevent the microbial spoilage in the emulsions, an antimicrobial agent (0.02 wt% sodium azide) was added to each protein solution. Chang et al. (2015) reported the solubility of the LPI at pH 3 as 56.2 ± 0.62 %.

3.3.3 Preparation of nanoemulsions

Nanoemulsions were prepared by adding 5 wt% canola oil to 95 wt% of the protein solutions (0.5 to 5 wt%), mixing with a rotor-stator blender (Polytron, Brinkman, ON, Canada) to form a coarse emulsion, followed by homogenization using a high-pressure homogenizer (Emulsiflex C3, Avestin Inc., Ottawa, ON, Canada) at 20,000 psi (equivalent to 137.9 MPa) for 6 cycles. The temperature of the emulsions during homogenization reached to ~60 ºC. The stability of the nanoemulsions was recorded for 28 d (4 weeks). All nanoemulsions were prepared in triplicate.

3.3.4 Droplet size distribution

Droplet size and distribution was measured using a static laser diffraction particle size analyzer (Mastersizer 2000, Malvern Instruments, Montreal, QC). The volume-weighted mean droplet diameter (d_{43}) and the size distribution were determined immediately after the preparation of the nanoemulsions and as a function of time (0, 7, 14, and 28 d). For more accurate measurement of individual un-flocculated droplet size, all samples were first diluted (1:5) with a 0.5 wt% Tween 20 in 0.1 M citrate buffer (pH 3) solution before measuring their droplet size.

3.3.5 Zeta potential

Surface charge or zeta potential of the oil droplets were determined using a Zetasizer Nano-ZS90 (Malvern Instruments, Westtborough, MA, USA) by measuring the electrophoretic mobility (U_E) of the LPI-coated droplets in a buffer solution (pH 3) (1 drop of emulsion added to 100 ml of citric buffer) in an electric field of where the droplets move towards the oppositely charged electrode. Zeta potential (ζ, mV) was determined by measuring the electrophoretic mobility (U_E) and then applying Henry's equation:

$$U_E = \frac{2\varepsilon \times \zeta \times f(k\alpha)}{3\eta} \quad \text{(eq. 3.1)}$$

where ε is the permittivity (F (Farad)/m), f (kα) is a function associated with the ratio of the particle radius (α) to the Debye length (k) and η is the viscosity (mPa·s) of the solution (water, 1 mPa.s). The Smoluchowski approximation f (kα) for this study was set to 1.5. Zeta potential was measured as a function of time (0, 7, 14, and 28 d) for all nanoemulsions stabilized with different LPI concentrations.

3.3.6 Accelerated gravitational separation

Long-term stability of the nanoemulsions was analyzed using a photocentrifuge dispersion analyzer (LUMiSizer, LUM Americas, Boulder, CO, USA) to determine the instability index as a function of time (0, 7, 14, and 28 d). In brief, 400 μL of freshly prepared nanoemulsions was transferred into 8 mm × 2 mm rectangular polycarbonate cuvettes and centrifuged at 2000g for 16 h. During centrifugation, transmission of an 865 nm laser through the sample was collected at 60 s intervals. The intensity of the transmitted light through the emulsion is based on the movements of the droplets and solid LPI particles under the centrifugal force. The final transmission profiles of the emulsions as a function of time and height of samples in the cuvettes give indication of kinetic stability of the emulsions under accelerated gravitation. Data analysis and calculation of separation or instability index was done using the SEPView software v 4.1 (LUM GmbH, Berlin, Germany).

3.3.7 Rheological properties of LPI nanoemulsions

The rheological properties of the lentil protein solutions and freshly prepared nanoemulsions were determined by a rheometer (AR G2, TA Instruments, Montreal, QC, Canada) equipped with a cone and plate geometry (40 mm, 2^o angle). All samples were run in two modes: 1) rotational mode, where the viscosity was measured as a function of shear rate (0.01 – 100 s^{-1}); and b) oscillatory mode, where the storage (G′) and loss (G″) modulus was measured as a function of strain (0.001 to 10%) at a constant frequency (6.28 rad/s) within the linear viscoelastic region (LVR).

3.3.8 Confocal laser scanning microscopy

The confocal laser scanning micrographs of freshly prepared nanoemulsions were taken using a Nikon C2 microscope (Nikon Inc., Mississauga, ON, Canada) using a combination of 543 and 633 nm lasers, a 60× Plan Apo VC (numerical aperture 1.4) oil immersion objective lens and 2.5 times digital zoom. All samples will be prepared by adding 0.01 wt% Nile red (excitation by 543 nm laser, emission collected in 573-613 range) to the oil phase prior to homogenization and 0.01 wt% fast green (excitation by 633 nm laser, emission collected using a 650 nm long pass filter) to the final nanoemulsion to stain the proteins within the continuous phase.

3.3.9 Statistics

All experiments were conducted in triplicate (for all protein concentrations) and reported as the mean ± one standard deviation. Statistical significance was determined using a two way analysis of variance (ANOVA) with a 95% confidence interval where $p < 0.05$ was considered as statistically significant. All the statistical analysis was done by using SPSS software (v24, IBM, USA).

3.4 Results and discussion

3.4.1 Droplet size distribution and surface charge

Extensive droplet and protein aggregation in the nanoemulsions led to an initial droplet size distribution (DSD) where most of the particles were > 10 μm (data not shown). Therefore, in order to break up flocculated droplets to measure individual droplet sizes, the nanoemulsions were mixed with 0.5 wt% Tween 20 buffer solution at pH 3 at a 1:5 nanoemulsion vs. Tween 20 volume ratio. Tween 20 is a small molecule emulsifier and more surface active than proteins. It has been shown that the addition of surface active small molecule emulsifiers would displace interfacial proteins from the oil droplet surface, thereby breaking any droplet flocculation (Wilde et al., 2004). In the present case, mixing Tween 20 with the nanoemulsions shifted their DSD towards a lower size. Even then, most nanoemulsions showed a bimodal DSD with one peak above 1 μm and another below (Figure 3.1). The peak < 1 μm is considered to be mostly due to free un-aggregated oil droplets, whereas the one > 1 μm from large protein aggregates and associated oil droplets (as shown below in the microscopy images, shown later). The nanoemulsions with 0.5 wt% LPI showed only a small shoulder above 1 μm, while the one with 1 wt% LPI did not show any second peak (Figure 3.1a). Probably, at 1 wt% LPI, most proteins are engaged in droplet stabilization and not much aggregation could be detected. At 0.5 wt%, we have insufficient protein to fully cover all droplets in the nanoscale range and the small shoulder above 1 μm could be due to large droplets or due to bridging flocculation (McClements, 2004). For 1.5 wt%, the droplet size distribution again became bimodal and the small peak between 1 to 10 μm could be due to the presence of excess proteins in the continuous phase (Figure 3.1c). Increasing LPI concentration from 1.5 to 3 wt% LPI reduced the height of the peak below 1 μm while the peak above increased due to increase in protein aggregate size (Figure 3.1c and d).

Reduction in oil droplet peak size (below 1 μm) with increase in protein concentration could be attributed to the loss of droplets entrapped in large protein aggregates. Excess protein in the 5 wt% LPI nanoemulsions transformed the whole system into strong gel (discussed in section 3.3) and the addition of Tween 20 solution was not enough to breakdown the droplet flocs from the

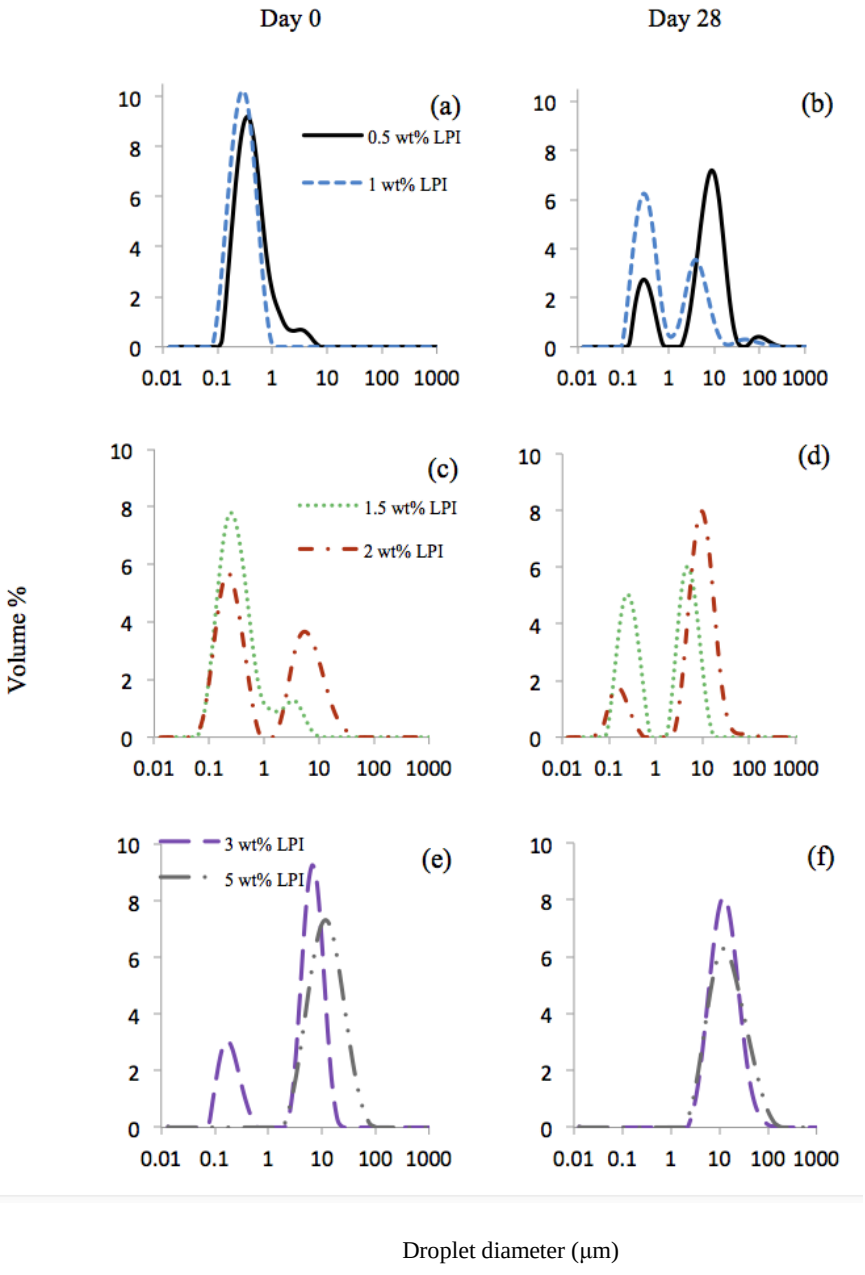

Figure 3.1 Droplet size distribution for nanoemulsions mixed with 0.5 wt% Tween 20 buffer solution (pH 3) in 1:5 ratio and prepared with: (a, b) 0.5 and 1, (c,d) 1.5 and 2, (e, f) 3 and 5 wt% LPI concentrations on day 0 (a, c, e) and day 28 (b, d, f).

strong protein aggregates, hence it showed a monomodal size distribution with a peak above 10 μm (Figure 3.1e).

After 28 days, DSD of nanoemulsions with 0.5 – 2 wt% LPI (Figure 3.1b and 1d) shifted towards larger peak, the peak < 1 μm decreased and the peak > 1 μm grew in size. This could be due to the formation of a stronger and larger protein network with time, which entrapped oil droplets. In the case of the 3 wt% LPI nanoemulsion (Figure 3.1f), the smaller peak < 1 μm disappeared as all the droplets were probably entrapped in the stronger protein network, which could not be disrupted by Tween 20 solution. The nanoemulsion prepared with 5 wt% LPI (Figure 3.1f), did not show any change in the size distribution from the initial state as it remains a strong gel after 28 days of storage.

In order to get an estimate of the average diameter (d_{32}) of the of the free oil droplets, only the peak < 1 μm was considered according to Yerramilli et al. (2017). From Figure 3.2a it can be seen that the average oil droplet size decreased with the increasing LPI concentration from 338 ± 27 nm for 0.5 wt% LPI nanoemulsions to 163 ± 4 nm for 3 wt% LPI nanoemulsions. For 5 wt% LPI nanoemulsions average droplet size could not be reported as no free droplets were detected. After 28 days of storage, average droplet size decreased, although not significantly ($p > 0.05$). This apparent decrease in average droplet size with time was due to the reduction in the the droplet peak < 1 μm as the large droplets were trapped in the growing protein aggregates. For 3 wt% LPI nanoemulsions after 28 days, the small droplet peak disappeared (Figure 3.1) and hence no average droplet size was calculated. It should also be noted that reporting average droplet size for these emulsions (with the presence of both large aggregates and free oil droplets) might not reveal the complete information on emulsion stability.

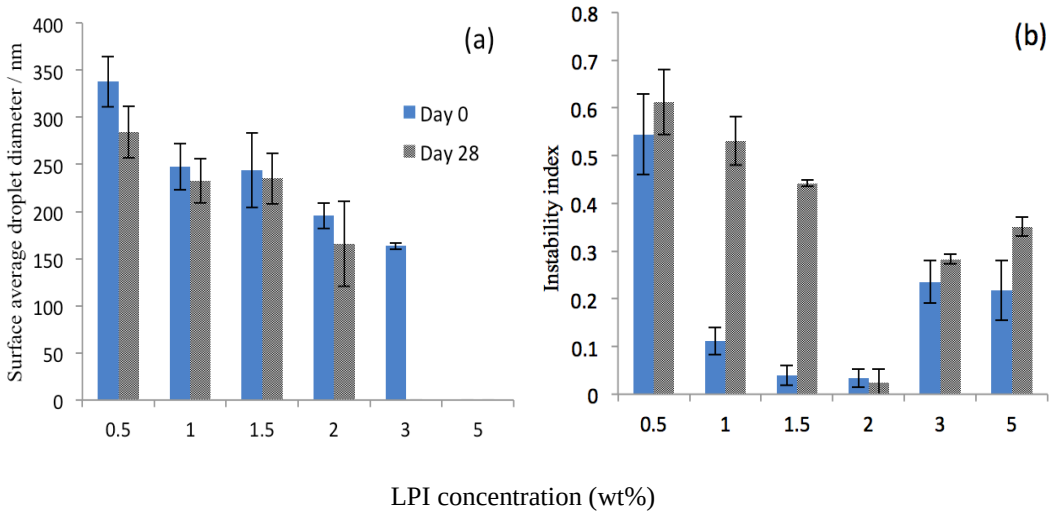

Figure 3.2 (a) Surface average droplet diameter from the peak below 1 μm and (b) instability indices for nanoemulsions mixed with 0.5 wt% Tween 20 buffer solution (pH 3) in 1:5 ratio and prepared with different LPI concentrations on day 0 and day 28. Data represent the mean ± one standard deviation (n=3).

Recently Joshi et al. (2012) prepared highly enriched LPI (protein content 90.2 %, dry basis)-stabilized conventional emulsions with 10% oil volume fractions at pH 7 using a microfludizer (50,000 psi for 5 passes). The authors observed decrease in average droplet size from 12.5 μm to 398 nm with an increase in aqueous phase protein concentration from 0.01 to 3.0 wt%, although no significant change in droplet size was observed above 1.0 wt% LPI. It was proposed that the oil-water interface was saturated by protein molecules at 1.0 wt% concentration. The authors also did not report any protein aggregation behaviour at higher LPI concentration. Such a large difference in average droplet size compared to our nanoemulsions, in spite of using a higher pressure microfluidozation process and similar protein extraction process could be explained by the differences in the interfacial tension of the protein isolates. We previously reported that the interfacial tension of 2 wt% LPI solution changed from 13.04 ± 0.52 mN/m at pH 3 to 9.10 ± 0.88 mN/m at pH 7 (Chang et al., 2015), while Joshi et al. (2012) reported equilibrium interfacial tension at pH 7 decreased from ~15 mN/m to ~13 mN/m when LPI concentration increased from 0.01 to 3.0 wt%. The authors also reported interfacial tension of 1 wt% LPI at pH 3, but the value (17 mN/m) was significantly higher than ours (14.76 ± 1.33 mN/m, data not shown). Perhaps lower interfacial tension of the LPI used in the present study and the use of lower pH improved its emulsification behaviour and nanoscale droplet formation ability.

Zeta potential of all nanoemulsions ranged from +19.46 mV to +15.79 mV (data not shown), although no significant difference was observed among the various samples ($p > 0.05$). It should be noted that the the zeta potential values reported here were obtained with the whole nanoemulsions diluted in buffer solution, so both the charge on free and aggregated proteins and oil droplets were counted. The pH of all nanoemulsions was maintained at 3, which is below the isoelectric point of LPI (Chang et al., 2015), hence the charge on the droplets and proteins were positive. The values of zeta potential also did not change after 28 days of storage ($p > 0.05$).

3.4.2 Accelerated storage stability

The accelerated storage stability of the nanoemulsions was determined using a photocentrifuge, which displays data in the form of transmission profiles (% transmission of laser through the samples) of emulsions as a function of time and sample height in the cuvette (Figure 3.3) (Lerche, 2002). It can be seen that as the position in the cuvette changed from 105

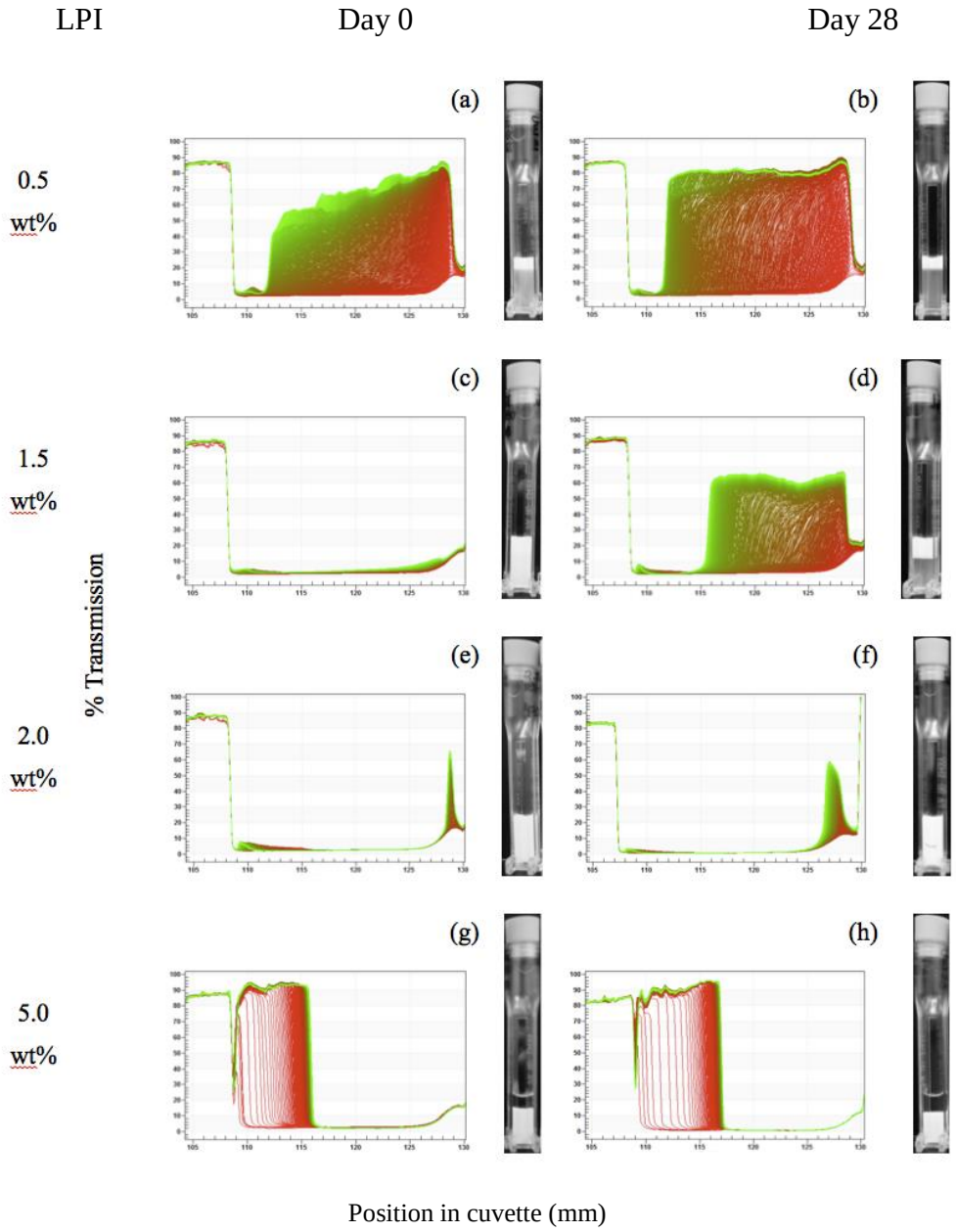

Figure 3.3 Photocentrifuge transmission profiles as a function of length of samples in cuvettes for the nanoemulsions made with (a, b) 0.5, (c, d) 1.5, (e, f) 2 and (g, h) 5 wt% LPI concentrations on day 0 (a, c, e, g) and day 28 (b, d, f, h). The color of the transmission profiles (collected every minute) changed from red to green as the time of centrifugation progressed from 0 to 16 hrs. Photos of the cuvettes after centrifugation are also shown.

mm, percent transmission of near 90% due to empty cuvette wall dropped to almost zero at about 109 mm indicating beginning of emulsion sample in the cuvette. Thereafter, the initial transmissions (red coloured lines) remained very close to zero, meaning no light was passing through the centrifuge tube due to homogeneous distribution of droplets and protein particles in the nanoemulsions. The change in transmission profiles near the very end of the cuvette (127 mm) collected at the beginning of each run (red lines) has been attributed to the effect of the cuvette wall (Lerche, 2002). As the time of centrifugation progressed, the oil droplets moved towards the top forming a cream layer and the bottom of the cuvette became depleted in droplets, which led to clarification. This behaviour can be clearly seen from the final transmission profiles (green coloured lines) for 0.5 wt% LPI nanoemulsion on both day 0 and day 28 (Figure 3.3a, b), where the band of near zero transmission at the top of the sample was due to the formation of cream layer and the band of high transmission was due to progressive clarification of the nanoemulsion with time (see the photo of the cuvette after centrifugation). From Figure 3.3a and b drop in transmission near the end of the cuvette length was also observed which could be attributed to the sedimentation of large protein aggregates at the bottom of the cuvette. It can also be seen that the degree of transmission or clarification increased after 28 days as the stability of the nanoemulsion decreased (also observed in the cuvette photo). This could be due to increase in overall size of the clusters with increased protein and droplet aggregation. As larger particles moved faster, better separation was observed after 28 days of storage. Similar behaviour of increase in particle size distribution with storage was also observed in DSD (Figure 3.1b).

Interestingly, nanoemulsions with 1.5 (Figure 3.3c) and 2 wt% LPI (Figure 3.3e) showed progressively lesser separation, meaning for the entire duration of centrifugation the droplets and protein particles did not phase separate or they were too thick to allow any light transmission. After 28 days, however, nanoemulsions with 1 (data not shown) and 1.5 wt% LPI showed significant phase separation, indicating destabilization (Figure 3.3d). It should be noted that after 28 days both the cream layer and the bottom sediment layer thickness increased with increase in protein concentration from 0.5 to 1.5 wt%. The increase in the thickness of the cream layer could be due to the migration of protein particles along with oil droplets towards the top of the nanoemulsion in the cuvettes, while the increase in the thickness of the bottom layer was due to the presence of excess free proteins in the continuous phase. Sedimentation of insoluble protein aggregates at the bottom of the cuvette can also be observed from the photo of the cuvette after

28 days (Figure 3.3d). The transmission of the middle clarified layer was also decreased with increase in protein concentration from 0.5 to 1.5 wt% (Figure 3.3b, d), which could be due to the presence of small oil droplets and protein aggregates in the 1.5 wt% LPI nanoemulsions that did not phase separate with time. The nanoemulsion with 2 wt% LPI (Figure 3.3e, f) was most stable as even after 28 days only very minor change in transmission profile was observed. This behaviour is in contrast with DSD (Figure 3.1d), where large protein aggregates hindered laser diffraction from small oil droplets and no indication of smaller droplet size of 2 wt% LPI nanoemulsion was obtained. It can be said that in this case the photocentrifuge was better able to identify emulsion stability under accelerated gravity.

Nanoemulsions with 3 (data not shown) and 5 wt% LPI (Figure 3.3g, h) showed quite different transmission profiles compared to the other samples. In this case, the whole emulsion (oil droplets as well as protein particles) formed the sediment layer towards the bottom of the cuvette leaving clear aqueous phase at the top. These nanoemulsions formed a thick gel and did not move freely when the glass vials containing the emulsions were tilted (not shown). Application of centrifugal force led to the compaction of the gel network made of protein and oil droplet aggregates by squeezing out the entrapped water (see photos of the cuvette after centrifugation). From the movement of transmission profiles, it can also be seen that the red lines were much more separated from each other in case of 5 wt% LPI nanoemulsions compared to the others, which indicates that the rate of movement was faster in the former. After 28 days of storage, not much change in transmission profiles was observed for these two nanoemulsions (Figure 3.3h), except that they were compacted even more than the fresh samples, indicating aging-related coarsening of the gel.

In order to get a proper comparison of nanoemulsions' long-term stability it is necessary to quantify the transmission profiles. In Figure 3.2b, instability index, calculated from the ratio of clarification due to phase separation to the maximum possible clarification, was used to compare the accelerated stability of the nanoemulsions (Detloff, Sobisch & Lerche, 2013). Instability index is a dimensionless number between 0 and 1, where 0 indicates no change in transmission and hence highest stability, and 1 represents a complete segregation of phases and hence lowest stability under the centrifugal field. From Figure 3.2b, it can be seen that in freshly-prepared state the lowest values of instability index or the best stability was shown by the nanoemulsions with 1.5, and 2 wt% LPI. After 28 days, instability indices increased for all nanoemulsions,

except for 2 wt% LPI, which showed no significant change in instability index as a function of time. Therefore, from the accelerated stability analysis, it can be concluded that the 2 wt% LPI nanoemulsion was the most stable and it should remain stable without any measurable phase separation for a very long time.

3.4.3 Rheology of the LPI nanoemulsions

As the nanoemulsions showed different thickness and consistency based on protein content it was important to quantitatively determine their rheological behaviour. Figure 3.4 shows viscosity as a function of shear rate for the homogenized LPI solutions (Figure 3.4a) and the corresponding nanoemulsions (Figure 3.4b). Both the nanoemulsions and protein solutions showed shear thinning behaviour; their viscosity decreased with increase in shear rate, indicating structure formation in a quiescent state that broke down during the application of shear. The viscosity of LPI solutions did not significantly change with LPI concentration until about 1.5 wt%, their after increased for 2, 3 and 5 wt% LPI solutions. The viscosity of all nanoemulsions was higher than the corresponding homogenized LPI solutions, but for 2, 3, and 5 wt% LPI nanoemulsions viscosity increased to a much greater extent, hypothesized due to a much more extensive protein-droplet network, resulting in higher shear thinning or pseudoplastic behaviour.

Figure 3.5 shows oscillatory strain sweep viscoelastic behaviour of the nanoemulsions. It can be seen that for all nanoemulsions, G′ was higher than G″ in the low-strain regime, which was followed by a crossover between G′ and G″ where the gel-network broke down. However, for the nanoemulsions with 0.5, 1 and 1.5 wt% LPI, the values of G′ were very low (0.05 to 0.3 Pa) indicating a weak gel was present. The nanoemulsion with 2 wt% LPI (Figure 3.5d) still showed G′ < 1 Pa, making it a weak gel, on the other hand, 3 and 5 wt% LPI nanoemulsion showed G′ >> G″ in the LVR and the values of G′ in the LVR was 17.5 Pa and 67.0 Pa, respectively. Of these two, the nanoemulsions with 3 wt% LPI flowed partially under gravity when the storage vials were laid horizontally (not shown) (Figure 3.5e). In the case of the 5 wt% LPI nanoemulsions, no flow under gravity was observed suggesting a strong gel was formed (Figure 3.5f). Overall, gel strength increased with increase in protein concentration. Gelation in emulsion in the presence of excess biopolymers is a well-known phenomena and has been attributed to depletion interaction by unabsorbed polymer in the continuous phase (Bergenholtz,

Poon, & Fuchs, 2003). In the present case, hydrophobic nature of the LPI may also promote protein aggregation in the continuous phase leading to a stronger gel formation.

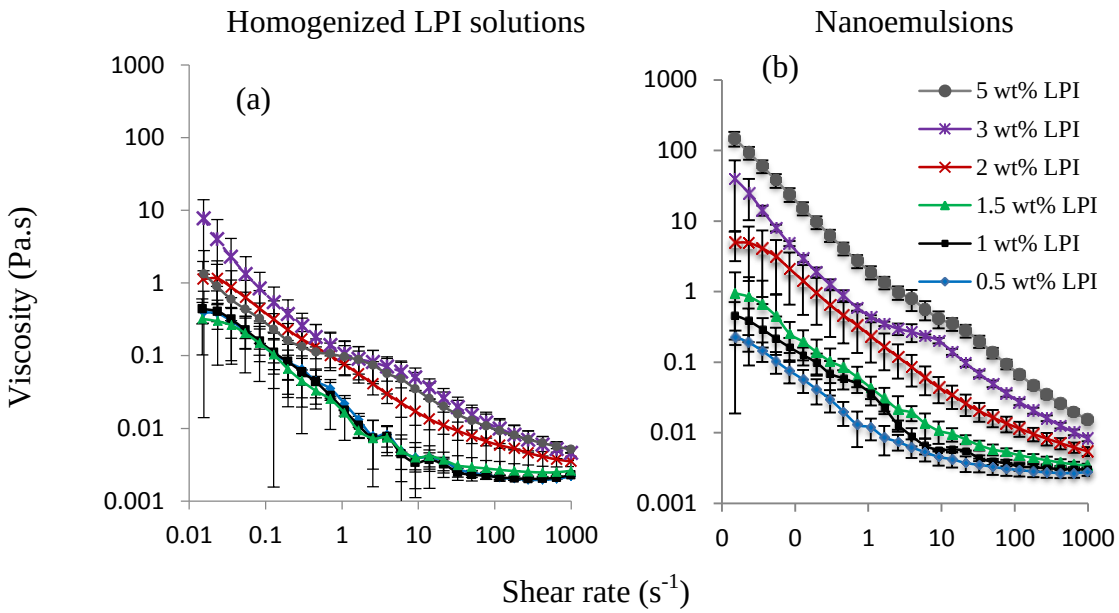

Figure 3.4 Average viscosity as a function of shear rate for (a) various LPI solutions and (b) nanoemulsions made with different concentrations of LPI. Error bars show ± one standard deviation.

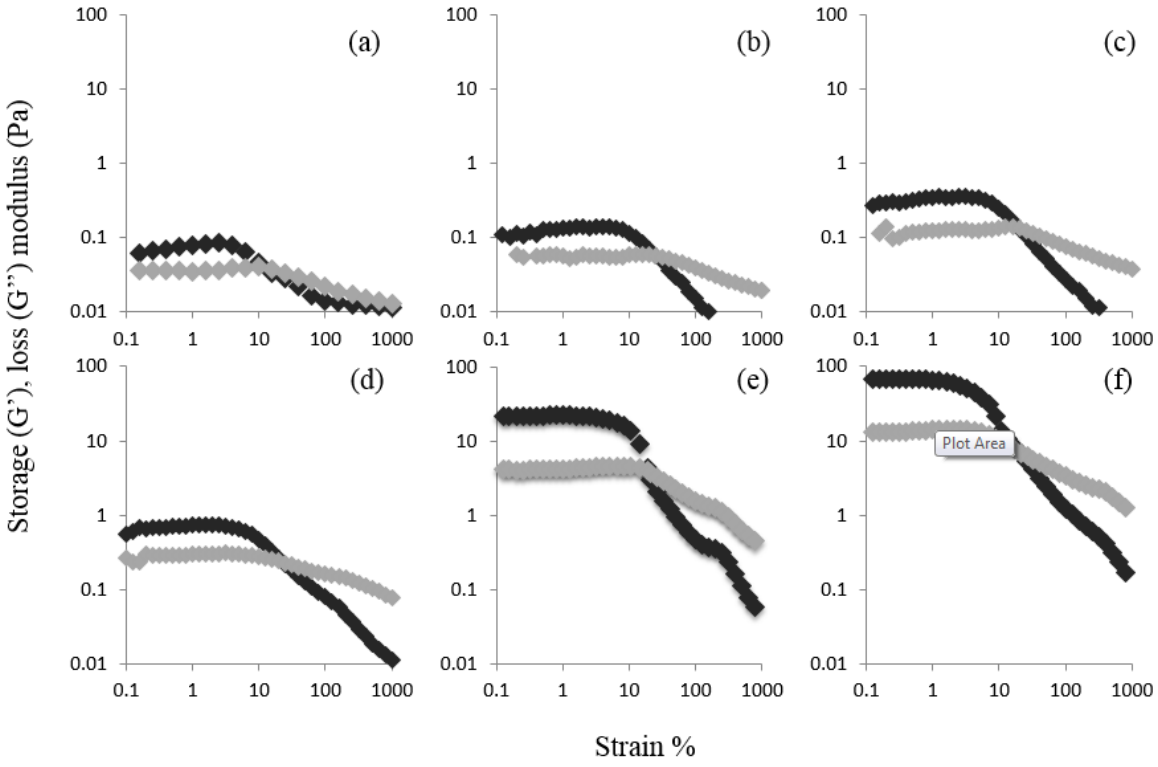

Figure 3.5 Change in storage (G′) (black symbols) and loss (G″) (grey symbols) moduli as a function of % strain for nanoemulsions-stabilized with (a) 0.5, (b) 1, (c) 1.5, (d) 2, (e) 3, and (f) 5 wt% LPI. Arrows in (f) indicate peaks in storage moduli responsible for structural breakdown events.

In the high-strain regime (⩾ 10 % strain) the nanoemulsion gels broke down (G′ < G″) which could be attributed to shear-induced disintegration of protein and oil droplet aggregates. The crossover strain required to break the nanoemulsion gel increased from 10% strain for 0.5 wt% LPI to 25% strain for 1 to 2 wt% LPI nanoemulsions. For 3 and 5 wt% LPI nanoemulsions, the crossover strain decreased to ~20% strain, indicating a fragile gel structure. These two nanoemulsion gels were stronger that the others, but broke down at a lower strain compared to 1-2 wt% LPI. Formation of a strong gel with just 5 wt% dispersed phase and 3-5 wt% LPI is a novel phenomenon and could be applied to a variety of food products with a low-fat requirement (e.g., salad dressing, spreads, etc.). Boye et al. (2010) investigated gelling properties of heat-treated (100 ºC for 1 hr) lentil protein concentrates (protein content ~80 wt%) and reported that a minimum of 8 - 12 wt% protein was needed to form firm gel, depending on the type of lentil (green or red) and the extraction process used (isoelctric precipitation or ultrafiltration). In the present case, presence of oil droplets facilitated gelation in lentil proteins at a lower concentration without any heat treatment. An idea about the internal microstructure of the protein-droplet aggregated gel network in the nanoemulsions can also be obtained from their yielding behaviour under oscillatory strain sweep (Figure 3.5). It can be seen that for 2 to 5 wt% LPI nanoemulsions G′ showed two inflection points as strain increased (shown by arrow in the figure). G″ also showed two inflection points or very small peaks, one in the proximity to the crossover of G′ and G″ (associated with yield strain) and the second one where G′ also showed an inflection. At lower LPI concentration (0.5 to 1.5 wt%) only the first inflection point in G′ can be observed which is associated with the yield strain of the gel. For 2 wt% LPI nanoemulsions the strains at the two inflection points were at around 5 and 200% (Figure 3.5d). For 3 and 5 wt% LPI nanoemulsions the low and high strain inflection points can be seen at around 8 and 250 % strain (Figure 3.5e), and 2.5 and 320 % strain (Figure 3.5f), respectively. This type of two-step yielding behaviour with increasing oscillatory strain sweep was also observed by others for attractive colloidal gels (Koumakis & Petekidis, 2011; Shao et al., 2013).

Koumakis and Petekidis (2011) used a suspension of hard spheres where attractive depletion interaction was induced by non-adsorbed linear polymers and proposed that the first yield strain was due to inter-cluster bond breaking, while the second one was related to the breaking of individual clusters into smaller fragments. Similarly, in the present case the first yield points in the denser nanoemulsions could be due to the rupture of interconnected clusters of

protein and oil droplets, while the second yield point can be ascribed to the break down of the individual aggregates of proteins and oil droplets in to find dispersions of free particles and oil droplets. Koumakis and Petekidis (2011) also noted that the second yield point or the second peak in G″ disappeared as the particle volume fraction decreased. Similarly, in the present case, below 2 wt% LPI only one inflection point in G′ and G″ can be seen, indicating lack of structural organization in the clusters and as the inter-cluster bonds break the whole system disintegrates.

3.4.4 Confocal microscopy

The microstructures of the nanoemulsions are shown in Figure 3.6. All nanoemulsions contain large protein aggregates along with numerous oil droplets. Many large oil droplets can be seen in 0.5 wt% LPI nanoemulsions, which is consistent with its largest droplet size distribution. No strong interconnected protein and oil droplet network can be viewed in the nanoemulsions with 0.5 to 1.5 wt% LPI, giving rise to lower viscosity (Figure 3.4) and weak gelation behaviour (Figure 3.5). The 2 wt% LPI nanoemulsions showed numerous protein aggregates and oil droplets, which led to higher viscosity than lower LPI containing nanoemulsions, but still a weak gelation behaviour. In contrast, 3 and 5 wt% LPI nanoemulsions showed extensively network of aggregated droplets and protein confirming their strong gelation behaviour as observed in the viscoelastic analysis (Figure 3.5).

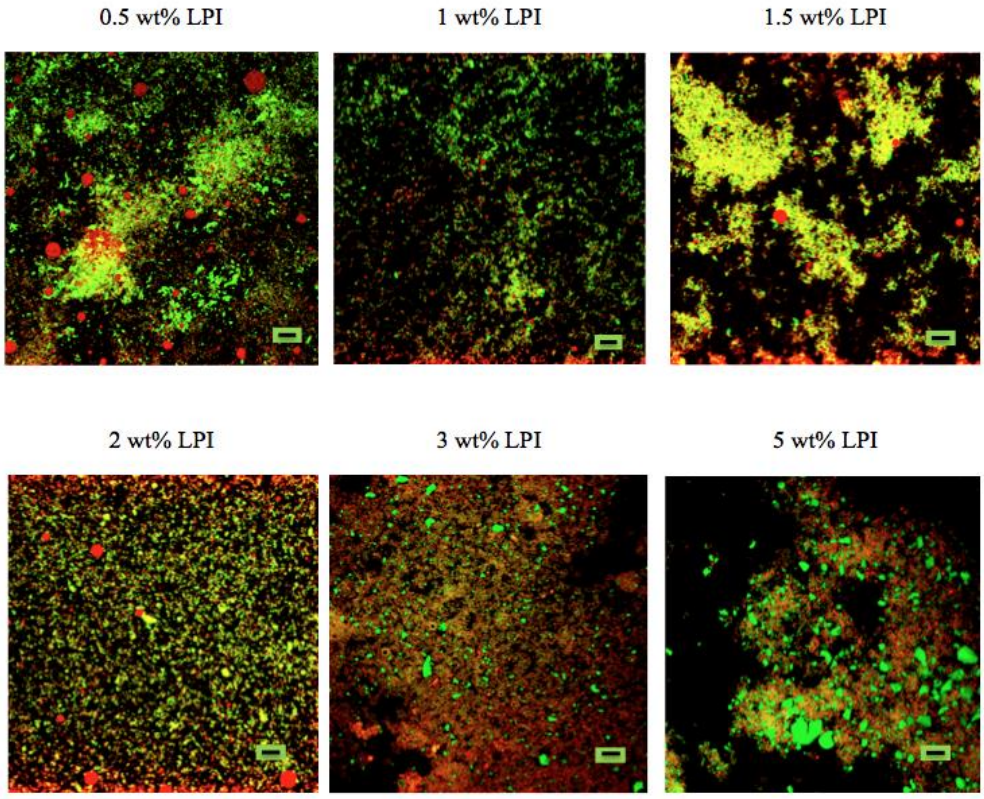

Figure 3.6 Confocal microscopy of nanoemulsions-stabilized with different LPI concentrations. Nile red was used to stain the oil droplets and the proteins in the continuous phase were stained with fast green. Scale bar 5 μm.

We have shown, for the first time, that LPI can be used to develop O/W nanoemulsions, although presence of insoluble fraction of LPI may still pose a problem for its utilization in beverage applications. It should be noted that the LPI used in the present study had 79.5 wt% proteins with the rest being carbohydrate, lipid, minerals and moisture, which does not take part in the emulsification. It may be possible to remove insoluble fractions of LPI by centrifugation, either prior to or after emulsification. However, centrifugation prior to emulsification may remove some of the surface active fractions of LPI that might be important in emulsion formation and stabilization under high-pressure homogenization. It will also be interesting to see whether any pre-treatment of the LPI solution (e.g., ultrasonication, high-pressure homogenization, breakdown of disulfide bonds, or hydrolysis) may improve their solubility and emulsification behaviour. Joshi et al. (2012) used dithiothreitol to reduce all intra- and inter-molecular disulfide bonds in LPI, which made the proteins more flexible and allowed faster diffusion to the oil/water interface during emulsification. The dissociation of the disulfide-bonded subunits also increased the protein solubility and improved their emulsion stabilization properties, although no significant decrease in emulsion droplet size was observed. On the other hand, Avramenko, Low, and Nickerson (2013) showed that enzymatic hydrolysis of LPI significantly decreased their emulsion stabilization properties (pH 7.8) due to reduction in surface hydrophobicity and inability to form a viscoelastic film at the oil droplet surface. Clearly, more research is needed to better understand effect of pre-treatment, and influence of different fractions of LPI and on the formation and stabilization of emulsions and nanoemulsions.

3.5 Conclusions

In conclusion, it was possible to develop stable O/W nanoemulsions using LPI as the sole emulsifier, although the presence of large insoluble protein aggregates in the continuous phase led to the extensive aggregation between the oil droplets and protein aggregates. Stable flowable nanoemulsions were formed at 1-2 wt% LPI concentrations, which may find applications in the pourable foods and beverages sector. Nanoemulsions with 0.5 wt% LPI were not stable, and phases separated over 28 days. The most stable nanoemulsions were formed at 2 wt% LPI, which was confirmed by accelerated stability analysis. All nanoemulsions showed shear thinning behaviour indicating structure formation in the quiescent state. However, the nanoemulsions with 3 and 5 wt% LPI concentration formed strong non-flowable gel and brokedown under high

shear, which could serve in applications associated with gelled-food products and controlled delivery of nutraceuticals or pharmaceutical compounds.

3.6 Connection to the next study

In the current study, the formation and stability of nanoemulsions as a function of lentil protein isolate (LPI) concentration (0.5 to 5.0 wt%) at pH 3.0 was investigated over a four-week period. Although stable and flowable nanoemulsions were formed at 1-2 wt% LPI concentrations, they destabilzied due to excessive protein aggregation. In order to improve LPI's emulsification behaviour, in the next study, protein solutions were homogenized at high-pressure prior to making the nanoemulsions and subsequently, their stability and lipid digestibility was tested.

4. EFFECTS OF HOMOGENIZATION OF LENTIL PROTEIN ISOLATE SOLUTIONS ON THE FORMATION, STABILITY AND LIPID DIGESTIBILITY OF NANOEMULSIONS

4.1 Abstract

Lentil protein isolate (LPI) solutions (1 – 2 wt%) were homogenized at 5,000 and 15,000 psi for 6 cycles before utilizing them to emulsify 5 wt% O/W nanoemulsions at 20,000 psi for 6 cycles. High-pressure homogenization significantly improved solubility of LPI, while their particle size distribution, surface hydrophobicity and interfacial storage moduli decreased. Interfacial tension of the LPI was not affected by the use of high-pressure homogenization. All nanoemulsions showed droplet flocculation and LPI aggregation, which was increased with protein concentration. The average free droplet size of the nanoemulsions significantly decreased from ~250 nm for unmodified LPI to less than 200 nm for homogenized LPI solutions, whereas no significant difference between 5,000 and 15,000 psi homogenization was observed. Although both the droplet size and instability indices of the nanoemulsions measured under accelerated gravitation increased after 28 days of storage, it was still much better than that from the nanoemulsions made with unmodified LPI solutions. An *in vitro* static digestion model using simulated stomach and intestine conditions was used to test the digestibility of the emulsified lipid by titrating the amount of free fatty acids released during lipolysis. It was observed that high-pressure homogenization of LPI significantly improved lipid digestibility from the nanoemulsions. It was proposed that both the higher interfacial area of smaller droplets and the weaker interfacial moduli of homogenized LPI-stabilized droplets were responsible for better proteolysis and removal of interfacial proteins by bile salts, leading to more accessibility of lipase towards the oil droplets. High-pressure homogenization of LPI could be novel way to utilize pulse proteins in the formation and stabilization of nanoemulsions and improved digestibility under gastro-intestinal conditions.

[2]Submitted to Food Hydrocolloids on June 22, 2017

4.2 Introduction

Nanoemulsions are dispersions of two immiscible phases with average droplet radii less than 100 nm (Mason et al., 2006). Nanoscale droplet size gives the nanoemulsions some unique properties compared to the microscale conventional emulsions, such as, enhanced physical stability and longer shelf life. Some nanoemulsions can have a transparent appearance; especially at the lower oil volume fractions therefore they can be used in the production of beverages and fortified drinks (Graves, 2008; Rao & McClements, 2011).

The choice of emulsifiers is crucial in the formation and stability of nanoemulsions. Quick migration to the oil droplet interface and the ability to provide strong repulsive forces are important properties of emulsifiers in providing a long-term stable nanoemulsions. Normally, low molecular weight emulsifiers are used to stabilize nanoemulsions because of their faster rate of diffusion towards the oil/water interface during homogenization and the ability to rapidly lower the interfacial tension (Pugnaloni et al., 2004). In the recent years there is a growing trend to replace synthetic emulsifiers with natural and healthier food ingredients. Proteins poccess good emulsifying properties due to their amphiphilic nature but they tend to migrate slowly to the oil/water interface due to their large molecular weight compared to low molecular weight emulsifiers, and therefore are not ideal for nanoemulsion formation (McClements et al., 2017; Donsi et al., 2010). However, there are many studies where proteins, mostly milk proteins, were used in the development of nanoemulsions. Ali et al. (2016) developed β-lactoglobulin stabilized nanoemulsions with droplets less 200 nm by using a low viscous oil and homogenized at 100 MPa for 4 passes.

Food manufacturers are trying to find alternative sources of proteins due to a growing world population as well as consumers dietary and religious preferences (Day, 2013). Seed storage proteins (lentil, pea chick pea, and faba bean) which are from plant sources have a potential to substitute animal proteins, but their functional properties are still not fully understood (Can Karaca et al., 2011). Plant proteins are larger in size than animal proteins and have globular conformation with hydrophobic groups buried inside the molecular structure; therefore a certain degree of unrevealing may improve their emulsification properties. It has been demonstrated that some plant proteins may provide significantly greater long-term stable emulsions compared to the animal proteins due to the formation of a thicker interfacial film. For example, the deamidated wheat gliadins formed 18 nm thick interfacial layer (Wong et al., 2011)

and the heat-treated soy proteins formed 30 – 40 nm thick interacial layer (Keerati-U-Rai & Corredig, 2010), while dairy protein β-lactoglobulin formed a 3.6 nm thick layer (Zhai et al., 2011).

Protein modifications (chemical, enzymatic or physical) can increase the charge, enhance the solubility by lowering the molecular weight and improve surface activity by exposure of the hydrophobic domains. Chemical and enzymatic modifications involve cleavage of peptide bonds into smaller peptides by proteolysis (Tavano, 2013). Avramenko et al. (2013) investigated the limited enzymatic hydrolysis on the physicochemical and emulsifying properties of lentil protein isolate (LPI) with different degree of hydrolysis (4 - 20%). It was found that surface hydrophobicity decreased for all hydrolyzed LPI solutions with increased degree of hydrolysis. Interfacial tension was lower for the hydrolyzed LPI solutions due to a better solubility and migration at the oil interface; however the emulsification properties decreased for all hydrolyzed LPI solutions due to lower hydrophobicity, which caused weaker attachment to the oil interface. They explained that exposure of hydrophobic groups after hydrolysis of LPI caused aggregation of peptides due to hydrophobic interaction and buried them again into larger moieties, which give rise to a new conformation of the protein.

High-pressure treatment may also affect the hydrophobic or electrostatic interactions and disulfide or hydrogen bonds, which are involved in stabilizing quaternary, tertiary and secondary protein structures (Messens, 1997). High-pressure homogenization generates proteins with a different degree of denaturation or unraveling which depend on pressure level, cycles, treatment time, temperature, pH and ionic strength (He et al., 2016). He et al. (2016) and De Maria at al. (2016) reported that high-pressure homogenization of bovine lactoferrin and bovine serum albumin caused modification in tertiary and secondary structure in a more unfolded conformation which improved solubility, foaming and emulsifying properties. At higher pressures, above 400 MPa, bovine serum albumin formed soluble high molecular weight aggregates. Molina et al., (2001) studied the effect of high-pressure treatment on the emulsification properties of soy protein isolate (SPI). At 400 MPa the hydrophobicity of 7S fraction was the highest with maximum emulsifying activity due to disruption into subunits, while for the 11S fraction hydrophobicity decrease due to re-aggregation because of the disulfide bond formation. The results showed that high-pressure treatment of SPI improved their emulsifying activity but decreased emulsion stability. Similar results were also found by Wang et al. (2008). Donsi et al.

(2010) developed pea protein stabilized nanoemulsions with the droplet size less than 200 nm. It was proposed that that high-pressure treatment caused changes in a protein structure by disruption of disulfide bonds which affected the exposure of hydrophobic groups.

To our knowledge, no previous research has been done on the effect high-pressure homogenization treatment on the LPI solution for the development of nanoemulsions. Therefore in this study, the effect of homogenization at different pressures and various LPI concentrations on the formation, stability and lipid digestibility of nanoemulsions was investigated. Based on initial research on the effect of LPI concentration on the formation of the most stable and flowable nanoemulsions, only 1, 1.5 and 2 wt% LPI concentrations were chosen for the present study.

4.3 Materials and methods

4.3.1 Materials

Lentil protein isolate (protein content 79.5% w/w, w.b.) was kindly provided by POS Bio-sciences (Saskatoon, SK, Canada), after being produced by alkaline extraction followed by isoelectric precipitation and spray drying at pilot scale. Canola oil used in this study was purchased from the local supermarket (Saskatoon, SK, Canada). The citric acid was purchased from VWR International (Edmonton, AB, Canada). All other chemicals were purchased Sigma-Aldrich (St. Louis, MO, USA) and were of reagent grade. Details of the reagents for in-vitro digestion tests and SDS PAGE are mentioned in the respective sections.

4.3.2 High-pressure homogenization of lentil proteins isolate solutions

Lentil protein solutions were prepared by dispersing the protein powder at different concentrations (1, 1.5, and 2 wt%) based on the protein content, in a 0.1 M citrate buffer (pH 3) using a magnetic stirrer at 500 rpm for 24 h at room temperature (22-23 ^{o}C). To prevent the microbial spoilage in the emulsions, an antimicrobial agent (0.02 wt% sodium azide) was added to each protein solution. Next, the LPI solution was ultra-sonicated for 20 min in an ultrasonic bath (Branson Ultrasonic Cleaner, Model 2510R-DTH, USA) at a frequency of 40 kHz and then homogenized at 5,000 psi and 15,000 psi pressures for 4 cycles in a high-pressure homogenizer (Emulsiflex C3, Avestin Inc., Ottawa, ON, Canada).

4.3.3 Nanoemulsion preparation

Immediately after homogenizing the protein solutions, they were mixed with 5 wt% canola oil and a coarse emulsion was prepared by mixing both the phases with a rotor-stator mixer (Polytron, Brinkman, ON, Canada). Thereafter, nanoemulsions were prepared in the high-pressure homogenizer (Emulsiflex C3, Avestin Inc., Ottawa, ON, Canada) at a pressure 20,000 psi (equivalent to 137.9 MPa) for 6 cycles. The samples were collected and stored in a refrigerator (4^oC) for further analysis.

4.3.4 Particle size distribution

Particle size distribution of unmodified and homogenized (at 5,000 and 15,000 psi, equvalent to 34.5 and 103.4 MPa) LPI solutions and also the nanoemulsions were measured using a static laser diffraction particle size analyzer (Mastersizer 2000, Malvern Instruments, Montreal, QC) immediately after the preparation of the nanoemulsions and as a function of time (0, 7, 14, and 28 d). The volume-weighted mean droplet diameter (d_{43}) and the size distribution were recorded for further analysis. For more accurate measurement of individual un-flocculated droplet size, a second experiment was done where all samples were diluted (1:5) with a 0.5 wt% Tween 20 in 0.1 M citrate buffer (pH 3) solution before measuring their droplet size.

4.3.5 Zeta potential

Surface charge or zeta potential of the oil droplets were determined using a Zetasizer Nano-ZS90 (Malvern Instruments, Westtborough, MA, USA) by measuring the electrophoretic mobility (U_E) of the LPI-coated droplets in a buffer solution (pH 3) (1 drop of emulsion added to 100 ml of citric buffer) in an electric field of where the droplets move towards the oppositely charged electrode. Zeta potential (ζ, mV) was determined by measuring the electrophoretic mobility (U_E) and then applying Henry's equation:

$$U_E = \frac{2\varepsilon \times \zeta \times f(k\alpha)}{3\eta} \qquad \text{(eq. 4.1)}$$

where ε is the permittivity (F (Farad)/m), f (kα) is a function associated with the ratio of the particle radius (α) to the Debye length (k) and η is the viscosity (mPa·s) of the solution (water, 1 mPa.s). The Smoluchowski approximation f (kα) for this study was set to 1.5. Zeta potential was

measured as a function of time (0, 7, 14, and 28 d) for all nanoemulsions stabilized with different LPI concentrations.

4.3.6 Accelerated gravitational separation

Long-term stability of the nanoemulsions was analyzed using a photocentrifuge dispersion analyzer (LUMiSizer, LUM Americas, Boulder, CO, USA) to determine the instability index as a function of time (0, 7, 14, and 28 d). In brief, 400 µL of freshly prepared nanoemulsions was transferred into 8 mm × 2 mm rectangular polycarbonate cuvettes and centrifuged at 2000 x g for 16 h. During centrifugation, transmission of an 865 nm laser through the sample was collected at 60 s intervals. The intensity of the transmitted light through the emulsion is based on the movements of the droplets and solid LPI particles under the centrifugal force. The final transmission profiles of the emulsions as a function of time and height of samples in the cuvettes give indication of kinetic stability of the emulsions under accelerated gravitation. Data analysis and calculation of separation or instability index was done using the SEPView software v 4.1 (LUM GmbH, Berlin, Germany).

4.3.7 Nanoemulsion viscosity

The viscosity of the nanoemulsions were determined by a rheometer (AR G2, TA Instruments, Montreal, QC, Canada) equipped with a cone and plate geometry (40 mm, 2^o angle) as a function of shear rate (0.01 – 100 s^{-1}).

4.3.8 Micro- and nanostructure of the nanoemulsions and protein particles

The confocal laser scanning micrographs of freshly prepared nanoemulsions were taken using a Nikon C2 microscope (Nikon Inc., Mississauga, ON, Canada) using a combination of 543 and 633 nm lasers, a 60× Plan Apo VC (numerical aperture 1.4) oil immersion objective lens and 2.5 times digital zoom. All samples will be prepared by adding 0.01 wt% Nile red (excitation by 543 nm laser, emission collected in 573-613 range) to the oil phase prior to homogenization and 0.01 wt% fast green (excitation by 633 nm laser, emission collected using a 650 nm long pass filter) to the final nanoemulsion to stain the proteins within the continuous phase. The microstructure of unmodified and homogenized protein solutions were also recorded using an optical microscope (Eclips E400, Nikon Mississauga, ON, Canada) using a 40x objective lens.

Nanostructure of LPI-stabilized droplets were also recorded using a Ultra High Resolution Cold-Emission Scanning Electron Microscope (SEM) (model SU8010, Hitachi High-Technologies Canada, Inc. Toronto, ON). Briefly, samples were dried on a metal plate and transferred into the SEM and images were captured at 40,000 and 100,000 magnification using 3,000 volt accelerating voltage and 3600 μm working distance.

4.3.9 Interfacial tension of protein solutions

Canola oil/water interfacial tension in presence of LPI was measured by using a tensiometer (Lauda TD2, GmbH & Co., Lauda-Königshofen, Germany) with a Du Noüy ring (20 mm diameter). Initially the ring was positioned below the oil-water interface and then slowly pulled through the interface. The interfacial tension was measured from the maximum force acted on the ring, just before it raptures.

4.3.10 Surface hydrophobicity of protein solutions

Surface hydrophobicity of the unmodified and homogenized (5,000 and 15,000 psi) LPI solutions was analysed by using a fluorescent probe 8-anilino-1-naphthalenesulfonic acid (ANS) that binds to the exposed hydrophobic groups of the amino acids of the protein generating fluorescence. The fluorescence intensity was measured using a FluoroMax-4 spectrofluorometer (Horiba Jobin Yvon Inc., NJ, USA). Fluorescence intensity of ANS protein solutions was obtained by subtracting the ANS blank and protein blanks. The surface hydrophobicity (S_0-ANS) is determined from the slope of the fluorescence intensity plotted as a function of protein concentration, prepared by dilution in the citric acid buffer.

4.3.11 Interfacial rheology of protein solutions

Interfacial rheology was determined in the rheometer (AR G2, TA Instruments, Montreal, QC, Canada) by using a Du Noüy ring geometry (10 mm diameter), in a glass wide mouth beaker (inner diameter 80 mm and depth 45 mm). Initially the interface between the unmodified or homogenized LPI solutions and canola oil was allowed to build for 1.5 hrs while the interfacial storage (G′) and loss (G″) modulus was recorded at a constant strain (0.01) and angular frequency (1 rad/s), thereafter the strength of the interface and its breakdown was

characterized by measuring the interfacial G′ and G″ as a function of strain (0.1 to 1000%) at a constant angular frequency (1 rad/s).

4.3.12 *In-vitro* digestion and determination of lipid digestibility

A static *in vitro* digestion model with simulated gastric and intestinal conditions as proposed by Minekus et al. (2014) (with a small modification) was used to study the structural changes during digestion and lipid digestibility of the LPI-coated oil droplets.

Preparation of stock solutions

The stock solutions of simulated gastric (SGF) and intestinal fluid (SIF) was made up with a mixtures of various sodium, potassium and magnesium and ammonium salts according to Table 1. For each of the simulated fluid (gastric or intestine) the corresponding volumes of stock solutions were mixed and diluted up to 400 ml using deionized water. The volumes of stock solution stated in Table 4.1 was calculated by Minekus et al. (2014) to give a correct final electrolyte concentrations of SGF and SIF at 500 ml, after the addition of emulsions, enzymes, bile extract, calcium salt solution and water. The $CaCl_2 (H_2O)_2$ solution was added directly in the simulated digestion mixture to prevent Ca^{2+} precipitation.

Table 4.1 Composition of stock solutions of simulated gastric fluid (SGF) and simulated intestinal fluid (SIF) according to Minekus et al. (2014). The compositions are adjusted to yield 500 ml when mixed with other ingredients.

			SGF (pH 3)		SIF (pH 7)	
	Stock conc.		Vol. of stock	Conc. in SGF	Vol. of stock	Conc. in SIF
	g/L	mol/L	mL	mmol/L	mL	mmol/L
KCl	37.3	0.5	6.9	6.9	6.8	6.8
KH_2PO_4	68	0.5	0.9	0.9	0.8	0.8
$NaHCO_3$	84	1	12.5	25	42.5	85
NaCl	117	2	11.8	47.2	9.6	38.4
$MgCl_2 \cdot 6\ H_2O$	30.5	0.15	0.4	0.5	1.1	0.33
$(NH_4)_2CO_3$	48	0.5	0.5	0.5	-	-
$CaCl_2 \cdot 2\ H_2O$	44.1	0.3	-	-	-	-

Gastric phase

Nanoemulsions prepared with unmodified and homogenized (at 5,000 and 15,000 psi) LPI solutions at concentrations 1, 1.5 and 2 wt% were digested by mixing them with a simulated gastric fluid (SGF) in a simulating stomach conditions. The SGF was prepared from the electrolyte stock solutions (Table 1) by adding the enzyme pepsin (P6887-1G) with activity 3,200 – 4,500 U/ml (Sigma Aldrich, St. Louis, MO), $CaCl_2 \cdot 22\ H_2O$ and water. Four parts of electrolyte solutions and 1 part of enzyme pepsin, $CaCl_2 \cdot 2\ H_2O$ solution and water was mixed which gave the correct ionic composition of SGF. Nanoemulsions were mixed with the SGF in 1:1 v/v where 10 ml of nanoemulsion was added to a 7.5 ml of SGF electrolyte stock solution, 1.6 mL of porcine pepsin in SGF solution, 5 μL of 0.3 M $CaCl_2 \cdot 2\ H_2O$ and 695 μL of water. The pH of the medium was adjusted to 3 by adding 1 M HCl. The nanoemulsion - SGF mixture (gastric chyme) was then incubated for 2 h at 37˚C in swirling motion (90 rpm) in a shaking water bath (Model G76, New Bruinswick scientific Co, Edison, NJ, USA).

Intestinal phase

After 2 hours of incubation in simulated gastric conditions the pH of the gastric chyme was adjusted to 7 by adding 1 M NaOH. The simulated intestinal fluid (SIF) was added to gastric chyme in 1:1 v/v to simulate the intestinal conditions. The SIF was prepared from the electrolyte stock solutions (Table 4.1) with the addition of enzyme porcine pancreatine (P7545) with lipase activity 2000 U/ml (Sigma Aldrich, St. Louis, MO), bile extract (B8631, Sigma Aldrich, St. Louis, MO), $CaCl_2\ (H_2O)_2$ and water. Four parts of SIF and 1 part of enzyme porcine pancreatin, porcine bile extract, $CaCl_2$ and water was mixed to obtain the correct composition of SIF. The pH of gastric chyme and SIF was adjusted to 7 prior to mixing them. The gastric chyme and SIF were then mixed in 1:1 v/v and stirred in a double jacketed glass vessel at a constant temperature of 37˚C. The release of free fatty acid (FFA) during lipid digestion was continuously measured by titrating with 0.1 M NaOH, to keep the final pH of the medoum at 7, using a pH-STAT autotitrator (907 Titrando, Metrohm, Switzerland) according to Li and McClements (2010). The percent FFA released was calculated from the number of moles of NaOH needed for neutralization of free fatty acid. It was assumed that 2 molecules of FFA were released from one molecule of triacylglycerol and one fatty acid remained as a monoacylglycerol. The percent FFA was calculated by using the following equation:

$$\%FFA = 100 \times (V_{NaOH} \times M_{NaOH} \times MW_{Lipid}) / (2 \times W_{Lipid}) \quad \text{(eq. 4.2)}$$

where V_{NaOH} is the volume of NaOH (ml), M_{NaOH} is the molarity of NaOH (0.1M), MW_{Lipid} is the average molecular weight of canola oil (882.92 g/mol) and W_{Lipid} is the weight of lipid in the nanoemulsion.

4.3.13 Statistics

All experiments were performed in triplicate (for all protein concentrations and all protein treatments) and reported as average and ± one standard deviation. Statistical analysis of the data was done by two-way analysis of variance (ANNOVA) with a Tukey *posthoc* test using SPSS software (v24, IBM, USA). $P < 0.05$ was considered significant.

4.4 Results and discussion

4.4.1 Particle size distribution, microstructure and dispersibility of homogenized LPI solutions

Prior to particle size measurements, all samples were diluted in a 0.5 wt% Tween 20 buffer solution (pH 3) at a sample to buffer ratio of 1:5 to break droplet flocculation and get a more accurate measurement of individual droplet size. Similar to the nanoemulsions, LPI solutions were also treated by Tween 20 buffer solutions, although aggregated protein particles would not breakdown by this method. Figure 4.1 shows a comparison of particle size distribution (PSD) of unmodified or unmodified, ultrasonicated and homogenized (5,000 and 15,000 psi pressures) LPI solutions. For all the LPI solutions with concentrations (1, 1.5, and 2 wt%) PSD has shifted towards the smaller size upon ultrasonication and homogenization compared to the control unmodified LPI solutions. For example, the peak ranging from 1 to 100 μm for unmodified LPI solution at 1.5 wt% (Figure 4.1b) shifted towards 1 to 22 μm for ultrasonicated LPI solution. Upon homogenization, a large peak appeared below 1 μm, indicating significant decrease in protein particle size. Homogenized LPI solution also showed small peaks in the range 1 to 100 μm, but these peaks are much smaller than the large submicron peaks. The size of these small peaks increased with increase in LPI concentration from 1 to 2 wt%, indicating increased presence of large aggregates of LPI. Not much difference in the PSD was observed

between LPI solutions homogenized at 5,000 and 15,000 psi. It was concluded that the 5,000 psi pressure was enough to break up the large protein aggregates. To confirm the

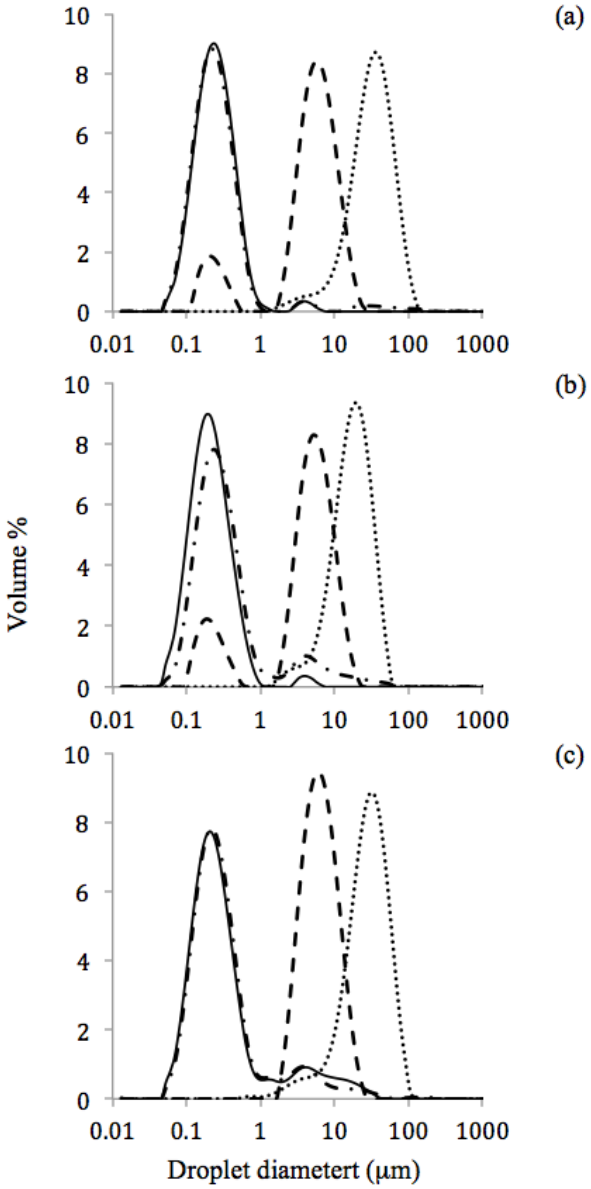

Figure 4.1 Particle size distribution of untreated LPI solutions (…..), ultrasonicated LPI solution (----) and the homogenized LPI solutions at 5,000 psi (-.-.-) and 15,000 psi (—) for: (a) 1 wt%, (b) 1.5 wt% and (c) 2 wt% LPI

difference between protein particle size, brightfield microscopy images of the unmodified and homogenized protein solutions were also recorded and data for only 1.5 wt% LPI is shown in Figure 4.2 (a, b, c). It can be observed that large particles and aggregates of LPI in the unmodified solution significantly decreased into a fine dispersion of particles, although numerous aggregates are still present. Similar to PSD, microscopy results also did not show much difference among the samples homogenized at 5,000 and 15,000 psi.

Homogenization of LPI solutions also improved their dispersibility, which is important for emulsification of oil droplets where only the dispersed and soluble fraction of LPI would move towards the freshly created droplets. Dispersibility of the LPI solutions was tested with the photocentrifuge dispersion analyzer where the movement of LPI particles under an accelerated gravitational field was recorded using laser transmission profiles as a function of time and length of the sample in cuvettes (Figure 4.2 d, e, f). It can be seen that, unmodified LPI solution quickly moved towards the bottom of the cuvettes and within few minutes of the total 8 hours run, the whole LPI was sedimented leaving a clear aqueous phase on the top (Figure 4.2d). For the LPI solution homogenized at 5,000 psi, the movement of the particles was much slower as indicated by the wide distribution of the red lines (Figure 4.2e). It took almost 8 hrs for the separation and even after that some LPI remained in the aqueous phase as indicated by the lower final transmission compared to the unmodified LPI solution. LPI solution homogenized at 15,000 psi showed even better dispersibility compared to 5,000 psi, as evident by even lower transmission at the end of the run (Figure 4.2f). An estimation of amount of sedimented LPI can also be obtained from the thickness of the lower layer, which decreased from unmodified to 5,000 psi and then again to 15,000 psi homogenized LPI solutions.

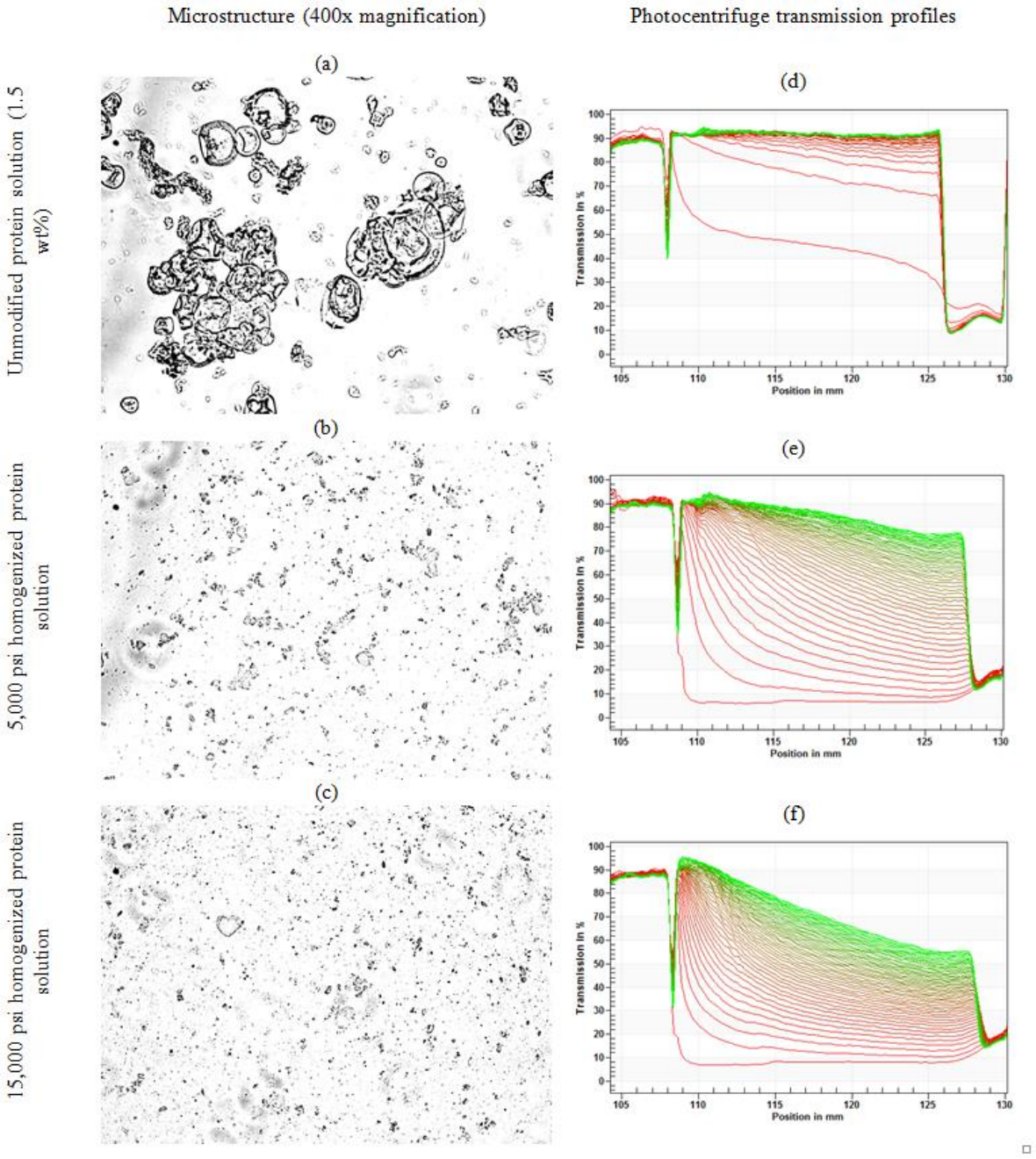

Figure 4.2 Microstructure (a, b, c) and photocentrifuge transmission profiles (d, e, f) of 1.5 wt% LPI solutions made with unmodified, un-homogenized (a, d), homogenized at 5,000 psi (b, e) and 15,000 psi (c, f). Transmission profile indicates dispersibility of the protein particles under accelerated gravitation (2000g). Red and green lines indicate initial and latest transmission profiles, respectively.

4.4.2 Nanoemulsion droplet size distribution

Figure 4.3 shows oil droplet size distributions of all nanoemulsions made with unmodified, 5,000 and 15,000 psi homogenized LPI at 1, 1.5, and 2 wt% concentrations in the aqueous phase. It can be seen that all nanoemulsions had bimodal distributions where the peak below 1 μm indicates oil droplets and smaller protein particles while the peak above 1 μm indicates aggregated protein particles in the continuous phase. Nanoemulsions prepared with 2 wt% unmodified LPI showed larger peaks above 1 μm than the nanoemulsions with unmodified 1 and 1.5 wt% LPI due to the presence of excess free proteins in the continuous phase. Homogenizing the protein solutions followed by emulsification significantly shifted the droplet size distribution towards smaller size. The peaks beyond 1 μm also became smaller as observed in the protein solution particle size distribution. No difference in the droplet size distribution was observed between the nanoemulsions prepared with 5,000 psi and 15,000 psi homogenized LPI solutions.

After 28 days, all nanoemulsions showed an increase in the size range of the droplet size distribution due to an increase in protein and droplet aggregation with time. However, nanoemulsions prepared with 1 and 1.5 wt% homogenized LPI (both 5,000 and 15,000 psi) showed less change in the droplet size distribution compared to the control indicating improvement in stability of nanoemulsions prepared with homogenized LPI solutions (Figure 4.3b and 4.3d). Nevertheless, the DSD of 2 wt% LPI-stabilized nanoemulsions with and without homogenized LPI solutions significantly shifted towards larger size after 28 days of storage (Figure 4.3f), indicating more protein aggregation with the time as protein concentration increased. Similar to what was observed for fresh nanoemulsions, homogenization of LPI solutions at 15,000 psi showed little improvement in the droplet size distribution compared to the 5,000 psi.

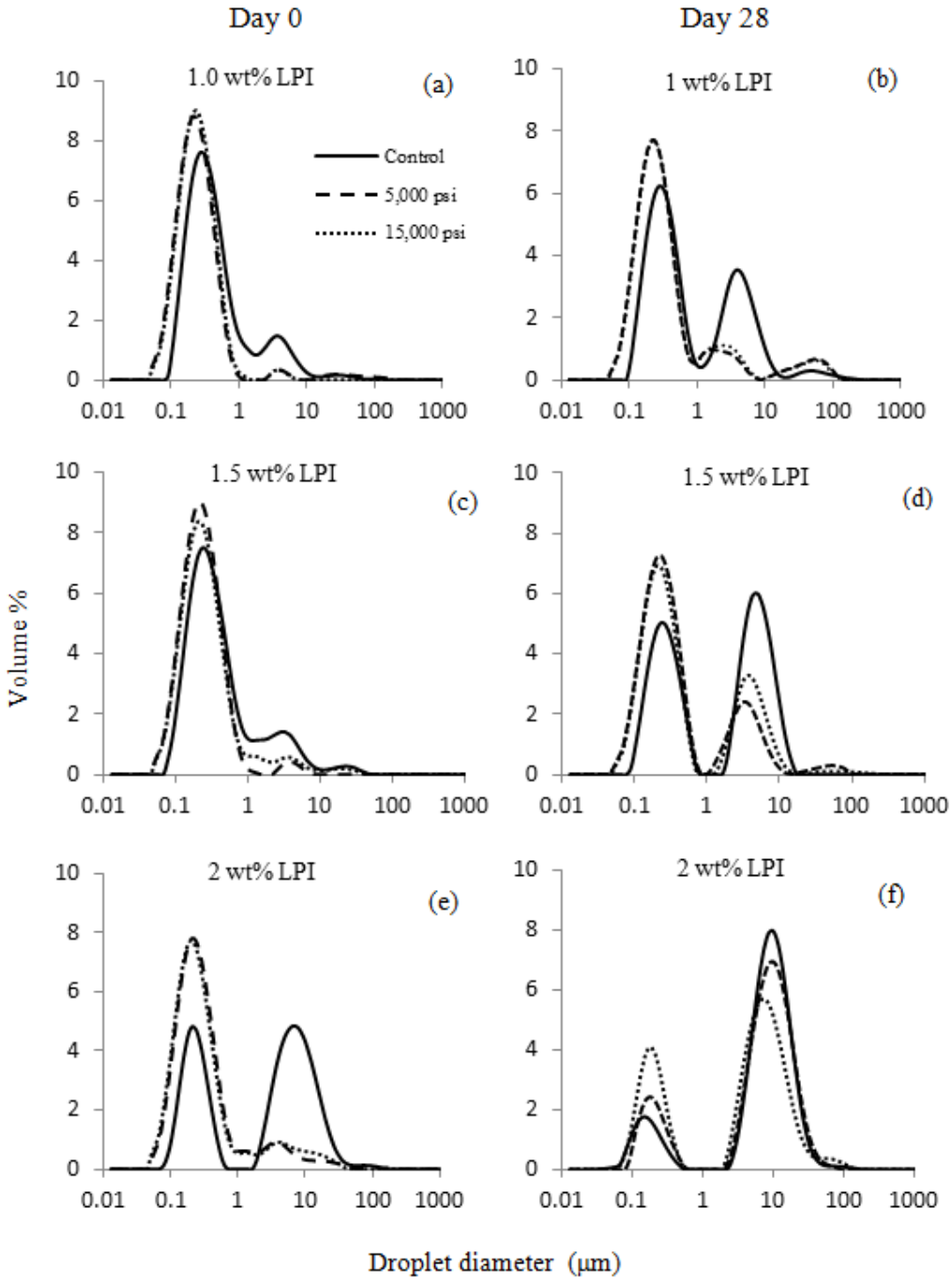

Figure 4.3 Droplet size distribution of freshly prepared nanoemulsions made with (- -) 5,000 and (…) 15,000 psi homogenized LPI and the nanoemulsions made with unmodified (---) LPI solution for 1 wt% (a, b), 1.5 wt% (c, d) and 2 wt% (e, f)

Surface average droplet diameter (d_{32}) of the nanoemulsions were determined from the peak in the droplet size distribution below 1 μm (Figure 4.4). Therefore, in the calculation of average droplet diameter only the free droplets below 1 μm was used, and the increase in droplet and protein aggregation with time (expressed in the second peak) was not considered. The average free droplet size for 1 and 1.5 wt% LPI-stabilized nanoemulsions (prepared with homogenized LPI solutions) decreased significantly compared to the unmodified LPI-stabilized nanoemulsions. For example, d_{32} for 1 wt% LPI-stabilized nanoemulsions decreased from 248 ± 28 nm in the unmodified LPI-nanoemulsions to 199 ± 32 nm in 5,000 psi homogenized LPI and to 196 ± 20 nm 15,000 psi homogenized LPI-nanoemulsions. Similarly, the average droplet size of 1.5 wt% LPI-stabilized nanoemulsions also decreased from 244 ± 36 nm for the unmodified to 180 ± 19 and 167 ± 13 nm in 5,000 psi and 15,000 psi homogenized LPI nanoemulsions, respectively. For 2 wt% LPI nanoemulsions no significant change in droplet size was observed between the control and 5,000 psi homogenized LPI-nanoemulsions. No difference in average free droplet diameter was observed after 28 days for all nanoemulsions (Figure 4.4b), however, this measure does not indicate the extensive protein and droplet aggregation upon storage which was evident from the droplet size distribution (Figure 4.3).

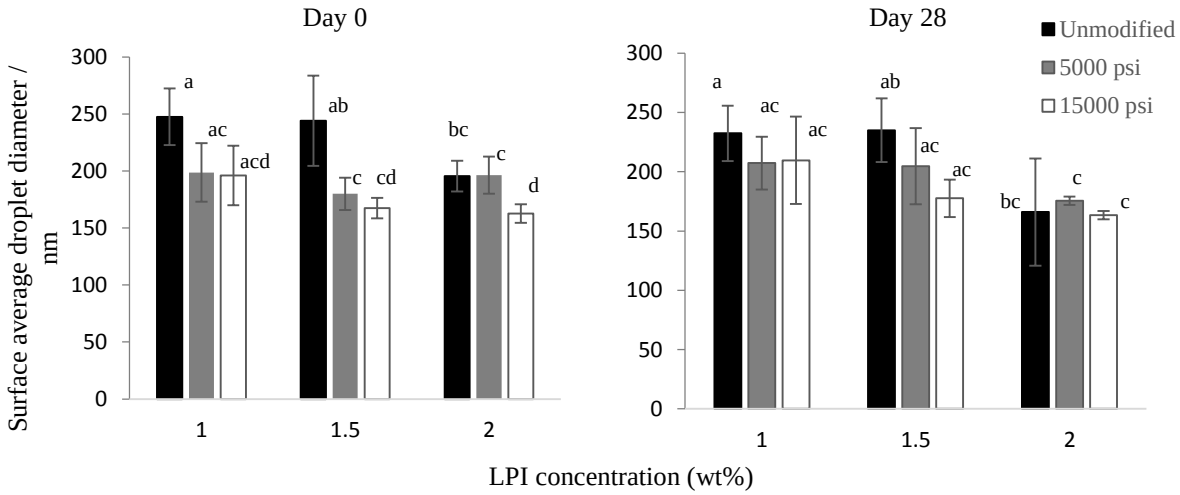

Figure 4.4 Surface average droplet diameter (d_{32}) for nanoemulsions prepared with unmodified LPI solutions (black) and with homogenized LPI solutions grey-5,000 psi) and (white-15,000 psi) on (a) day 0 and (b) day 28 for 1, 1.5, and 2 wt% LPI concentrations. Data with different letters on day 0 and day 28 graphs are significantly different ($p < 0.05$). No significant difference was observed in the data obtained from the same sample on day 0 and day 28.

Zeta-potential for all the nanoemulsions was between +17 to +19 mV at pH 3, while the values for the protein solutions were significantly lower (ranged between +15 to +16 mV) (Figure 4.5). The increase in zeta potential when the proteins are present at the oil droplets surface could be due to surface denaturation of protein. During emulsification, the lentil protein molecules changes their conformation and open up their structure exposing the hydrophobic portion for adsorption in the oil phase and the hydrophilic amino acids in the aqueous phase. It is possible that such re-organization of protein's molecular structure at the oil droplet surface led to an increase in exposure of charged amino acids leading to a higher zeta potential for the protein coated oil droplets compared to the proteins themselves. There was no significant difference in zeta-potential between 5,000 and 15,000 psi homogenized LPI or with various LPI concentrations. However, as a function of time, zeta potential of the nanoemulsions significantly decreased, which could be due to re-organization of the proteins at the oil droplet surface or interaction with neighbouring molecules leading to a shielding of the charged amino acids.

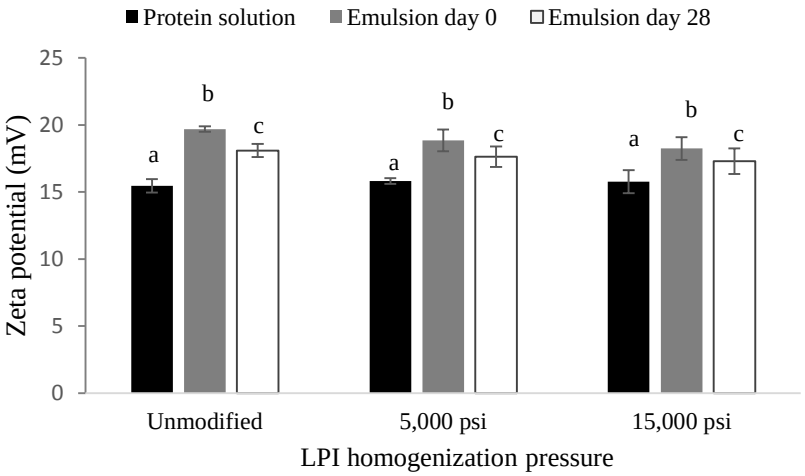

Figure 4.5 Zeta potential for unmodified and high-pressure homogenized LPI solutions and nanoemulsions on day 0 and day 28 for 1.5 wt% LPI concentrations. Data with different letters are significantly different ($p < 0.05$).

4.4.3 Storage stability of the nanoemulsions under accelerated gravitation

The accelerated storage stability of the nanoemulsions was also determined in the photocentrifuge similar to the protein solutions. In Figure 4.6 transmission profiles of nanoemulsions with 1.5 wt% protein are shown. It can be seen that for freshly prepared nanoemulsions no difference in the transmission profiles can be seen between unmodified and homogenized LPI. All of them showed no movement under accelerated gravitation, which must be due to the improved stability of the nanoemulsions. It should be noted that when the protein solutions were tested under similar condition (Figure 4.2), extensive sedimentation was observed leaving a clear aqueous phase on top. Therefore, no separation for the nanoemulsions indicates that by emulsification, it was possible to overcome the insolubility in LPI. Nevertheless, after 28 days all nanoemulsions showed phase separation under accelerated gravitation where a low transmission near the top followed by a high transmission region in the middle and sedimentation of LPI at the bottom of the cuvettes. The change in transmission profiles of all the nanoemulsions after 28 days indicates increase in protein aggregation upon storage which could negatively impact nanoemulsion stability. The thickness of the upper low-transmission opaque region was lower in case of unmodified LPI compared to the homogenized ones. As all nanoemulsions have only 5 wt% oil phase, the extent of the upper opaque layer indicates the presence of LPI along with oil droplets. The microstructure of the nanoemulsions (shown below in Figure 4.8) showed an extensive aggregated state of oil droplets and LPI particles, which could be responsible for the formation of thick opaque layer at the top of the emulsions. It was possible that the presence of finer LPI particles and smaller oil droplets in the homogenized nanoemulsions improved their stability, hence less movement of the emulsion layer was observed in them.

In order to quantify the stability under accelerated gravitation, the instability indices of all nanoemulsions was calculated from their transmission profiles and shown in bottom panel of Figure 4.6. Instability index is a measure of emulsion stability where a maximum value of 1 refer to complete destabilization or separation of the phases under the centrifugal force and zero refers to highly stable emulsions with no separation of the phases. Overall, instability indices decreased as the LPI concentration increased from 1 to 2 wt% LPI ($p < 0.05$) because of the increased viscosity (shown below) for the 2 wt% LPI-stabilized nanoemulsion which slowed down movement of droplets and protein aggregates under accelerated gravity. On day 0 all

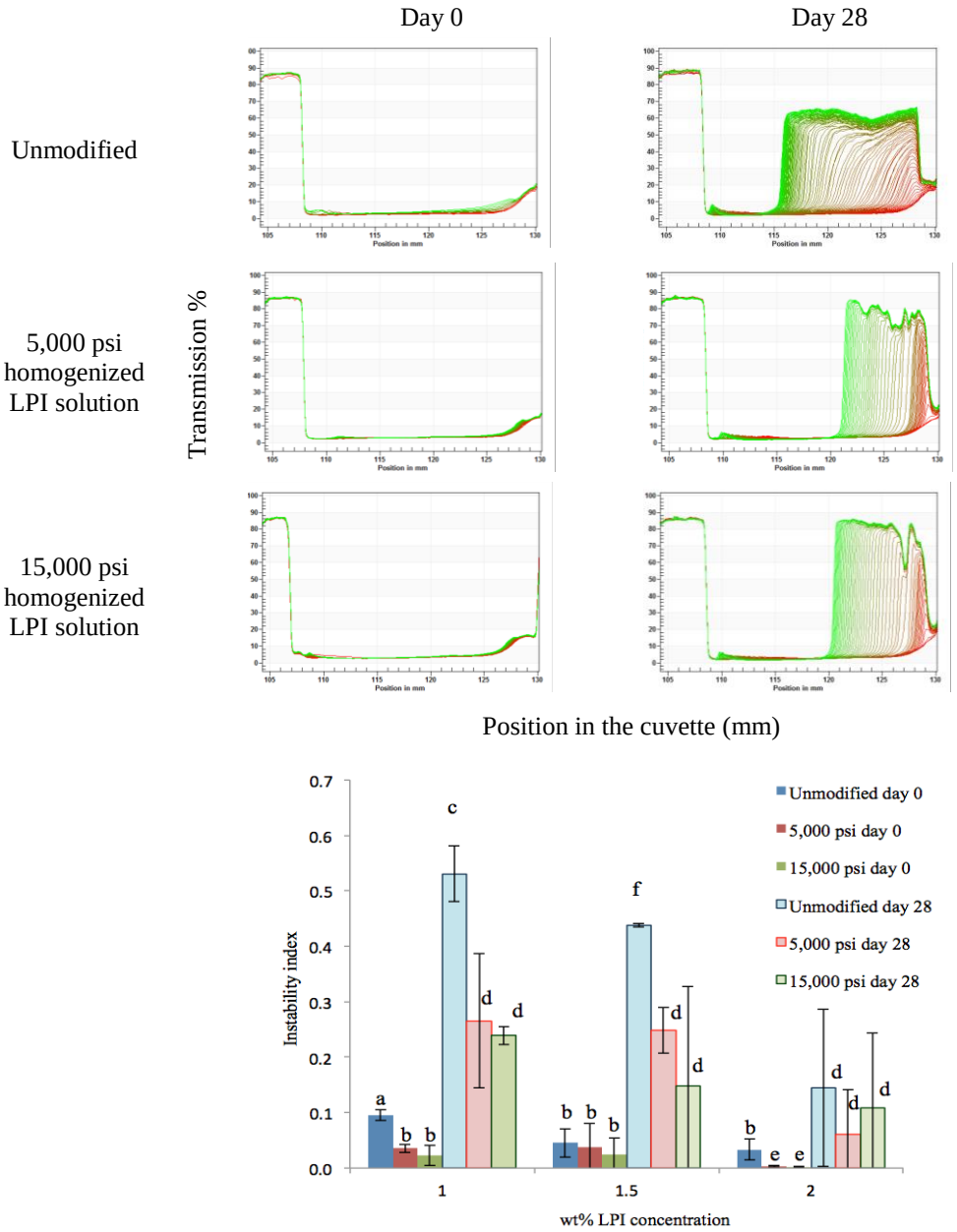

Figure 4.6 Top: Photocentrifuge transmission profiles of nanoemulsions prepared with 1.5 wt% LPI on day 0 and day 28. Bottom: Instability indices of all the nanoemulsions prepared with unmodified, 5,000 and 15,000 psi homogenized LPI solutions at 1, 1.5, and 2 wt% concentration calculated from photocentrifugal transmission profiles on day 0 and day 28. Data with different letters are significantly different ($p < 0.05$).

nanoemulsions were very stable and almost no difference was observed among the various nanoemulsions, except at 1 wt% LPI, where high-pressure homogenization of LPI solutions significantly improved stability of nanoemulsions ($p < 0.05$). After 28 days instability indices significantly increased from day 0, but the values for homogenized samples were significantly lower ($p < 0.05$) than the unmodified LPI containing samples, except for 2 wt% LPI, where increased viscosity due the presence of higher amount of LPI prevented droplet movement and hindered laser transmission. Increase in instability indices with time is consistent with the droplet size distribution results, which showed extensive increase in the peak above 1 μm due to protein aggregation.

4.4.4 Viscosity of LPI nanoemulsions

The viscosity of the nanoemulsions prepared by homogenized LPI solutions was measured and compared with the control in order to understand whether their flow behaviour was impacted due to the high-pressure treatment of LPI solutions. For all nanoemulsions viscosity decreased as the shear rate increased, indicating shear thinning behaviour (Figure 4.7). Low shear viscosity of the nanoemulsion also increased with increase in protein concentration. For example, viscosity of the nanoemulsions with unmodified LPI at 0.01 s^{-1} shear rate was 0.5, 1.0, and 5.0 for 1, 1.5 and 2 wt% LPI, respectively. The significantly higher initial viscosity of 2 wt% LPI-stabilized nanoemulsions compared to the 1 or 1.5 wt% LPI-stabilized nanoemulsions could be due to the formation of stronger and larger protein-droplet network which was also evident from the PSD data and supports our hypothesis behind its decreased instability index. The viscosity of 1 and 1.5 wt% LPI-stabilized nanoemulsions (prepared by high-pressure treated LPI solutions) at 5,000 and 15,000 psi did not change compared to the unmodified control (Figure 4.7a and 7b). The 2 wt% LPI-stabilized nanoemulsion (prepared by high-pressure treated LPI solution) showed slightly higher initial viscosity compared to the unmodified sample (Figure 4.7c).

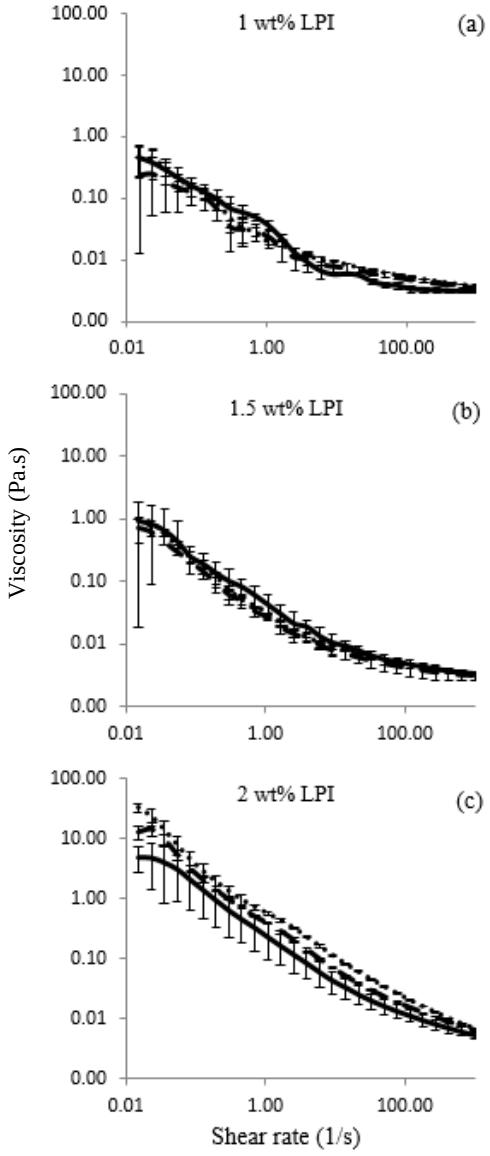

Figure 4.7 Viscosity of nanoemulsion; (--) prepared with unmodified LPI solution, (- -) 5,000 psi and (….)15,000 psi LPI homogenized for (a) 1 wt% LPI (b) 1.5 wt% LPI and c) 2 wt% LPI as a function of shear rate. Overall data for different protein treatments at a particular concentration were not significantly different, however, initial values of viscosity for different concentrations of LPI were significantly different.

4.4.4 Microstructure of LPI nanoemulsions

Confocal microscopy was used to compare the microstructure of all LPI-stabilized nanoemulsions with and without the protein homogenization step (Figure 4.8). All the nanoemulsions made with unmodified proteins contained large aggregates along with oil droplets. No strong interconnected protein and oil droplet network can be viewed in the nanoemulsions with 1 and 1.5 wt% LPI, giving rise to their lower viscosity compared to 2 wt% LPI nanoemulsions, which showed numerous protein aggregates and oil droplets. The most striking difference in the microstructure of the nanoemulsions made with homogenized LPI is the lack of protein aggregates. Homogenizing LPI prior to emulsification significantly reduced their size. Nevertheless, few large aggregates of proteins can still be observed and their number increased with increase in protein concentration. The microstructure of the nanoemulsions also showed extremely small oil droplets, most of them in an aggregated state possibly due to depletion flocculation by excess unadsorbed LPI and its non-protein components and hydrophobic interactions among the LPI-coated droplets. For some large free oil droplets, interfacial proteins can also be seen (arrow in Figure 4.8). The nanoemulsions stabilized by 2 wt% LPI showed more protein and droplet aggregation than 1 or 1.5 wt% LPI-stabilized nanoemulsions which are consistent with the droplet size distribution (Figure 4.4) and viscosity data (Figure 4.7). Increase in droplet aggregation with protein concentration could also be related to the presence of excess soluble proteins leading to depletion flocculation (Yerramilli & Ghosh, 2017). SEM images of LPI nanoemulsions also showed aggregated droplet structure (Figure 4.9). The 100,000 times magnified SEM images also showed the presence of smooth coating of proteins on the nanodroplets surface.

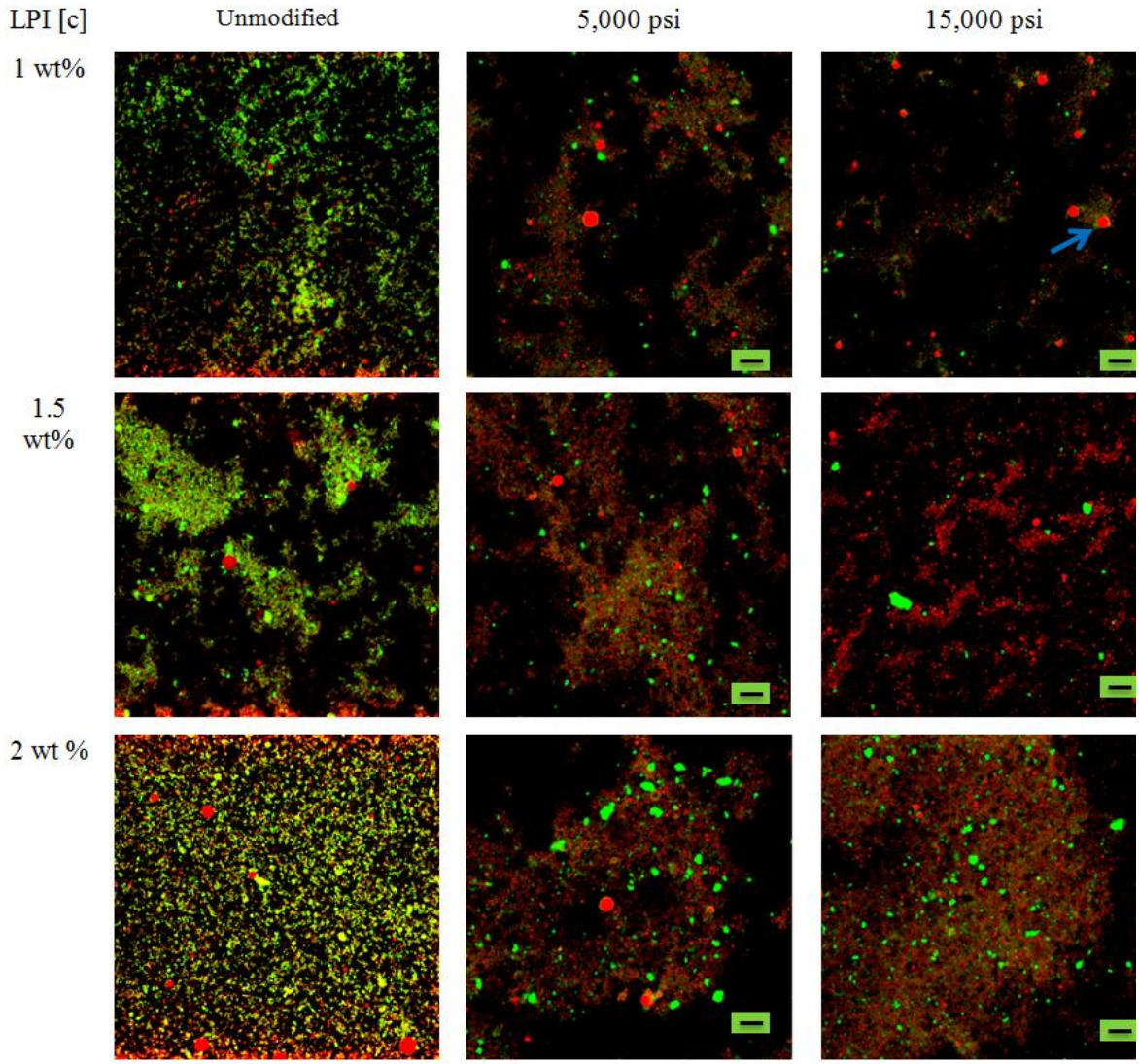

Figure 4.8 Images from confocal microscopy at 1500x magnification for 1, 1.5 and 2 wt% LPI-stabilized nanoemulsion prepared with unmodified and 5,000 and 15,000 psi homogenized LPI solutions. The red color represents the oil droplets while the green color represents the LPI in the continuous phase of the nanoemulsions. Arrow indicates presence of protein at the oil droplet surface. Scale bar measures 5 μm.

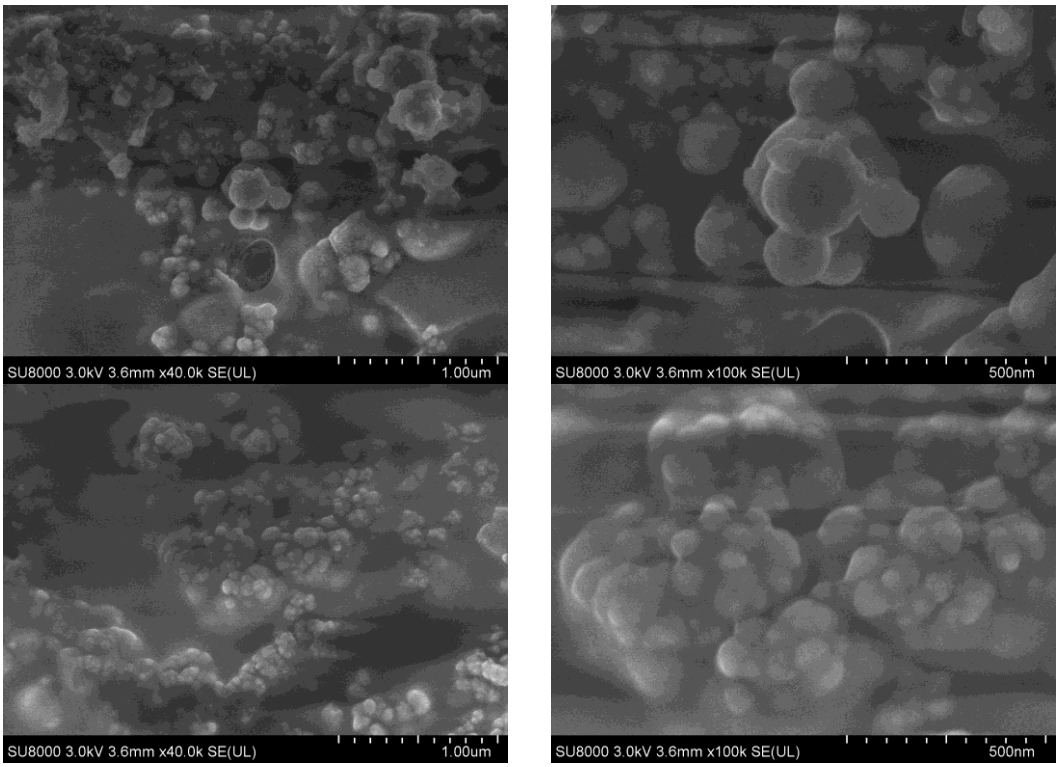

Figure 4.9 SEM images of 5,000 psi homogenized LPI (1.5 wt%)-stabilized nanoemulsions under two different magnifications. Scale bars and magnifications are indicated on the images.

4.4.5 Mechanism of improved stabilization of homogenized LPI nanoemulsions

Results from droplet size distribution, average droplet size, stability under accelerated gravitation and microstructure of the LPI nanoemulsions indicates that high-pressure homogenization of LPI prior to emulsification significantly improved the stability under 28 days of storage, although no difference between the two protein homogenization pressures was observed. Microscopy showed reduction in protein particle size and aggregation behaviour upon homogenization, although significant droplet aggregation was evident. In order to understand the mechanism of improved emulsification behaviour of the homogenized LPI, we determined oil/water interfacial tension, surface hydrophobicity and interfacial rheology of the protein solutions upon high-pressure homogenization. As a control, unmodified LPI solutions were also tested.

Interfacial tension

Figure 4.10a shows the oil/water interfacial tension values of the protein solutions as a function of concentration and homogenization condition. Addition of LPI in the aqueous phase significantly decreased the interfacial tension from 22.5 ± 0.85 without proteins to 12.68 to 14.84 in presence of proteins. No significant difference in the interfacial tension was observed when LPI concentration increased from 1 to 2 wt% ($p > 0.05$), which indicates that 1 wt% LPI was enough to saturate the oil/water interface. There is a trend of decreasing interfacial tension from unmodified to 5,000 and 15,000 psi homogenization condition, however, the values are not significantly different from each other ($p > 0.05$). Bouaouina et al. (2006) investigated interfacial tension and emulsification behaviour of dynamic high-pressure treated whey protein isolates using an ultra high-pressure homogenizer at different pressures up to 300 MPa. Similar to the present case, the authors also observed significant decrease in protein particle size upon high-pressure homogenization which was responsible for faster surface adsorption kinetics of the homogenized proteins and led to a rapid initial decrease in dynamic interfacial tension as a funcion of time compared to the unmodified proteins. However, after about an hour, equilibrium interfacial tension did not show any significant change between the high-pressure treated and unmodified proteins. In the present case only the equilibrium interfacial tension was measured and similar to Bouaouina et al. (2006), no difference was observed.

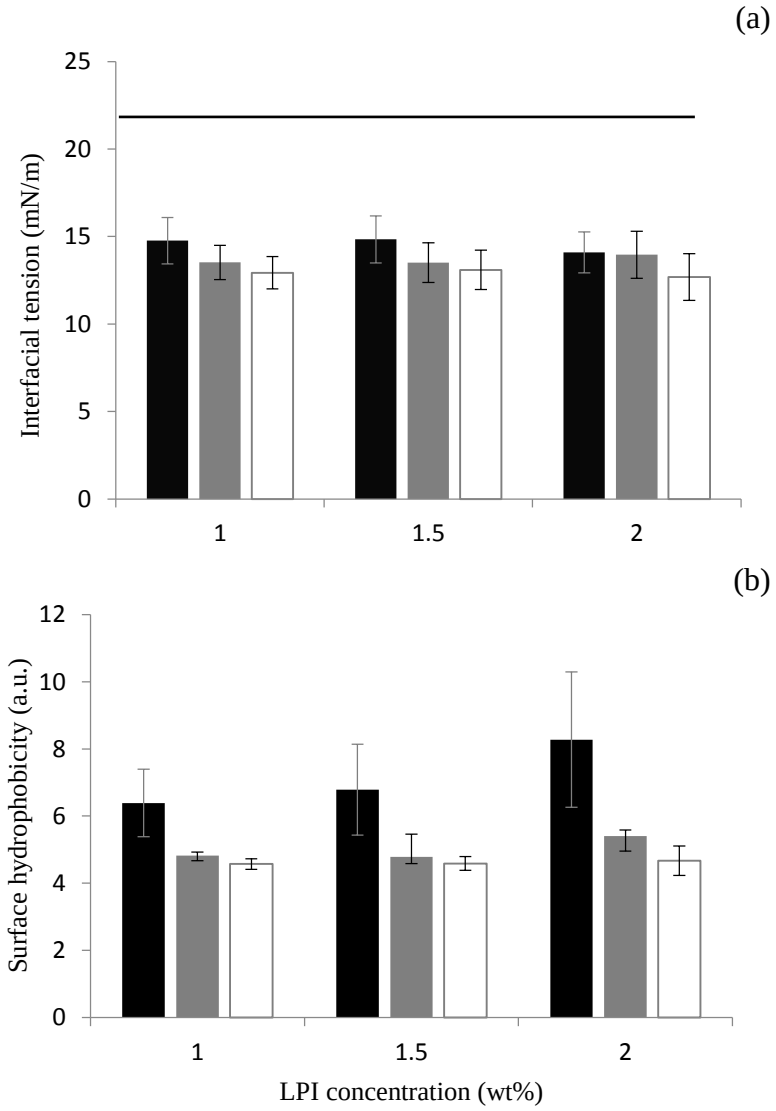

Figure 4.10 (a) Interfacial tension and (b) surface hydrophobicity of LPI solutions (black-unmodified) and high-pressure homogenized at (grey-5,000 psi) and (white-15,000 psi) pressure at different concentrations. Black line on (a) indicates oil/water interfacial tension without any proteins.

Surface hydrophobicity

Surface hydrophobicity of the protein solutions as a function of concentration and homogenization condition is given in Figure 4.10b. No significant difference in surface hydrophobicity was observed as the LPI concentration increased from 1 to 2 wt% ($p > 0.05$). However, surface hydrophobicity significantly decreased when the protein solutions were homogenized compared to the unmodified protein solution ($p < 0.05$). For example, at 1.5 wt% surface hydrophobicity decreased from 6.79 ± 1.35 for unmodified LPI to 4.59 ± 0.21 for 15,000 psi homogenized LPI solution. No significant difference in surface hydrophobicity was observed between 5,000 and 15,000 psi homogenization of protein solution ($p > 0.05$). Many authros studied effect high-pressure treatment on soy protein's hydriphobicity and generally an increase in surface hydrophobicity was obsered with increase in pressure above 200 MPa due to partial unravelling of the buried hydrophobic groups, although the extent of increase was found to be concentration and pH dependent (Molina et al., 2001; Puppo et al., 2004). For example, Wang et al. (2008) found that below 3 wt% SPI, surface hydrophobicity increased when pressure inceased from 0.1 to 600 MPa, while for 5 wt% SPI it slowly increased till 400 MPa, follwoed by a significant decrease at 600 MPa. It was proposed that at higher protein concentration and pressure upto 400 MPa partially unfolded proteins could re-aggregate partially leading to a less increase in the hydrophobicity, while at 600 MPa, completely denatured proteins re-associates due to exposure of hydrophobic groups and further decrease in hydrophobicity. Nevertheless, Puppo et al. (2004) observed that for 1 wt% soy protein isolates at pH 3 increasing pressure from 0.1 to 200 MPa showed a decrease in surface hydrophobicity follwoed by rapid increase at 400 MPa. Similarly, in the present case, decrease in surface hydrobicity upon homogenization at 5,000 psi (34 MPa and 15,000 psi (103 MPa) could be due to aggregation of LPI molecules, thereby re-covering them within the interior of a larger aggregates.

Interfacial rheology

Protein's adsorption at the oil/water interface significantly improves interfacial strength and the ability to resist deformation (Freer et al., 2004). Depending on the protein type, conformation, and the nature of the intra- and intermolecular interactions at the oil droplet surface a protein-stabilized interface may display viscous (e.g., flexible and disordered beta casein) or viscoelastic (e.g., globular and ordered lysozyme) behaviour (Freer et al., 2004). The

adsorption process of both types of proteins to the oil/water interface follow a three-step regimes, which starts with movement of proteins towards the interface (regime I), formation of monolayer (regime II) and finally adsorption of multilayer of proteins and formation of network or crosslinks among the adsorbed protein molecules (regime III) (Baldursdottir et al., 2010). In most cases, detection of protein adsorption at the interface in the regime I is not possible using interfacial rheology measurement, as no interactions happened among the very few molecules at the interface. In the present case evolution of interfacial moduli of LPI was measured as a function of time for 1.5 hrs (Figure 4.11). It can be seen that the measurement starts after the cross over of G' over G", followed by a rapid increase in the first 1000 s, indicating significant interfacial interaction among the LPI molecules which may already fall in the regime III. Similar behaviour of evolution of interfacial rheology was also observed for lysozyme. It was proposed that it was not possible to detect the rapid rate of diffusion (regime I) and monolayer formation (regime II) (Baldursdottir et al., 2010). Lysozyme is a small protein with a molecular mass of 14.3 kDa and fast movement is not surprising. However, LPI are multimeric proteins with many subunits where the molecular mass range from 300-400 kDa for hexameric legumin and 150 kDa for trimeric vicilin (Barbana & Boye, 2011). It is surprising that instead of such a large structure, LPI display such a fast movement towards the oil/water interface. Perhaps, the non-disulfide bonded individual subunits of vicilin with lower molecular mass were moving quickly towards the interface and their unfolding and quick adsorption at the interface led to the faster formation of monolayer of proteins. From Figure 4.11a, it can also be observed that as a function of time, G' increased and even after 1.5 hrs (5400 s) no plateau was observed, while G" remain almost constant. It could be due to the multilayer formation and continuous evolution of the interfacial intermolecular interactions among the various fractions of LPI. A similar behaviour was also observed for lysozyme (Baldursdottir et al., 2010).

The determination of time evolution of interfacial moduli was followed by a strain sweep measurement, where the strength of the interfacial elastic network among the LPI molecules were tested by breaking it under high strain (Figure 4.11b). For clarity only the data for 1.5 wt% proteins are presented, all other concentrations showed similar behaviour, which was summarized by comparing the plateau G' and crossover G' in (Figure 4.11c and 8d, respectively. At a lower strain both G' and G" remain constant with the values of G' significantly higher than G". The strong plateau in G' where the moduli are independent of applied strain indicates

formation of strong gelation network at the interface. At about 10% strain G' dropped sharply, indicating yielding in the gel network. Between 30 – 40 % strain crossover of the G' and G" was observed which corresponds to complete breakdown of the interfacial gel network. Beyond the crossover strain G' continuously dropped and G" remains higher that G', indicating fluid-like behaviour of the interfacial proteins due to the lack of interaction and broken network among the LPI molecules.

In order to compare how the effect of high-pressure homogenization and different LPI concentrations influence interfacial rheological behaviour, the plateau G' values from the strain sweep data for all samples were plotted in Figure 4.11c. In general, no change in G' was observed as a function of protein concentration. However, considerable differences were observed between the unmodified and high-pressure homogenized LPI at the interface. In all cases, surface shear modulus (G') for unmodified LPI was significantly higher than both the 5,000 and 15,000 psi homogenized LPI solutions ($p < 0.05$). No significant difference in the crossover G' (Figure 4.11d) or crossover strain was observed among the various samples ($p < 0.05$), indicating indifferent mechanisms for strain-induced breakdown of interfacial elastic membrane.

The difference in plateau G' values of the oil/water interface made up with unmodified and homogenized protein solutions could be used to explain formation and stability of the emulsions formed by them. During emulsion formation, as the protein molecules adsorbed onto a freshly created bare droplet surface, a stronger elastic interface may be better able to prevent droplet disruption under the applied homogenization shear, thereby the droplet size of the emulsion would be higher compared to an emulsion with lesser elastic interface (Langevin, 2000). On the other hand, a stronger elastic interface may be better able to prevent re-coalescence of droplets during homogenization (Schubert and Engel, 2004), therefore a balance between these two opposing factors is needed to generate stable emulsion with small droplets in the nanoscale range. The observation of protein-covered droplet's ability to prevent deformation was also observed by Fischer and Windhab (2011). Similarly, Bouyer et al. (2011) found that gum Arabic formed a stronger elastic interface compared to beta-lactoglobulin and consequently the average droplet size of the resultant emulsion was higher. Both the emulsifiers showed similar interfacial tension, therefore, gum Arabic's ability to prevent droplet disruption during homogenization may have led to a large droplet size compared to beta-lactoglobulin, although

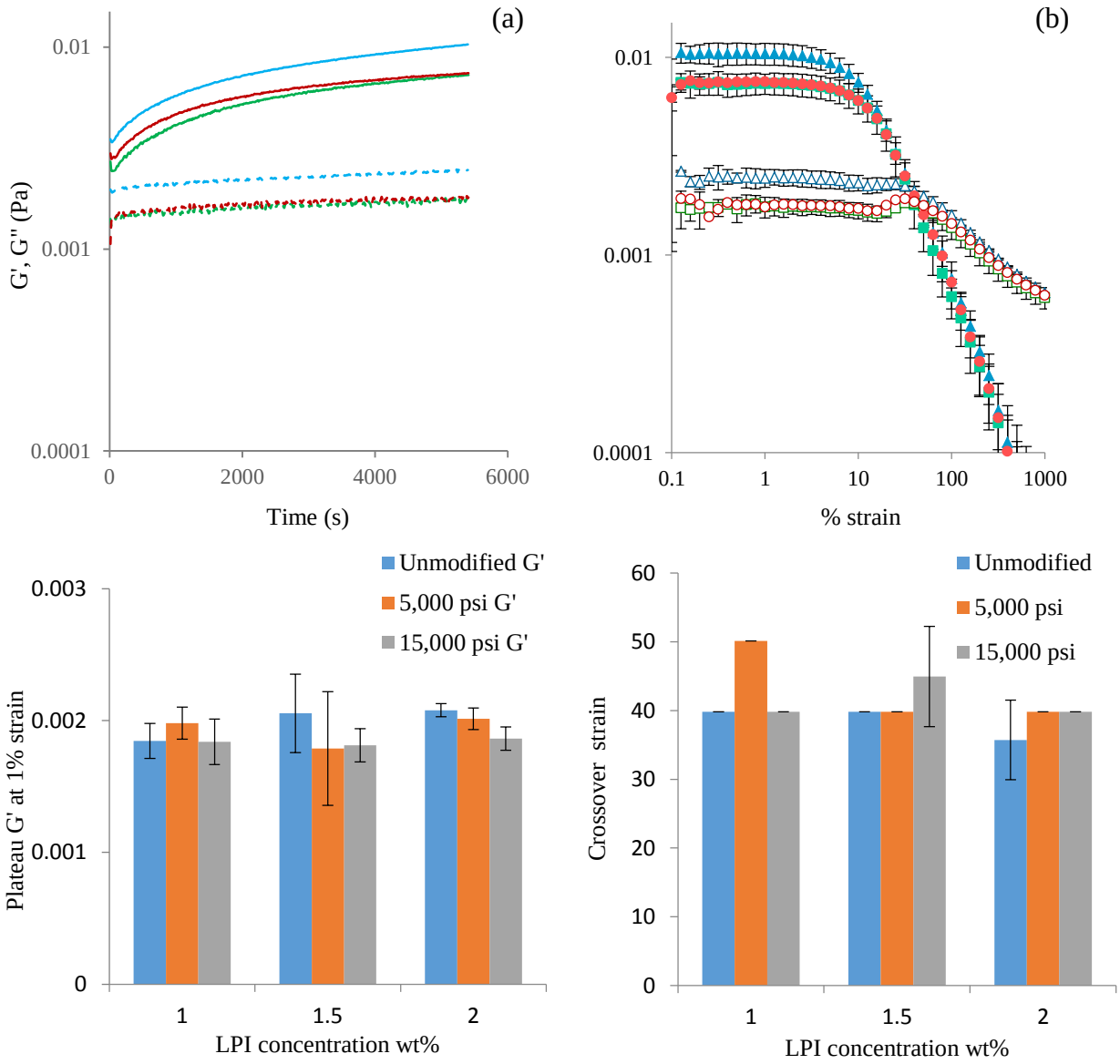

Figure 4.11 Interfacial rheology of LPI solutions prepared with (5,000-green and 15,000-red psi) and without (unmodified-blue) homogenization; solid line, G' and dashed line, G''. (a) Initially, the interface was allowed to form at a constant strain (0.01) and angular frequency (1 rad/s) for 1.5 hrs, followed by (b) strain sweep rheology at a constant angular frequency (1 rad/s). Data for only 1.5 wt% LPI solutions are shown (a) and (b). (c) Plateau G' and (d) crossover G' extracted from the strain sweep rheology data are also shown for better comparison among the different samples.

the authors offered no mechanism. In the present case, the average droplet size and the size distributions of the emulsions made with unmodified LPI solutions were larger than the emulsions made with homogenized-LPI solutions. Therefore, prevention of droplet disruption was more dominant for the nanoemulsions made with unmodified LPI solution, which could be ascribed to their higher interfacial elastic modulus (Figure 4.11c).

4.4.6 Lipid digestibility

Lipid digestibility from oil-in-water nanoemulsion is an indication of the ability of the nanoemulsion to deliver bioactive lipid and lipid-soluble compounds during digestion in gut. In many cases, the interfacial layer around the oil droplets stand as barriers against digestive enzymes and bile salts. Proteins, being more biocompatible, are expected to be easily attacked by proteolytic enzymes, thereby facilitating adsorption of bile salt during intestine digestion leading to displacement of the hydrolysed and reminder of the original proteins from the oil droplet surface. Bile adsorption at the oil/water interface assist attack by lipase and hydrolysis of the lipid in to free fatty acids (FFA) and a mixture of mono and diglyceride. In this work the percent FFA released from the nanoemulsions prepared with unmodified and homogenized LPI after 2 h in simulated stomach conditions followed by 2 h in simulated instential fluids was investigatedand the released FFA was titrated with NaOH in order to determine the extent of lipid digestion. With 1 wt% unmodified LPI percent FFA released from the nanoemulsions was 40.76 ± 1.7. Homogenizing the LPI led to a significant increase in the release of FFA (54.5 ± 3.5 %) compared to the unmodified form ($p < 0.5$), however there was no difference between those nanoemulsions prepared with LPI homogenized at 5,000 and 15,000 psi ($p > 0.05$). The values of % FFA released are also in accordance with the interfacial elastic modulus of the proteins (Figure 4.11), which showed higher elastic modulus for the unmodified LPI compared to the homogenized LPI. It is well reported in literature that higher value of interfacial elasticity may lead to lower breakdown of the interface during in vitro digestion (Singh, Ye and Horne, 2009). As the LPI concentration increased to 1.5 and 2 wt% no significant differences in % FFA release were found between the nanoemulsions prepared with the unmodified LPI (49.4 ± 7.9 %) or homogenized LPI (58.3 ± 7.1 %) ($p > 0.05$). There was also no difference in the amount released between the 1.5 wt% (53.8 ± 9.8 %) and 2 wt% (56.9 ± 5.0 %) LPI nanoemulsions ($p > 0.05$). It

could be due to the presence of higher amount of LPI at the oil droplet surface preventing digestion and non-protein components (carbohydrates) in the continuous phase interferring with the enzymes and bile salts.

4.5 Conclusions

The most stable and flowable nanoemulsions (1, 1.5 and 2 wt% LPI) from the previous work were further investigated in order to improve nanoscale droplet formation and long-term storage stability. High-pressure homogenization of LPI solutions decreased the droplet size of the nanoemulsions below 200 nm and increased their accelerated storage stability compared to the unmodified LPI-stabilized nanoemulsions. Confocal microscopy showed less protein aggregation for the nanoemulsions, prepared with high-pressure treated LPI solutions, compared to the control which was also evident from the lower viscosity of the nanoemulsions. No significant change in the surface average droplet size, or in microstructure was observed between the 5,000 and 15,000 psi homogenized LPI nanoemulsions, indicating 5,000 psi pressure was enough to induce protein disintegration and improvement in their emulsification ability. Homogenization of protein solution did not improve their interfacial tension, however, surface hydrophobicity significantly dropped. Interfacial rheology of the protein solutions indicated stronger network of protein at the droplet surface for the unmodified LPI compared to the homogenized LPI, which also reflected in the lipid digestibility of the nanoemulsions. Unmodified LPI with stronger interface was less digestible under in vitro digestion condition compared to the homogenized ones, which showed possible improvement in the delivery of lipid soluble bioactives. After 28 days, a significant increase in protein aggregation was observed making the nanoemulsions unstable towards phase separation. The storage stability of the nanoemulsions could be further improved by centrifugal separation of the insoluble LPI from the nanoemulsions or from the homogenized-LPI solutions prior to emulsification. Finally, it can be concluded that LPI has a potential to be utilized as an emulsifier in the development of nanoemulsions, although further work is needed to prevent protein re-aggregation with time.

5. GENERAL DISCUSSION

Plant proteins represent a promising alternative to animal-derived proteins and other synthetic compounds as emulsifiers in food applications, since they are sustainable, low in cost, and considered as natural ingredients (leading to cleaner labels) (Day, 2013). Because of their good emulsifying properties they also have a role in the production of oil-in-water nanoemulsions (Donsi et al., 2010). This type of emulsion has tremendous potential in the food and beverage, cosmetic and pharmaceutical sectors since they have the ability to deliver poorly water-soluble ingredients and significantly prolong the product's shelf life (Mason et al., 2006). The overarching goal of the present research was to utilize lentil protein isolate (LPI) for stabilizing oil-in-water nanoemulsions to improve their shelf life and for the delivery of a sensitive core ingredient (omega-3 fatty acid rich oils). Chang et al. (2015) investigated the emulsifying properties of pea, lentil, soy and canola protein isolates in coarse emulsions at different pHs, and found LPI at pH 3 showed the greatest emulsifying properties. At this pH, LPI also displayed the greatest solubility, surface hydrophobicity and formed strong viscoelastic interfaces than at other pHs. Therefore, for this thesis research, LPI was dispersed in a citric buffer at pH 3 for investigating the formation and stability of nanoemulsions.

In the initial study, the effect of LPI concentration (0.5 – 5 wt% LPI) on the formation and flow behaviour of nanoemulsions were investigated, along with their stability over 28 d of storage. All nanoemulsions showed a bimodal droplet size distribution with a smaller peak <1 μm and larger peak >10 μm. A similar particle size distribution was found >10 μm for a protein control solution, indicating the presence of large protein aggregates most likely present within the continuous phase of the nanoemulsions. To obtain a more accurate measurement of droplet size within the nanoemulsion, the droplets average diameter (d_{32}) was determined considering only the peak <1 μm. The average droplet diameter was found to decrease from 338 ± 27 nm to 163 ± 4 nm with increasing LPI concentration from 0.5 to 3 wt%, which then remained constant after 28 d of storage. Findings suggest that smaller droplets were formed at higher LPI concentrations due to the presence of enough protein for adsorption to the bare droplet surface

during homogenization leading to saturation coverage. Accelerated storage stability measured by using a photocentrifuge revealed best stability was obtained for the 1, 1.5 and 2 wt% LPI stabilized nanoemulsions; the 0.5 wt% LPI-stabilized nanoemulsion almost completely separated indicating poor longterm stability; whereas the 3 and 5 wt% LPI-stabilized nnaoemulsions showed rapid separation with droplet-protein gel network sedimentation at the bottom caused by strong aggregation of proteins and droplets. Rheological properties were determine for all LPI solutions and nanoemulsions by measuring their steady shear viscosity and oscillatory strain sweep viscoelastic behaviour. Viscosity measured as a function of shear rate showed shear thinning behaviour for all LPI solutions and nanoemulsions. Viscosity of the nanoemulsions was found to be higher compared to LPI solutions, however for the 2, 3 and 5 wt% LPI-stabilized nanoemulsions, a large increase in viscosity was observed due to the formation of strong protein-droplet network. Viscoelastic behaviour was determined by measuring the dynamic storage (G′) and loss (G″) moduli as a function of strain. The G′ for the 0.5, 1 and 1.5 wt% LPI stabilized nanoemulsions was found to be < G″indicating fluid-like behaviour, whereas for the 2 wt% LPI stabilized nanoemulsions G′ increased and became > G″ suggesting a weak gel-like network was being formed. However, for the 3 and 5wt% LPI stabilized nanoemulsions, G′ increased to a greater extent than at the 2wt% level indicating strong network was being formed. Gelation behaviour was also confirmed by visual observation where nanoemulsions stabilized with 3 and 5 wt% LPI did not flow in response to the force of gravity. It was postulated that gel strength increased with increasing LPI concentration due to the aggregation of unabsorbed proteins in the continuous phase of the nanoemulsions. Extensive protein-protein and protein-droplets aggregation at higher LPI concentration was also observed using confocal scanning laser microscopy. The ability to form a strong viscoelastic gel at the 3 and 5 wt% LPI concentrations with entrapped oil nanodroplets could have potential applications in the food, cosmetic and pharmaceutical sectors. The most stable and flowable nanoemulsions were formed at 1, 1.5 and 2 wt% LPI concentrations, however protein aggregation within the continuous phase was still present which would cause phase separation over an extended time.

Many studies have been conducted in the literature to alter the protein's properties (i.e., solubility, surface activity and size) in an effort to improve their emulsifying properties (Messens, 1997). Therefore in the second study, the effect of shear modification of the LPI at different homogenization pressures and concentrations on the formation and stability of

nanoemulsions was investigated. Based on the first study, the 1, 1.5 and 2 wt% LPI concentrations were chosen to investigate the shear modification at 5,000 and 15,000 psi (via 4 passes through the high-pressure homogenizer) of the LPI solutions prior to nanoemulsions formation. Modification was thought to alter their surface activity and size to help improve their emulsifying properties. These concentrations were chosen since the nanoemulsions formed with unmodified LPI were all found to be stable and non-gelling.

Initially, LPI solutions were subjected to ultasonication to help first break up the protein aggregates, resulting in a shift in particle size distribution from 1 – 100 μm to 1 – 22 μm. After homogenization within the high-pressure homogenizer, aggregate sizes were <1 μm, with a few larger peaks. The latter tended to increase with increasing LPI concentration due to more protein-protein aggregation. Homogenization was found to significantly improve the solubility of LPI relative to the unmodified form, however no differences in solubility was observed between the 5,000 or 15,000 psi pressure indicating that 5,000 psi pressure was sufficient to break up the larger LPI aggregates. While no significant difference was observed for the interfacial tension between different concentrations or different treatments of LPI solutions, the surface hydrophobicity was decreased significantly with homogenization.

Nanoemulsions stabilized by homogenized LPI were found to have a similar bimodal droplet size distribution as those with unmodified LPI, however the distribution was shifted to smaller sizes for all samples. The average droplet size decreased form ~250 nm to <200 nm in the first peak, whereas the second peak (>10 μm) decreased in magnitude indicating that less protein aggregation was occurring. No difference in droplet size distribution was observed between LPI homogenized at different pressures. Less protein aggregation in pre-treated nanoemulsions was also confirmed by using confocal scanning laser microscopy. After 28 d of storage, the droplet size distribution started to shift towards larger sizes due to protein aggregation for all nanoemulsions, however the ones stabilized with homogenized LPI was to a lesser extent suggesting improved stability. It was postulated that the lower surface hydrophobicity of the pre-homogenized LPI solutions may have resulted in less protein aggregation occurring within the pre-homogenized nanoemulsion.

An *in vitro* lipid digestibility model involving simulated gastric and intestine fluids was used to measure the release of free fatty acids from the LPI-stabilized nanoemulsions. Lipid digestibility of the 1 wt% LPI stabilized nanoemulsions was found to increase for homogenized

LPI-stabilized nanoemulsions compared to the unmodified one. Interfacial rheology indicated that the homogenized LPI interfacial film had lower G′ values than the un-modified LPI film indicating a weaker viscoelastic film was being formed. Subsequently, this allowed for easier displacement of protein from the interface by bile salts and give better accessibility for the lipase (Maldonado-Valderrama et al., 2011). No difference in lipid digestibility was observed between unmodified and homogenized LPI nanoemulsions at the 1.5 and 2 wt% LPI concentrations probably due to denser adsorption of proteins on the oil droplets surface and the presence of other insoluble components (carbohydrates, lipids etc.) of the LPI.

Overall, homogenization of the LPI solutions resulted in nanoemulsions that were more stable and had greater digestibility than that without modification. Findings could significantly improve their applications in the food, cosmetic and pharmaceutical sectors since they show improved quality attributes (i.e., stability and release/digestibility).

6. OVERALL CONCLUSIONS

The initial study enable us to gain a better understanding of the impact LPI concentration on the ability to form stable nanoemulsions, as well to understand the change in flow behaviour as a function of LPI concentration. Nanoemulsions stabilized with 0.5 wt% LPI destabilized over the 28 d period due to insufficient coverage of oil droplet surface. The most stable and flowable nanoemulsions were formed at a LPI concentration of 1, 1.5 and 2 wt% LPI concentration, with 2 wt% LPI stabilized nanoemulsion showing the greatest stability because of excess unabsorbed proteins in the continuous phase which formed a protein-droplet network that prevented the movement of droplets (creating a weak gel-like structure). However, protein aggregation with time at these concentrations lead to phase separation and destabilization of the nanoemulsions, therefore further improvement to the emulsifying properties of LPI is warranted. Fluid nanoemulsions at pH 3 and low oil volume fractions stabilized solely by lentil protein as a natural ingredient can be applied in the beverage sector as a base for sports drinks and various juices. The addition of flavors, colors or bioactive compounds within the omega-3 fatty acid rich canola oil phase could provide better protection against oxidation to prevent off flavors and discoloration of the product, or for controlled delivery purposes. Nanoemulsions stabilized with 3 and 5 wt% LPI also showed good stability with very small droplet size. However the higher amount of unabsorbed protein in the continuous phase caused extensive droplet-protein aggregation resulting in the formation of a viscoelastic gel with many potential applications in food industry. Formation of gel at only 5 wt% canola oil could be used in development of low fat products such as spreads or creams.

The second study gave us a better understanding of the effect of high-pressure homogenization on the modification of LPI as a means of improving the shelf life and properties of the formed nanoemulsions. Homogenization of LPI prior to nanoemulsion formation showed significantly improved emulsifying properties, such as fewer aggregates, greater solubility and lower surface hydrophobicity than unmodified LPI. They also formed more stable nanoemulsions with smaller droplet sizes. Because of these properties, homogenized LPI was

postulated to migrate at a faster rate to the interface where it then is absorbed. The homogenized LPI also led to nanoemulsions with a weaker) viscoelastic interfacial film, which allowed for improved lipid digestibility relative to when unmodified LPI stabilized the interface since greater pepsin hydrolysis and easier displacement of proteins by bile salts allowed for greater accessibility of the lipases. Higher lipid digestibility can influence the nutritional value of a product by improving the delivery of bioactive compounds within the oil phase. High-pressure homogenization of LPI (a physical treatment of protein) is an effective strategy for modifying protein functionality for enhanced emulsification, which can then be applied to improve products within the food, cosmetic or pharmaceutical sectors.

7. FUTURE STUDIES

Nanoemulsions developed as part of this work showed improved long-term stability due to reduced average oil droplet size and less protein aggregation in the continuous phase. This was achieved through the disruption of large protein aggregates to smaller protein particles using high-pressure homogenization (at 5,000 and 15,000 psi). In many studies, higher pressures were used to modify the conformation of proteins, with changes to quaternary, tertiary and secondary structure being observed with pressures between 200 – 600 MPa (equivalent to 29,000 – 87,000 psi) (De Maria et al., 2016; Puppo et al., 2004). Unfolding of proteins due to a high-pressure leads to the exposure of hydrophobic domains or charged amino acids which enhance the surface activity of the protein and efficiency in reducing the droplet size (Puppo et al., 2005). There are also other strategies for modifying the protein structure, including chemical and enzyme modification; enzymatic hydrolysis/ high-pressure treatments (Chen et al., 2016); or heat/ enzymatic hydrolysis (Avramenko, 2016). Another strategy to improve the long-term stability of nanoemulsions could be with the removal of insoluble proteins within the LPI by centrifugation or filtration prior to emulsification. This would prevent the sedimentation of large insoluble protein aggregates, fibers and polysaccharides. This would be especially important in beverage-type products where sedimentation and aggregation of particles are not desired. The formation of nanoemulsions using only the soluble proteins of LPI (unmodified and modified) should be explored.

In addition, the formation of nanoemulsions-based gel-like structures should also be explored further for potential applications. Having strong protein-droplet aggregation at higher protein concentrations and low oil volume fractions result in the formation of viscoelastic gel which has a potential applications in controlled food structure (e.g., in low fat products) and for controlled delivery purposes. However a more comprehensive gelation study needs to be carried out involving the nanoemulsion-based gel, including the impact of temperature, time and salts on the network strength, melting profiles, swelling properties and morphology.

Another method to reduce the oil droplet size and improve the long-term stability of LPI-stabilized nanoemulsions would be solvent evaporation. In this method a regular micron size emulsion of oil-solvent mixture is prepared and the solvent is evaporated under vacuum leaving the interfacial protein layer intact and leading to shrinkage of the micron size oil droplets into nanodroplets. Some examples of common solvents used in food industry are hexane and ethyl acetate. Removal of solvent from the oil droplets will not affect the interfacial protein layer, but shrink the micron size oil droplets into nanodroplets. After complete evaporation of solvent we will have an oil-in-water nanoemulsion stabilized with thick layer of proteins (Lee et al., 2011). Moreover, the higher the initial amount of organic solvent mixed with the oil the smaller would be the final oil droplet size after evaporation (Fryd & Mason, 2010).

One of the most promising potential for nanoemulsions, especially in the applications of beverages, is the delivery of nutrients or bioactive compounds. Incorporation of bioactive components such as omega-3 fatty acids, β-carotene or curcumin (Komaiko et al., 2016; Salvia-Trujillo et al., 2013; Zou et al., 2015) into a food or beverage could have positive effect on the health (McClements et al., 2016). Our *in vitro* study showed that nanoemulsions prepared with high-pressure treated LPI had higher lipid digestibility due to smaller oil droplet size and weaker interfacial film which can improve the bioaccessibility of potential bioactive component. However, these compounds might be more susceptible to oxidation due to a higher surface area, therefore their oxidative stability should to be further studied. Some bioactive components could get degraded on the way through the gastrointestinal tract due to changes in physiological conditions (pH, ionic strength or enzymes) (Kenmogne-Domguia et al., 2014). Therefore nanoemulsions could be tested for a targeted release of bioactive component or lipids using a layer-by-layer technique. In this method, oil droplets are stabilized by multiple interfacial layers due to electrostatic attraction of oppositely charged biopolymers (protein and polysaccharide). They could pass harsh chemical conditions of the stomach without destabilization and then release the bioactives at the location of action (e.g., small intestine) (McClements et al., 2008). This knowledge could also be used for the delivery and controlled release of bioactive ingredients into the nanoemulsions.

8. REFERENCES

Acosta, E. (2009). Bioavailability of nanoparticles in nutrient and nutraceutical delivery. *Current Opinion in Colloid & Interface Science, 14*(1), 3-15.

Ali, A., Mekhloufi, G., Huang, N., & Agnely, F. (2016). β-lactoglobulin stabilized nanemulsions—Formulation and process factors affecting droplet size and nanoemulsion stability. *International Journal of Pharmaceutics, 500*(1-2), 291-304.

Armand, M., Pasquier, B., André, M., Borel, P., Senft, M., Peyrot, J., Salducci J., Portugal, H., Jaussan, V., Lairon, D. (1999). Digestion and absorption of 2 fat emulsions with different droplet sizes in the human digestive tract. *The American Journal of Clinical Nutrition, 70*(6), 1096-106.

Arzeni, C., Pérez, O. E., & Pilosof, A. M. R. (2012). Functionality of egg white proteins as affected by high intensity ultrasound. *Food Hydrocolloids, 29*(2), 308-316.

Avramenko, N. A., Low, N. H., & Nickerson M. T. (2013). The effects of limited enzymatic hydrolysis on the physicochemical and emulsifying properties of a lentil protein isolate. *Food Research International, 51*(1), 162-169.

Avramenko, N.A., Chang, C., Low, N. H., & Nickerson, M. T. (2016). Encapsulation of flaxseed oil within native and modified lentil protein-based microcapsules. *Food Research International, 81*, 17-24.

Baldursdottir, S. G., Fullerton, M. S., Nielsen, S. H., & Jorgensen, L. (2010). Adsorption of proteins at the oil/water interface—Observation of protein adsorption by interfacial shear stress measurements. *Colloids and Surfaces B: Biointerfaces, 79*(1), 41-46.

Barbana, C., & Boye, J. I. (2011). Angiotensin I-converting enzyme inhibitory properties of lentil protein hydrolysates: Determination of the kinetics of inhibition. *Food Chemistry, 127*(1), 94-101.

Bergenholtz, J., Poon, W. C. K., & Fuchs, M. (2003). Gelation in model colloid−polymer mixtures. *Langmuir, 19*(10), 4493-4503.

Bouaouina, H., Desrumaux, A., Loisel, C., & Legrand, J. (2006). Functional properties of whey proteins as affected by dynamic high-pressure treatment. *International Dairy Journal, 16*(4), 275-284.

Bouyer, E., Mekhloufi, G., Potier, I. L., Kerdaniel, T. d. F. D., Grossiord, J.-L., Rosilio, V., & Agnely, F. (2011). Stabilization mechanism of oil-in-water emulsions by β-lactoglobulin and gum arabic. *Journal of Colloid and Interface Science, 354*(2), 467-477.

Boye, J. I., Aksay, S., Roufik, S., Ribéreau, S., Mondor, M., Farnworth, E., & Rajamohamed, S. H. (2010). Comparison of the functional properties of pea, chickpea and lentil protein concentrates processed using ultrafiltration and isoelectric precipitation techniques. *Food Research International, 43*(2), 537-546.

Chang, C., Tu, S., Ghosh, S., & Nickerson, M.T. (2015). Effect of pH on the inter-relationships between the physicochemical, interfacial and emulsifying properties for pea, soy, lentil and canola protein isolates. *Food Research International, 77 (3),* 360-367.

Chantrapornchai, W., & McClements, D. J. (2002). Influence of NaCl on optical properties, large-strain rheology and water holding capacity of heat-induced whey protein isolate gels. *Food Hydrocolloids, 16*(5), 467-476.

Chen, L., Chen, J., Yu, L., & Wu, K. (2016). Improved emulsifying capabilities of hydrolysates of soy protein isolate pretreated with high-pressure microfluidization. *LWT - Food Science and Technology, 69,* 1-8.

Dagorn-Scaviner, C., Gueguen, J., & Lefebvre, J. (1987). Emulsifying properties of pea globulins as related to their adsorption behaviours. *Journal of Food Science, 52*(2), 335-341.

Damodaran, S. (2005). Protein stabilization of emulsions and foams. *Journal of Food Science, 70*(3), R54-R66.

Day, L. (2013). Proteins from land plants – Potential resources for human nutrition and food security. *Trends in Food Science & Technology, 32*(1), 25-42.

De Maria, S., Ferrari, G., & Maresca P. (2016). Effects of high hydrostatic pressure on the conformational structure and the functional properties of bovine serum albumin. *Innovative Food Science and Emerging Technologies, 33,* 67-75.

Detloff, T., Sobisch, T., Lerche, D. (2013) Instability Index. *Dispersion Letters Technical* T4, 1-4.

Dickinson, E. (1994). Protein-stabilized emulsions. *Journal of Food Engineering*, *22*(1), 59-74.

Dickinson, E., Radford, S. J., & Golding, M. (2003). Stability and rheology of emulsions containing sodium caseinate: combined effects of ionic calcium and non-ionic surfactant. *Food Hydrocolloids, 17*(2), 211-220.

Donsì, F., Senatore, B., Huang, Q., & Ferrari, G. (2010). Development of novel pea protein-based nanoemulsions for delivery of nutraceuticals. *Journal of Agricultural and Food Chemistry, 58*(19), 10653-10660.

Duranti, M. (2006). Grain legume proteins and nutraceutical properties. *Fitoterapia, 77*(2), 67-82.

Euston, S. R., Finnigan, S. R., & Hirst, R. L. (2000). Aggregation kinetics of heated whey protein-stabilized emulsions. *Food Hydrocolloids, 14*(2), 155-161.

Fernandez-Avila, C., Arranz, E., Guri, A., Trujillo, A. J., & Corredig, M. (2016). Vegetable protein isolate-stabilized emulsions for enhanced delivery of conjugated linoleic acid in Caco-2 cells. *Food Hydrocolloids, 55*, 144-154.

Fischer, P., & Windhab, E. J. (2011). Rheology of food materials. *Current Opinion in Colloid & Interface Science, 16*(1), 36-40.

Freer, E. M., Yim, K. S., Fuller, G. G., & Radke, C. J. (2004). Interfacial rheology of globular and flexible proteins at the hexadecane/water interface: comparison of shear and dilatation deformation. *Journal of Physical Chemistry B, 108*(12), 3835-3844.

Fryd, M. M., & Mason, T. G. (2010). Time-dependent nanoemulsion droplet size reduction by evaporative ripening. *The Journal of Physical Chemistry Letters, 1*(23), 3349-3353.

Gillingham, L. G., Harris-Janz, S., & Jones, P. J. H. (2011). Dietary monounsaturated fatty acids are protective against metabolic syndrome and cardiovascular disease risk factors. *Lipids, 46*(3), 209-228.

Golding, M., & Wooster, T. J. (2010). The influence of emulsion structure and stability on lipid digestion. *Current Opinion in Colloid & Interface Science, 15*(1), 90-101.

Graves, S. M. (2008). *The formation, optical properties, and structure of nanoemulsions.* Ph.D. thesis, University of California, Los Angeles, USA, pp. 59-60 .

He, X., Mao, L., Gao, Y., & Yuan, F. (2016). Effects of high-pressure processing on the structural and functional properties of bovine lactoferrin. *Innovative Food Science and Emerging Technologies, 38,* 221-230.

Hu, H., Wu, J., Li-Chan, E. C. Y., Zhu, L., Zhang, F., Xu, X., Fun, G., Wang, L., Huang, L., Pan, S. (2012). Effects of ultrasound on structural and physical properties of soy protein isolate (SPI) dispersions. *Food Hydrocolloids, 30*(2), 647-655.

Jarpa-Parra, M., Bamdad, F., Tian, Z., Zeng, H., Temelli, F., & Chen, L. (2015). Impact of pH on molecular structure and surface properties of lentil legumin-like protein and its application as foam stabilizer. *Colloids and Surfaces B: Biointerfaces, 132*, 45-53.

Jiang, L., Wang, J., Li, Y., Wang, Z., Liang, J., Wang, R., Zhang, M. (2014). Effects of ultrasound on the structure and physical properties of black bean protein isolates. *Food Research International, 62*, 595-601.

Joshi, M., Adhikari, B., Aldred, P., Panozzo, J. F., Kasapis, S., & Barrow, C. J. (2012). Interfacial and emulsifying properties of lentil protein isolate. *Food Chemistry, 134*(3), 1343-1353.

Karaca, A. C., Low, N. H., & Nickerson, M. T. (2011). Emulsifying properties of chickpea, faba bean, lentil and pea proteins produced by isoelectric precipitation and salt extraction. *Food Research International, 44*(9), 2742-2750.

Karaca, A. C., Nickerson, M. T., & Low, N.H. (2011). Lentil and chickpea protein-stabilized emulsions: Optimization of emulsion formulation. *Journal of Agricultural and Food Chemistry, 59*(24), 13203-13211.

Keerati-U-Rai, M., & Corredig, M. (2009). Effect of dynamic high-pressure homogenization on the aggregation state of soy protein. *Journal of Agricultural and Food Chemistry, 57*(9), 3556-3562.

Keerati-U-Rai, M., & Corredig, M. (2010). Heat-induced changes occurring in oil/water emulsions stabilized by soy glycinin and β-conglycinin. *Journal of Agricultural and Food Chemistry, 58*(16), 9171-9180.

Kenmogne-Domguia, H. B., Moisan, S., Viau, M., Genot, C., & Meynier, A. (2014). The initial characteristics of marine oil emulsions and the composition of the media inflect lipid oxidation during in vitro gastrointestinal digestion. *Food Chemistry, 152*, 146-154.

Komaiko, J., Sastrosubroto, A., & McClements, D. J. (2016). Encapsulation of ω-3 fatty acids in nanoemulsion-based delivery systems fabricated from natural emulsifiers: sunflower phospholipids. *Food Chemistry, 203*, 331-339.

Koumakis, N., & Petekidis, G. (2011). Two step yielding in attractive colloids: transition from gels to attractive glasses. *Soft Matter, 7*(6), 2456-2470.

Lam, R. S. H., & Nickerson, M. T. (2013). Food proteins: a review on their emulsifying properties using a structure–function approach. *Food Chemistry, 141*(2), 975-984.

Lam, R. S. H., & Nickerson, M. T. (2015). The effect of pH and temperature pre-treatments on the structure, surface characteristics and emulsifying properties of alpha-lactalbumin. *Food Chemistry, 173*, 163-170.

Lam, R. S. H., & Nickerson, M. T. (2015). The effect of pH and temperature pre-treatments on the physicochemical and emulsifying properties of whey protein isolate. *LWT - Food Science and Technology, 60*(1), 427-434.

Langevin, D. (2000). Influence of interfacial rheology on foam and emulsion properties. *Advances in Colloid and Interface Science, 88*(1), 209-222.

Lawrence, M. J., & Rees, G. D. (2012). Microemulsion-based media as novel drug delivery systems. *Advanced Drug Delivery Reviews, 64*, 175-193.

Lee, H., Yildiz, G., Dos Santos, L. C., Jiang, S., Andrade, J. E., Engeseth, N. J., & Feng, H. (2016). Soy protein nano-aggregates with improved functional properties prepared by sequential pH treatment and ultrasonication. *Food Hydrocolloids, 55*, 200-209.

Lee, S., Choi, S., Li, Y., Decker, E., & McClements, D. (2011). Protein-stabilized nanoemulsions and emulsions: Comparison of physicochemical stability, lipid oxidation, and lipase digestibility. *Journal of Agricultural and Food Chemistry, 59*(1), 415-27.

Lerche, D. (2002). Dispersion stability and particle characterization by sedimentation kinetics in a centrifugal field. *Journal of Dispersion Science and Technology, 23*(5), 699-709.

Li, Y., & McClements, D. J (2010). New mathematical model for interpreting pH-stat digestion profiles: impact of lipid droplet characteristics on in vitro digestibility. *Journal of Agricultural and Food Chemistry, 58*(13), 8085-8092.

Liang, H.-N., & Tang, C.-H. (2013). Emulsifying and interfacial properties of vicilins: role of conformational flexibility at quaternary and/or tertiary levels. *Journal of Agricultural and Food Chemistry, 61*(46), 11140-11150.

Lin, L., Allemekinders, H., Dansby, A., Campbell, L., Durance-Tod, S., Berger, A., & Jones, P. (2013). Evidence of health benefits of canola oil. *Nutrition Reviews, 71*(6), 370-385.

Lobo, L. (2002). Coalescence during Emulsification. *Journal of Colloid and Interface Science, 254*(1), 165-174.

Maldonado-Valderrama, J., Wilde, P. J., Mulholland, F., & Morris, V. J. (2012). Protein unfolding at fluid interfaces and its effect on proteolysis in the stomach. *Soft Matter, 8*(16), 4402-4414.

Maldonado-Valderrama, J., Wilde, P., Macierzanka, A., & Mackie, A. (2011). The role of bile salts in digestion. *Advances in Colloid and Interface Science, 165*(1), 36-46.

Mason, T. G., Wilking, J. N., Meleson, K., Chang, C. B., & Graves, S. M. (2006). Nanoemulsions: formation, structure, and physical properties. *Journal of Physics: Condensed Matter, 18*(41), R635-R666.

McClements, D. J. (2004). Protein-stabilized emulsions. *Current Opinion in Colloid & Interface Science, 9*(5), 305-313.

McClements, D. J. (2005). *Food emulsions: principles, practices, and techniques* (2nd ed.. ed.). Boca Raton: Boca Raton : CRC Press.

McClements, D. J. (2010). Design of nano-laminated coatings to control bioavailability of lipophilic food components. *Journal of Food Science, 75*(1), R30-R42.

McClements, D. J., & Li, Y. (2010). Review of in vitro digestion models for rapid screening of emulsion-based systems. *Food & Function, 1*(1), 32-59.

McClements, D. J., & Rao, J. (2011). Food-grade nanoemulsions: formulation, fabrication, properties, performance, biological fate, and potential toxicity. *Critical Reviews in Food Science and Nutrition, 51*(4), 285-330.

McClements, D. J., Bai, L., & Chung, C. (2017). Recent advances in the utilization of natural emulsifiers to form and stabilize emulsions. *Annual Review of Food Science and Technology, 8*(1), 205-236.

McClements, D. J., Decker, J., Park, E., & Weiss, A. (2008). Designing food structure to control stability, digestion, release and absorption of lipophilic food components. *Food Biophysics, 3*(2), 219-228.

McClements, D. J., Saliva-Trujillo, L., Zhang, R., Zhang, Z., Zou, L., Yao, M., & Xiao, H. (2016). Boosting the bioavailability of hydrophobic nutrients, vitamins, and nutraceuticals in natural products using excipient emulsions. *Food Research International, 88*, 140-152.

Meleson, K., Graves, S. M., & Mason, T. G. (2004). Formation of concentrated nanoemulsions by extreme shear. *Soft Materials, 2*(2-3), 109-123.

Messens, W., Van Camp, J., & Huyghebaert, A. (1997). The use of high-pressure to modify the functionality of food proteins. *Trends in Food Science & Technology, 8*(4), 107-112.

Minekus, M., Alminger, M., Alvito, P., Ballance, S., Bohn, T., Bourlieu, C., Carrire, F., Corredig, M., Dupont, D., Dufour, C., Egger, L., Golding, M., Karakaya, S., Kirkhus, B., Le Feunteun, S., Lesmes, U., Macierzanka, A., Mackie, A., Marze, S., McClements, D. J., Mnard, O., Recio, I., Santos, C. N., Singh, R. P., Vegarud, G. E., Wickham, M. S. J., Weitschies, W., Brodkorb, A. (2014). A standardised static in vitro digestion method suitable for food an international consensus. *Food & Function, 5*(6), 1113-1124.

Mishchuk, N.A., Miller, R., Steinchen, A., & Sanfeld, A. (2002). Conditions of coagulation and flocculation in dilute mini-emulsions. *Journal of Colloid and Interface Science, 256*(2), 435-450.

Molina, E., Papadopoulou, A., & Ledward, D. A. (2001). Emulsifying properties of high-pressure treated soy protein isolate and 7S and 11S globulins. *Food Hydrocolloids, 15*(3), 263-269.

Mun, S., Decker, E. A., & McClements, D. J. (2007). Influence of emulsifier type on in vitro digestibility of lipid droplets by pancreatic lipase. *Food Research International, 40*(6), 770-781.

Norton, J. E., Gonzalez Espinosa, Y., Watson, R. L., Spyropoulos, F., & Norton, I. T. (2015). Functional food microstructures for macronutrient release and delivery. *Food & Function, 6*(3), 663-678.

O'Sullivan, J., Murray, B., Flynn, C., & Norton, I. (2015). The effect of ultrasound treatment on the structural, physical and emulsifying properties of animal and vegetable proteins. *Food Hydrocolloids,* 53, 141-154.

Oomah, B. D., Patras, A., Rawson, A., Singh, N., & Compos-Vega, R. (2011). Chemistry of Pulses. In B. Tiwari, A. Gowen & B. M. McKenna (Eds.), *Pulse foods: processing , quality and nutraceutical applications* (1st ed., pp. 9-56). Burlington, MA: Elsevier.

Peng, W., Kong, X., Chen, Y., Zhang, C., Yang, Y., & Hua, Y. (2016). Effects of heat treatment on the emulsifying properties of pea proteins. *Food Hydrocolloids, 52,* 301-310.

Pinnamaneni, S., Das, N. G., & Das, S. K. (2003). Comparison of oil-in-water emulsions manufactured by microfluidization and homogenization. *Die Pharmazie, 58*(8), 554-558.

Protonotariou, S., Evageliou, V., Yanniotis, S., & Mandala, I. (2013). The influence of different stabilizers and salt addition on the stability of model emulsions containing olive or sesame oil. *Journal of Food Engineering, 117*(1), 124-132.

Pugnaloni, L.A., Dickinson, E., Ettelaie, R., Mackie, A.R., & Wilde, P. J. (2004). Competitive adsorption of proteins and low-molecular-weight surfactants: Computer simulation and microscopic imaging. *Advances in Colloid and Interface Science, 107*(1), 27-49.

Puppo, C., Chapleau, N., Speroni, F., De Lamballerie-Anton, M., Michel, F., Añón, C., & Anton, M. (2004). Physicochemical modifications of high-pressure-treated soybean protein isolates. *Journal of Agricultural and Food Chemistry, 52*(6), 1564-71.

Qian, C., & McClements, D. J. (2011). Formation of nanoemulsions stabilized by model food-grade emulsifiers using high-pressure homogenization: factors affecting particle size. *Food Hydrocolloids, 25*(5), 1000-1008.

Rao, J., & McClements, D. J. (2011). Formation of flavor oil microemulsions, nanoemulsions and emulsions: influence of composition and preparation method. *Journal of Agricultural and Food Chemistry, 59*(9), 5026-5035.

Reiffers-Magnani, C. K., Cuq, J. L., & Watzke, H. J. (2000). Depletion flocculation and thermodynamic incompatibility in whey protein stabilised O/W emulsions. *Food Hydrocolloids, 14*(6), 521-530.

Sagalowicz, L., & Leser, M. E. (2010). Delivery systems for liquid food products. *Current Opinion in Colloid & Interface Science, 15*(1), 61-72.

Salvia-Trujillo, L. Qian, C., Martín-Belloso, O., & McClements, D. J. (2013). Influence of particle size on lipid digestion and β-carotene bioaccessibility in emulsions and nanoemulsions. *Food Chemistry, 141*(2), 1472-1480.

Salvia-Trujillo, L., Fumiaki, B., Park, Y., & McClements, D. J. (2017). The influence of lipid droplet size on the oral bioavailability of vitamin D2 encapsulated in emulsions: an in vitro and in vivo study. *Food & Function, 8*(2), 767-777.

Schubert, H., & Engel, R. (2004). Product and formulation engineering of emulsions. *Chemical Engineering Research and Design, 82*(9), 1137-1143.

Severin, S., & Xia, W. S. (2006). Enzymatic hydrolysis of whey proteins by two different proteases and their effect on the functional properties of resulting protein hydrolysates. *Journal of Food Biochemistry, 30*(1), 77-97.

Shao, Z., Negi, A. S., & Osuji, C. O. (2013). Role of interparticle attraction in the yielding response of microgel suspensions. *Soft Matter, 9*(22), 5492-5500.

Silletti, E., Vingerhoeds, M. H., Norde, W., & van Aken, G. A. (2007). The role of electrostatics in saliva-induced emulsion flocculation. *Food Hydrocolloids, 21*(4), 596-606.

Silva, J. L., & Weber, G. (1993). Pressure stability of proteins. *Annual Review of Physical Chemistry, 44*, 89-113.

Singh, H., & Sarkar, A. (2011). Behaviour of protein-stabilised emulsions under various physiological conditions. *Advances in Colloid and Interface Science, 165*(1), 47-57.

Singh, H., Ye, A., & Horne, D. (2009). Structuring food emulsions in the gastrointestinal tract to modify lipid digestion. *Progress in Lipid Research, 48*(2), 92-100.

Surh, J., & McClements, D. J. (2008). Influence of salt concentrations on the stabilities and properties of sodium caseinate stabilized oil-in-water emulsions. *Food Science and Biotechnology, 17*(1), 8-14.

Tadros, T., Izquierdo, P., Esquena, J., & Solans, C. (2004). Formation and stability of nano-emulsions. *Advances in Colloid and Interface Science, 108*, 303-318.

Tavano, O. L. (2013). Protein hydrolysis using proteases: an important tool for food biotechnology. *Journal of Molecular Catalysis B: Enzymatic*, 90, 1-11.

Walstra, P. (2002). *Physical chemistry of foods*. New York, NY: Marcel Dekker.

Wang, X., Jiang, Y., Wang, Y.-W., Huang, M.-T., Ho, C.-T., & Huang, Q. (2008). Enhancing anti-inflammation activity of curcumin through O/W nanoemulsions. *Food Chemistry, 108*(2), 419-424.

Wang, X.-S., Tang, C.-H., Li, B.-S., Yang, X.-Q., Li, L., & Ma, C.-Y. (2008). Effects of high-pressure treatment on some physicochemical and functional properties of soy protein isolates. *Food Hydrocolloids, 22*(4), 560-567.

Wilde, P., Mackie, A., Husband, F., Gunning, P., & Morris, V. (2004). Proteins and emulsifiers at liquid interfaces. *Advances in Colloid and Interface Science, 108–109*, 63-71.

Wong, B. T., Zhai, J., Hoffmann, S. V., Aguilar, M., Augustin, M.-I., Wooster, T. J., & Day, L. (2011). Conformational changes to deamidated wheat gliadins and β-casein upon adsorption to oil–water emulsion interfaces. *Food Hydrocolloids*, 27(1), 91-101.

Wooster, T. J., Golding, M., & Sanguansri, P. (2008). Impact of oil type on nanoemulsion formation and Ostwald ripening stability. *Langmuir*, *24*(22), 12758-12765.

Yaghmur, A., Aserin, A., & Garti, N. (2002). Phase behaviour of microemulsions based on food-grade nonionic surfactants: effect of polyols and short-chain alcohols. *Colloids and Surfaces A: Physicochemical and Engineering Aspects*, *209*(1), 71-81.

Ye, A. (2008). Interfacial composition and stability of emulsions made with mixtures of commercial sodium caseinate and whey protein concentrate. *Food Chemistry, 110*(4), 946-952.

Yerramilli, M., & Ghosh, S. (2016). Long-term stability of sodium caseinate-stabilized nanoemulsions. Journal of Food Science and Technology. 54(1), 82–92.

Yerramilli, M., Longmore, N., & Ghosh, S. (2017). Improved stabilization of nanoemulsions by partial replacement of sodium caseinate with pea protein isolate. *Food Hydrocolloids, 64*, 99-111.

Zhai, J., Wooster, T. J., Hoffmann, S. V., Lee, T.-H., Augustin, M. A., & Aguilar, M.-I. (2011). Structural rearrangement of β-lactoglobulin at different oil-water interfaces and its effect on emulsion stability. *Langmuir: The ACS Journal of Surfaces and Colloids, 27*(15), 9227-9236.

Zhao, G., Liu, Y., Zhao, M., Ren, J., & Yang, B. (2011). Enzymatic hydrolysis and their effects on conformational and functional properties of peanut protein isolate. *Food Chemistry, 127*(4), 1438-1443.

Zou, L., Liu, W., Liu, Chengmei, X., H., & McClements, D. J. (2015). Utilizing food matrix effects to enhance nutraceutical bioavailability: increase of curcumin bioaccessibility using excipient emulsions. *Journal of Agricultural and Food Chemistry, 63*(7), 2052-62.